AD-A084 662 SRI INTERNATIONAL MENLO PARK CA F/G 18/3
LABORATORY INVESTIGATION OF CONTAINMENT IN UNDERGROUND NUCLEAR --ETC(U)
JAN 78 J C CIZEK, A L FLORENCE DNA001-77-C-0025
UNCLASSIFIED DNA-4846F NL

1 OF 2
AD A 084662

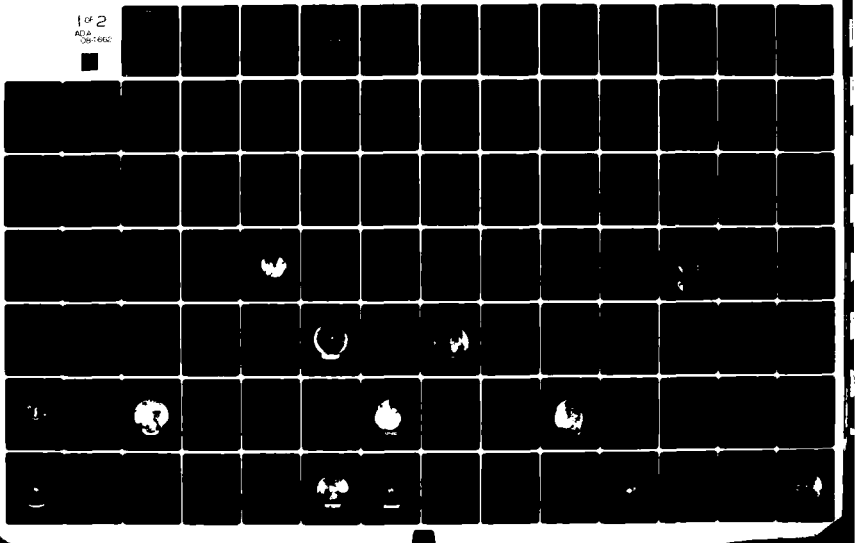

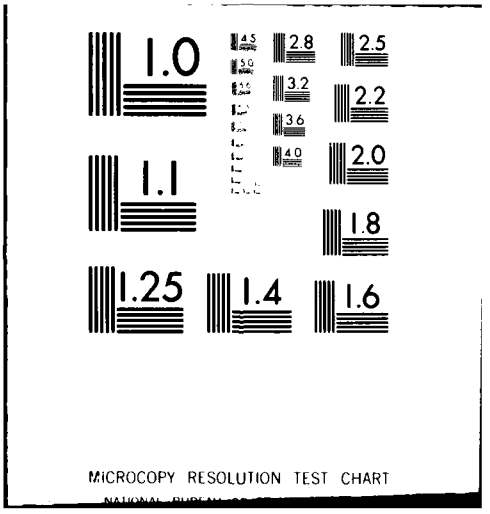
1.0
1.1
1.25
1.4
1.6
1.8
2.0
2.2
2.5
2.8
3.2
3.6
4.0
4.5
5.0
MICROCOPY RESOLUTION TEST CHART

DNA 4846F

LABORATORY INVESTIGATION OF CONTAINMENT IN UNDERGROUND NUCLEAR TESTS

J. C. Cizek
A. L. Florence
SRI International
333 Ravenswood Avenue
Menlo Park, California 94025

1 January 1978

Final Report for Period 1 January 1977—30 November 1977

CONTRACT No. DNA 001-77-C-0025

APPROVED FOR PUBLIC RELEASE;
DISTRIBUTION UNLIMITED.

THIS WORK SPONSORED BY THE DEFENSE NUCLEAR AGENCY
UNDER RDT&E RMSS CODE B345077462 J24AAXYX98341 H2590D.

Prepared for
Director
DEFENSE NUCLEAR AGENCY
Washington, D. C. 20305

Destroy this report when it is no longer needed. Do not return to sender.

PLEASE NOTIFY THE DEFENSE NUCLEAR AGENCY, ATTN: STTI, WASHINGTON, D.C. 20305, IF YOUR ADDRESS IS INCORRECT, IF YOU WISH TO BE DELETED FROM THE DISTRIBUTION LIST, OR IF THE ADDRESSEE IS NO LONGER EMPLOYED BY YOUR ORGANIZATION.

UNCLASSIFIED

SECURITY CLASSIFICATION OF THIS PAGE *(When Data Entered)*

REPORT DOCUMENTATION PAGE		READ INSTRUCTIONS BEFORE COMPLETING FORM
1. REPORT NUMBER DNA 4846F	2. GOVT ACCESSION NO. AD-A084 662	3. RECIPIENT'S CATALOG NUMBER
4. TITLE *(and Subtitle)* LABORATORY INVESTIGATION OF CONTAINMENT IN UNDERGROUND NUCLEAR TESTS		5. TYPE OF REPORT & PERIOD COVERED Final Report for Period 1 Jan 77—30 Nov 77 6. PERFORMING ORG. REPORT NUMBER SRI PYU-5958
7. AUTHOR*(s)* John C. Cizek Alexander L. Florence		8. CONTRACT OR GRANT NUMBER*(s)* DNA 001-77-C-0025 ✓
9. PERFORMING ORGANIZATION NAME AND ADDRESS SRI International 333 Ravenswood Avenue Menlo Park, California 94025		10. PROGRAM ELEMENT, PROJECT, TASK AREA & WORK UNIT NUMBERS Subtask J24AAXYX983-41
11. CONTROLLING OFFICE NAME AND ADDRESS Director Defense Nuclear Agency Washington, D.C. 20305		12. REPORT DATE 1 January 1978 13. NUMBER OF PAGES 136
14. MONITORING AGENCY NAME & ADDRESS*(if different from Controlling Office)*		15. SECURITY CLASS *(of this report)* UNCLASSIFIED 15a. DECLASSIFICATION DOWNGRADING SCHEDULE

16. DISTRIBUTION STATEMENT *(of this Report)*

Approved for public release; distribution unlimited.

17. DISTRIBUTION STATEMENT *(of the abstract entered in Block 20, if different from Report)*

18. SUPPLEMENTARY NOTES

This work sponsored by the Defense Nuclear Agency under RDT&E RMSS Code B345077462 J24AAXYX98341 H2590D.

19. KEY WORDS *(Continue on reverse side if necessary and identify by block number)*

Nuclear	Fracture Initiation
Underground	Overburden
Containment	Stemming
Cavity	
Hydrofracture	

20. ABSTRACT *(Continue on reverse side if necessary and identify by block number)*

As part of the DNA stemming and containment program for underground nuclear testing, laboratory investigations were conducted to further develop a containment experiment for studying residual stress fields around exploded cavities. A comparison of hydrofracture pressures for exploded and unexploded cavities revealed the existence of this stress field and its benefit to containment. Fundamental containment mechanisms were investigated by studying the effects of changes in basic experimental parameters. The data generated

DD FORM 1 JAN 73 1473 EDITION OF 1 NOV 65 IS OBSOLETE

UNCLASSIFIED

SECURITY CLASSIFICATION OF THIS PAGE *(When Data Entered)*

20. ABSTRACT (Continued)

provide results suitable for development of new containment theories as well as for correlation with predictions of existing computer codes.

SUMMARY

The purpose of this project is to conduct laboratory containment experiments in support of the DNA stemming and containment program for underground nuclear tests. Over the years, the DNA stemming and containment program has consisted of five main parts:

(1) Code development and application for ground motion, tunnel closure, and grout flow calculations.

(2) Material properties determination.

(3) Laboratory investigations.

(4) Scaled high explosive tests.

(5) Field diagnostics.

SRI has been conducting the laboratory investigations.

During this phase of the laboratory program, a previously developed containment experiment was used for further study of the residual stress surrounding an exploded cavity in a rheological material. The experimental data generated are suitable as a basis for development of containment theories as well as for correlation with predictions of existing codes.

In the basic containment experiment, a small spherical charge is cast in a sphere of rock-matching grout (RMG) with properties similar to those of Nevada Test Site tuff. The RMG sphere is hydraulically pressurized to represent overburden. The explosive is detonated and the residual gases are released by drilling into the cavity. Dyed fluid is pumped into the cavity at a constant flow rate until fracture occurs and a steady radial pressure gradient is established. The internal pressure is removed and then the external pressure is removed. The cracked sphere is drained and tapped into two parts by use of a chisel, and the exposed fracture plane is photographed.

The following experimental parameters were investigated:

- Charge size. Charges containing two different amounts of high explosive were used.
- Overburden. Exploded cavities were tested at two different external pressures. A range of external pressures was applied to spheres with unexploded cavities.
- Viscosity. Hydrofracture was performed with two different fluids.
- Flow rate. Cavities were pressurized at two different rates.
- Cavity size. Three unexploded cavity sizes were tested.

In addition, the effects of material strength, creep, cavity imperfections, cavity lining, and simulated geological and test site features were investigated.

Findings to date are as follows:

- Unexploded cavity reproducibility was good.
- For the larger explosive charge, reproducibility was good. Fracture initiation pressures were significantly higher than those in the corresponding unexploded cavity tests.
- For the smaller charge, reasonably reproducible fracture initiation pressures were followed by a spectrum of cavity pressures. The pressures required for fracture initiation were only slightly higher than those in the corresponding unexploded cavity tests.
- Fracture initiation in unexploded and exploded cavities was correlated with a pronounced spike on the hydrofracture pressure record.
- Fracture initiation pressure in unexploded cavities increased with increasing overburden, increasing material strength and decreasing cavity size.
- Increased overburden had negligible influence on fracture initiation pressure for exploded cavities.

- Lower viscosity hydrofracture fluid and slower flow rate lowered fracture initiation pressures for unexploded and exploded cavities.
- Simulated faults and interfaces strongly influenced fracture patterns and subsequent flow in unexploded and exploded cavity tests.
- Venting of detonation gases to an adjoining tunnel degrated the containment capability of an exploded cavity.
- Imperfections in the walls ofan unexploded cavity reduced containment capability.
- Prolonged material relaxation following detonation resulted in hydrofracture pressures at the lower end of the exploded cavity spectrum.

The existence of a residual stress field was demonstrated for the larger charge by the increased hydrofracture pressure. However, further work is required to explain the spectrum of cavity pressures associated with the smaller charge. Also, conclusions not related to reproducibility, overburden, or fracture initiation are based on a maximum of three tests. Hence further testing is required to confirm these results.

PREFACE

This research was conducted under Contract DNA001-77-C-0025 in support of the DNA stemming and containment program for underground nuclear tests.

The authors are indebted to the technical monitor, Carl Keller (FCDNA) for ideas and overall guidance, to Don Gardiner of Terra Tek, Inc., for material testing, and to Dick Stowe of Waterways Experiment Station for information on the preparation of granite simulant. In addition, the insights provided by the theoretical work of the containment communities at Systems, Science and Software and Pacifica Technology are appreciated.

Finally, the authors are indebted to R. W. Gates and L. J. Dary for performing the experiments and suggesting improvements, and to G. R. Abrahamson for overall supervision.

RELEVANT CONVERSION FACTORS

To Convert From	To	Multiply By
atmosphere (normal)	kilo pascal (kPa)	1.013 25 X E +2
bar	kilo pascal (kPa)	1.000 000 X E +2
foot	meter (m)	3.048 000 X E -1
inch	meter (m)	2.540 000 X E -2
mil	meter (m)	2.540 000 X E -5
ounce	kilogram (kg)	2.834 952 X E -2
poise	kilogram/meter-second (kg/m·sec)	1.000 000 X E -1
pound-force (lbf avoirdupois)	newton (N)	4.448 222
pound-force/inch^2 (psi)	kilo pascal (kPa)	6.894 757
pound-mass (lbm avoirdupois)	kilogram (kg)	4.535 924 X E -1

CONTENTS

ILLUSTRATIONS

TABLES

1. INTRODUCTION

In underground nuclear tests, radioactive gases must be prevented from entering the atmosphere. In general, this requirement will be met if experimental tunnels leading from the nuclear device cavity are stemmed successfully and if the residual cavity gases are contained by the adjacent surrounding medium. The residual stress field created around the cavity by the explosion probably aids containment. Although containment has been achieved for many years and stemming has generally been successful in recent nuclear tests, reliability is uncertain and planned tests still require extensive containment evaluation.

Over the years, the DNA stemming and containment (SAC) program has consisted of five main parts: code development for ground motion, tunnel closure, and grout flow calculations; material properties determination; laboratory investigations; scaled high explosive tests; and field diagnostics. SRI has been conducting the laboratory investigations.[1-4]

Laboratory investigations during the last year have focused mainly on containment. One purpose of the experimental program has been to determine the fracture initiation pressure of a cavity generated under a variety of conditions. Another purpose is to validate the calculated nature[1,4] of the residual stress field as a major containment feature of underground nuclear tests. The data generated in the laboratory are suitable for correlation with the predictions of existing codes. The experimental technique may also be used to determine the influence of major geological and test site features. Although the experiment may not be regarded as a small-scale version of an explosively simulated underground nuclear test, simulation is good enough to provide the correct important mechanisms required in a study of containment.

In a standard containment experiment, a small spherical charge is cast in a sphere of rock-matching grout (RMG) with properties similar to

those of Nevada Test Site tuff. The RMG sphere is hydraulically pressurized to represent overburden. The explosive is detonated and the residual gases are released by drilling into the cavity. Dyed fluid is pumped into the cavity at a constant flow rate until fracture occurs and a steady radial pressure gradient is established. The internal pressure is removed and then the external pressure is removed. The cracked sphere is drained and tapped into two parts by use of a chisel, and the exposed fracture plane is photographed. The effect of the explosively generated residual stress field is assessed by conducting a separate hydrofracture on a sphere with an unexploded cavity equal in size to the corresponding exploded cavity.

Although emphasis was placed on reproducibility, additional investigations were made in the following areas:

- Charge size. Explosive charges containing 1/4 and 1/2 gram of PETN* were used.
- Overburden. External pressure in the range 0-2000 psi was applied.
- Viscosity. Hydrofracture was performed by pumping dyed glycerol or dyed water. Viscosity of these fluids is 660 and 1 centipoise, respectively.
- Flow rate. Hydrofracture fluid was pumped into the cavities at the rate of 0.71 or 4.26 cm^3/min.
- Cavity size. Unexploded cavities with 11/16-, 1-, and 2-inch diameters were tested.
- Material strength. Two rock-matching grouts, 2C3 and 2C4, and two grainte simulants, GS2 and GS3, were tested.
- Geology. Simulated geological and test site features included faults, interfaces, nearby tunnels and cavities, and a tunnel extending from the explosive source.
- Creep. Prior to hydrofracture of exploded cavities, material relaxation periods as long as 97 hours were allowed.
- Imperfection sensitivity. Unexploded cavities with and without notches in the cavity wall were tested.

*Pentaerythritol tetranitrate ($C_5H_8O_{12}N_4$).

- Cavity lining. The surface of several unexploded cavities was lined with glass.

- Fracture initiation and growth. Hydrofracture was terminated at various stages of development.

The main findings of the above work include:

- Reproducibility with unexploded cavities was good.

- Reproducibility with 1/2-gram charges was good. Fracture initiation pressure was 35% higher than for the corresponding unexploded cavity in the case of RMG 2C3. For RMG 2C4 the increase was 47%.

- Reproducibility with 1/4-gram charges was good up to fracture initiation, but a spectrum of cavity pressures followed. The increase in fracture initiation over the value of the corresponding unexploded cavity was 5% for RMG 2C4 spheres.

- Fracture initiation pressure for an unexploded cavity increased with increasing overburden, increasing material strength, and decreasing cavity size.

- An increase in overburden had negligible influence on exploded cavity tests.

- Lower viscosity hydrofracture fluid and slower hydrofracture flow rate reduced fracture initiation pressure in unexploded and exploded cavities.

- Venting of detonation gases along a tunnel significantly reduced containment capability of exploded cavities.

- Imperfections in the wall of an unexploded cavity reduced containment capability.

- Prolonged material relaxation following detonation resulted in hydrofracture pressures at the lower end of the 1/4-gram charge spectrum.

Except for reproducibility, overburden, and fracture initiation, the above findings are based on a maximum of three tests in each category. A detailed distribution of all tests is given in Section 3 (Table 3.1).

2. EXPERIMENTAL DEVELOPMENT

2.1 CONCEPT

The experiment shown schematically in Figure 2.1 was devised[4] to simulate in the laboratory the conditions in an underground nuclear test. A small spherical explosive charge representing the device is sealed and cast in a much larger sphere of rock-matching grout (RMG) with properties similar to those of Nevada Test Site tuff (Figure 2.1a). The grout surface is sealed and hydraulically pressurized to represent overburden (Figure 2.1b). The explosive is detonated and the residual gases released (Figure 2.1c). Fluid is pumped into the cavity at a constant flow rate until fracture occurs and a steady flow develops along the fracture surface (Figure 2.1d).

The final stages of gas release and cavity pressurization are included to determine the effect of the residual stress field by comparing the cavity pressures required to crack the RMG sphere with and without residual stresses. In the experiments without a residual stress field, spherical cavities are cast in the grout sphere; these unexploded cavities are the same size as the exploded cavities.

2.2 EXPERIMENTAL APPARATUS

External pressure is applied by means of the apparatus shown in Figure 2.2. A 12-inch-diameter RMG sphere is shown inside a steel vessel containing water under pressure. The sphere is suspended from the lid by a steel tube cast in the grout, this tube is also used to position the charge, guide the detonator cables, and drill into the cavity after detonation. The water in the vessel is maintained at a constant pressure throughout the test by incorporating a high-pressure gas reservoir and valve in the water supply line.

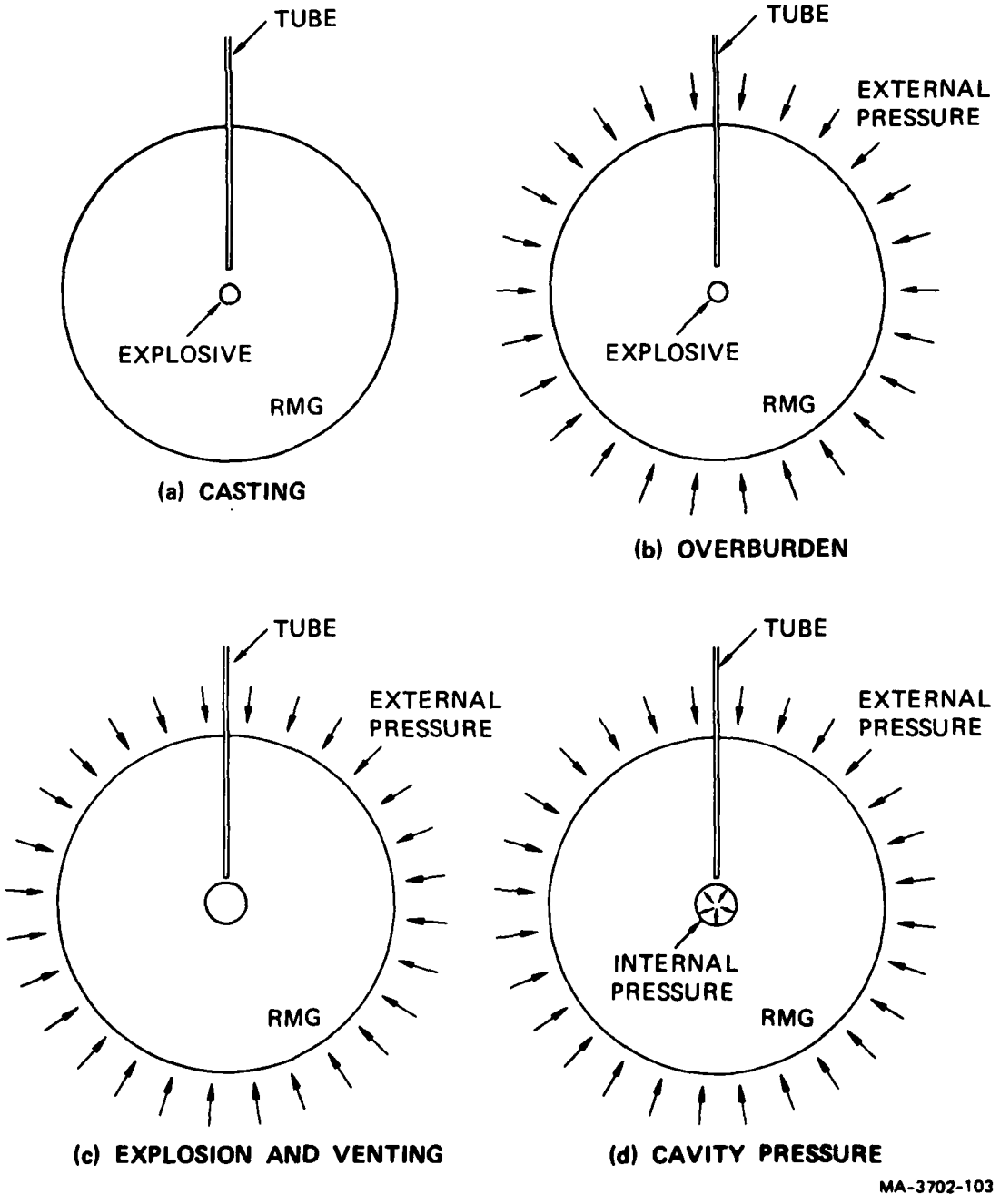

FIGURE 2.1 SEQUENCE OF OPERATIONS IN CONTAINMENT EXPERIMENT

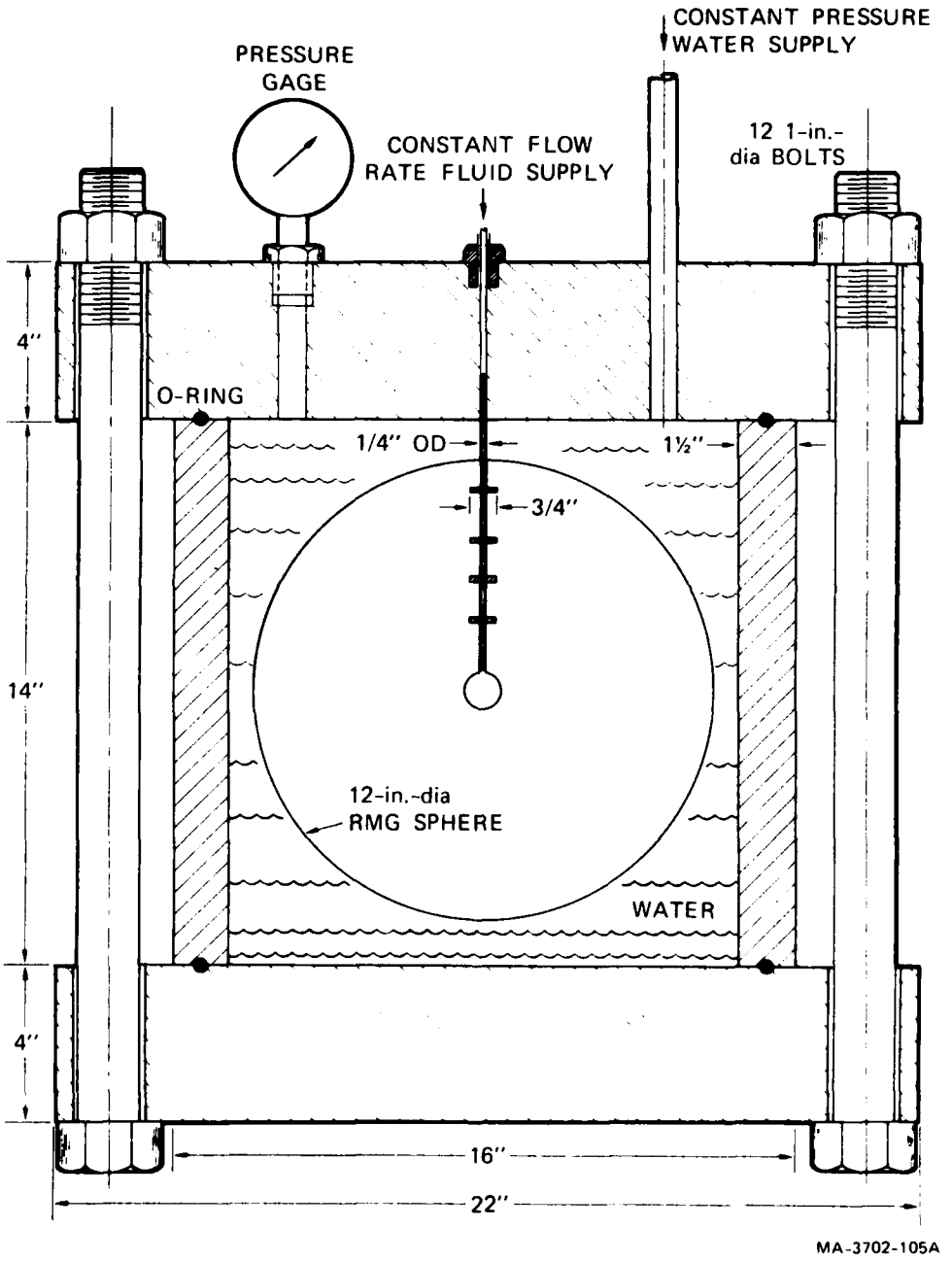

FIGURE 2.2 CONTAINMENT EXPERIMENT APPARATUS

The constant flow rate system shown schematically in Figure 2.3 was introduced to make the apparatus conform with standard hydrofracture practice. The specifications of this system are as follows:

Motor: Dayton Gear motor Model 5K933, 1/4 hp, 6 rpm, 600 in-lb torque

Pump: High Pressure Equipment Co. Model 87-6-5
60 cm^3 capacity, 5000 psi maximum pressure
4.26 cm^3/min flow rate (0.71 cm^3/revolution)

System: Fluid: dyed glycerin or dyed water
Volume (excluding pump) 31.33 cm^3

The motor shaft rotates at a constant angular velocity of 6 rpm. A slotted tubular coupling allows an extension of the shaft to translate as well as rotate. The shaft extension is threaded and rotates in a fixed threaded bearing, resulting in a constant velocity translation of the pump piston. Hence, fluid is driven at a constant rate of 4.26 cm^3/min into the cavity supply line (Figure 2.3). Fluid flow is recorded automatically with pen and chart by measuring the voltage change across an angular potentiometer geared to the rotating shaft; a constant chart speed introduces time, and calibration test results relate flow to voltage change. Similarly, pressure is recorded by measuring the voltage change across a calibrated resistance pressure transducer. A slower flow rate of 0.71 cm^3/min was made possible through a modification of the gear system.

2.3 MATERIAL PROPERTIES

Figures 2.4 and 2.5 show strength properties of a rock-matching grout, SRI RMG 2C3, used in early tests and the average properties from many samples of Nevada Test Site tuff for comparison. The grout mixture and its physical properties are given in Tables 2.1 and 2.2. Unconfined crush strength data are shown in Figure 2.6. Scatter in this data prompted development of new grout, RMG 2C4, with similar but more consistent strength. The mixture and physical properties of RMG 2C4 are included in Tables 2.1 and 2.2. Unconfined crush strength data are shown in Figure 2.7.

Table 2.1

MIXTURES[a] FOR SRI RMG 2C3 AND SRI RMG 2C4

Component	RMG 2C3	RMG 2C4
Type I-II Portland cement	31.95%	32.691%
Sand (20-40 Monterey)	21.40%	21.896%
Barite (barium sulfate)	20.40%	20.848%
Bentonite (gel)	2.80%	2.837%
CFR 2 (concrete friction reducing compound)	0.08%	0.078%
Water	23.37%	21.650%

[a]28-day aging procedure: Sealed in plastic and submerged in water with the following temperature sequence: raise to 50°C over 8-hr period, hold at 50°C for 48-hr, lower to 22°C over 6-hr period.

Table 2.2

PHYSICAL PROPERTIES OF SRI RMG 2C3, RMG 2C4, AND GS3

Sample	Density (g/cm^3)			Water by Wet Weight (%)	Porosity (%)	Saturation (%)	Air Voids (%)
	Aged	Dry	Grain				
2C3	2.13	1.72	2.95	19.2	42	98	1
2C3	2.18	1.79	2.95	17.9	40	98	1
2C3	2.16	1.75	2.94	19.0	41	100	0
2C4	2.15	1.76	2.90	18.1	39	99	0.5
2C4	2.15	1.75	2.87	18.6	39	100	0
2C4	2.18	1.79	2.88	17.7	38	100	0
GS3	2.42	2.27	2.80	6.3	19	82	3.5

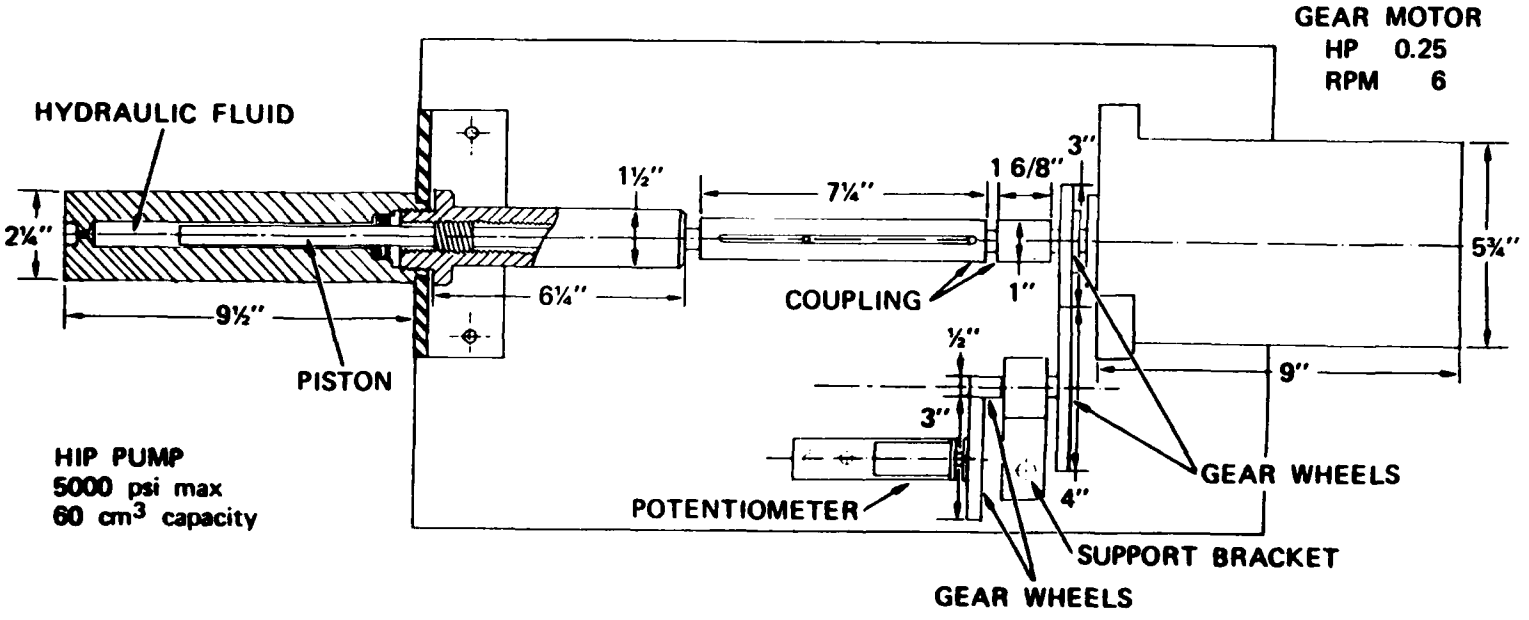

FIGURE 2.3 CONSTANT FLOW-RATE HYDROFRACTURE SYSTEM

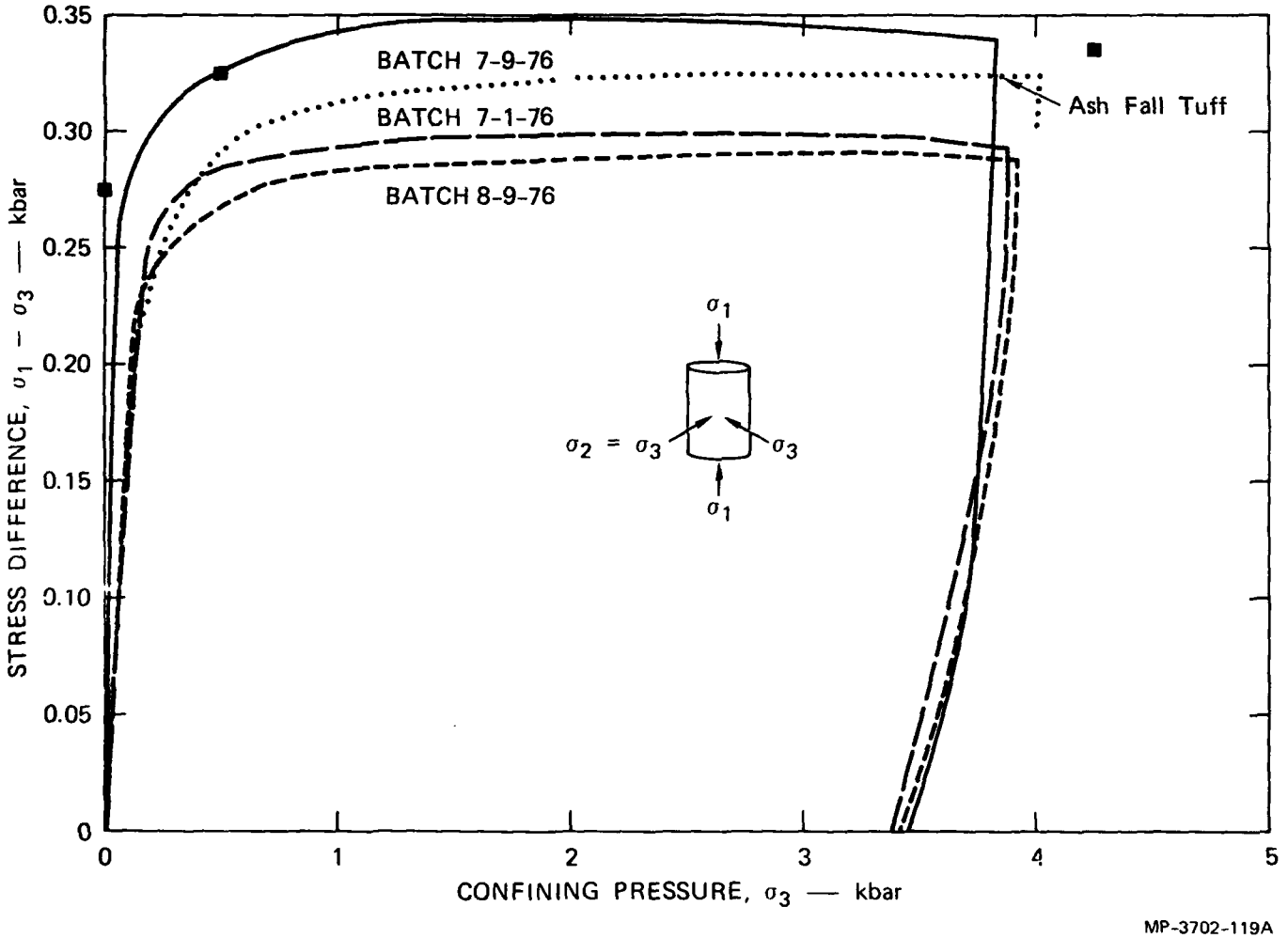

FIGURE 2.4 STRENGTH PROPERTIES OF THE ROCK-MATCHING GROUT SRI RMG 2C3: STRESS DIFFERENCE VERSUS CONFINING PRESSURE

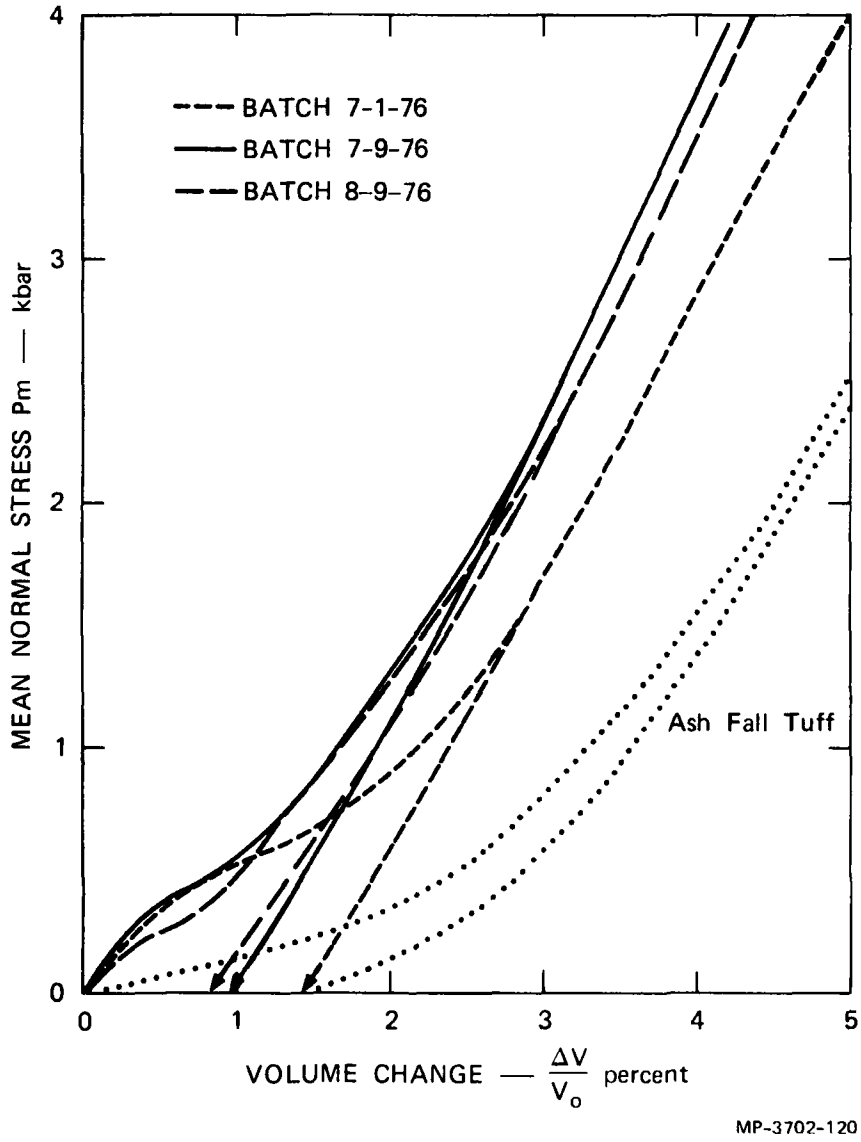

FIGURE 2.5 STRENGTH PROPERTIES OF THE ROCK-MATCHING GROUT SRI RMG 2C3: MEAN NORMAL STRESS VERSUS VOLUME CHANGE

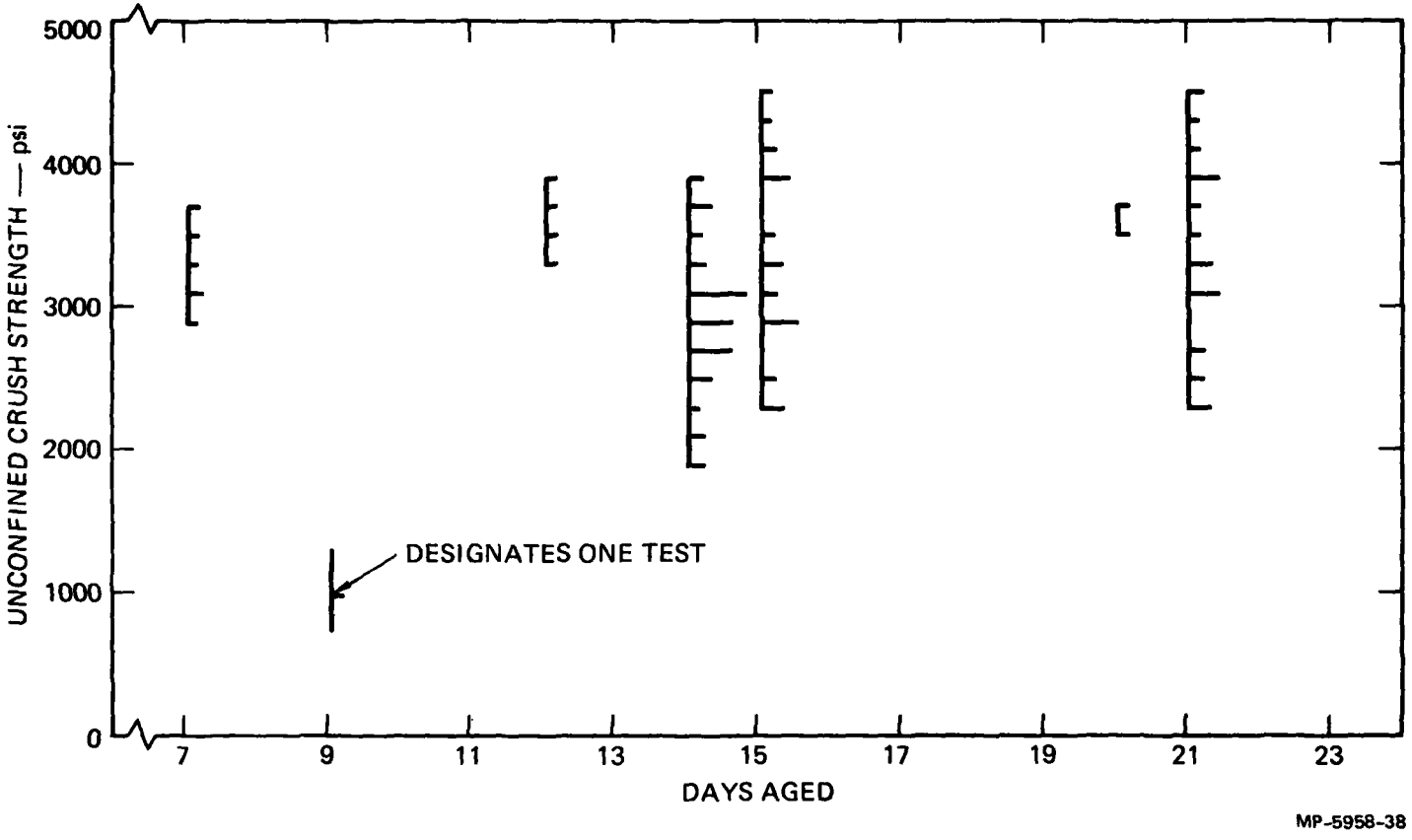

FIGURE 2.6 UNCONFINED CRUSH STRENGTH OF THE ROCK-MATCHING GROUT SRI RMG 2C3

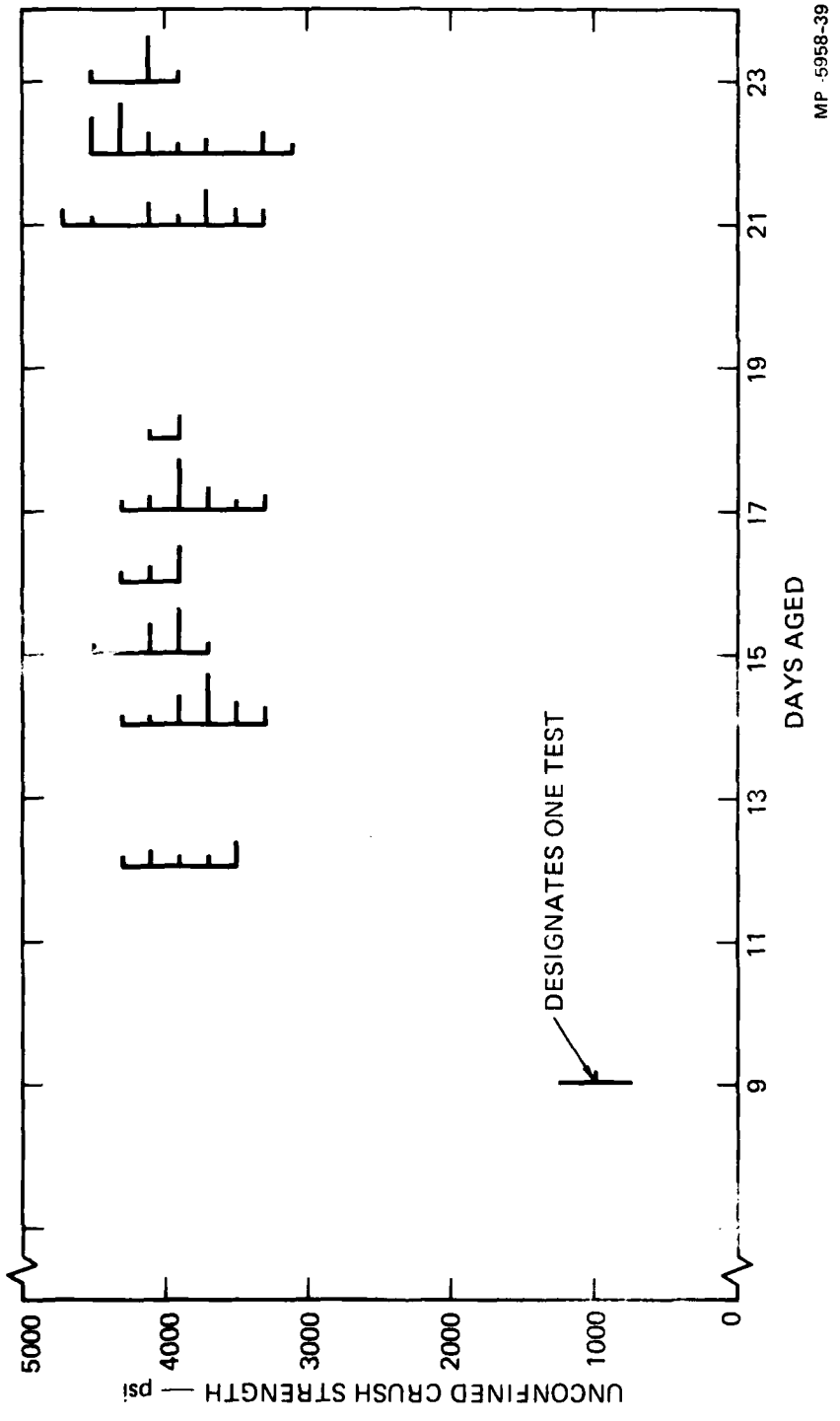

FIGURE 2.7 UNCONFINED CRUSH STRENGTH OF THE ROCK-MATCHING GROUT SRI RMG 2C4

Figures 2.8 and 2.9 show additional strength properties of RMG 2C4. For comparison, properties of a modified granite simulant, GS3, are also shown. Physical properties for GS3 are given in Table 2.2. Unconfined crush strength data are shown in Figure 2.10. The stronger granite simulant was developed for studying the effect on containment of (1) material strength and (2) an interface between dissimilar materials. Waterways Experiment Station, Vicksburg, Mississippi, supplied the original mixture design information that led to the development of GS3.

2.4 UNEXPLODED CAVITIES

The basic configuration for unexploded cavity tests is shown in Figure 2.11. Three different methods were used to form the central cavity. In one method two orthogonal wire hoops, with diameters equal to the desired cavity diameter, were soldered to the outside of the steel access tube. A balloon was inserted through the tube and expanded to the desired size with water. The wire cage held the balloon in place. After the sphere was cast and cured, the balloon was removed but the wire cage remained embedded in the surrounding material. This was the standard method of forming the cavity.

In a second method, the wire hoops were temporarily fastened to allow the balloon to take a spherical shape and then removed. This design was developed to study the significance of imperfections induced by the embedded wire cage. Hence experiments using this design were termed imperfection sensitivity tests.

The third method made use of a thin glass sphere epoxied to the end of the access tube. An opening in the sphere allowed fluid to flow into the cavity. Since the glass restricts flow to the surrounding material, experiments using this design were termed cavity lining tests.

2.5 EXPLODED CAVITIES

The basic configuration for exploded cavity tests is shown in Figure 2.12. Explosive charges containing nominally 1/2 gram and 1/4 gram

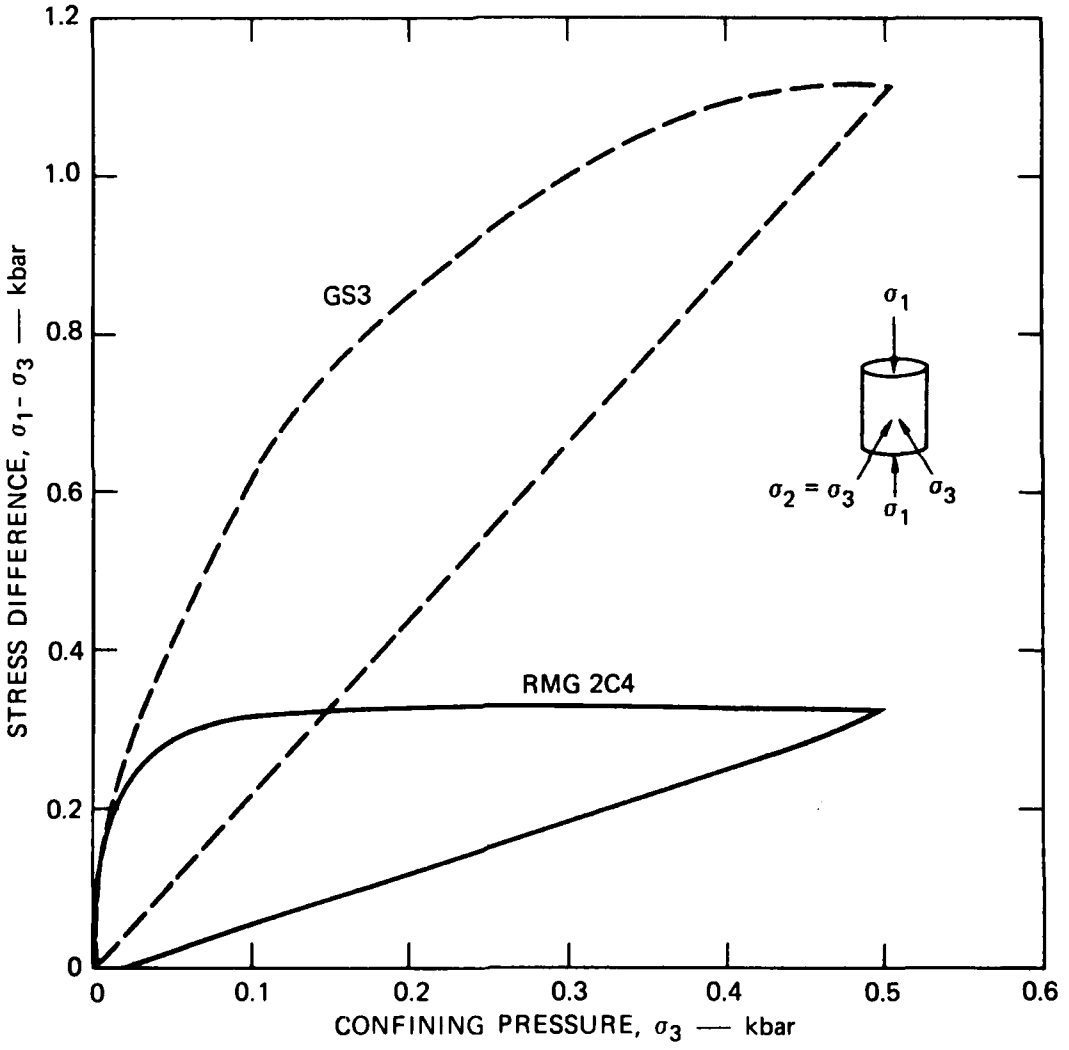

FIGURE 2.8 STRENGTH PROPERTIES OF THE ROCK-MATCHING GROUT SRI RMG 2C4 AND THE MODIFIED GRANITE SIMULANT GS3: STRESS DIFFERENCE VERSUS CONFINING PRESSURE

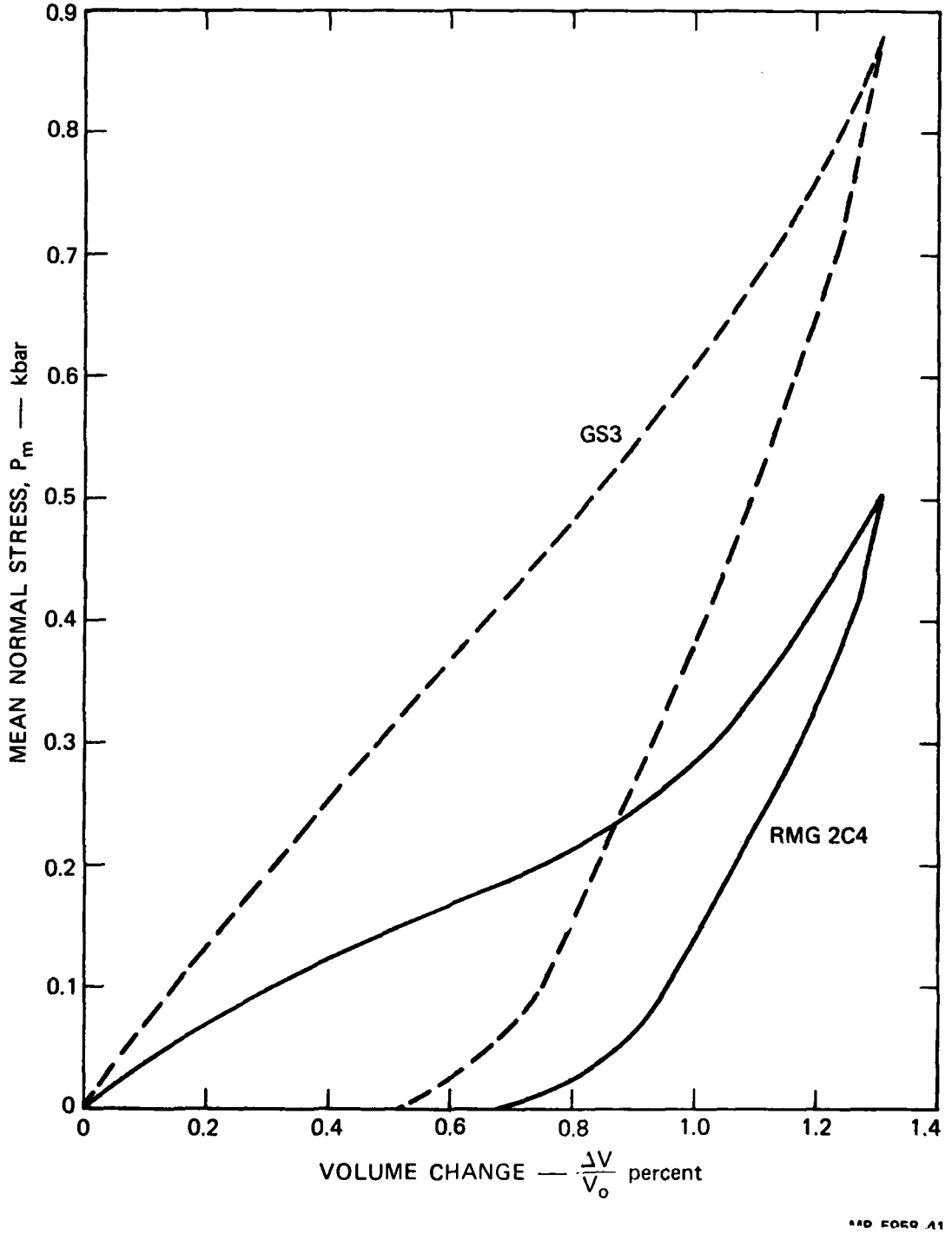

FIGURE 2.9 STRENGTH PROPERTIES OF THE ROCK-MATCHING GROUT SRI RMG 2C4 AND THE MODIFIED GRANITE SIMULANT GS3: MEAN NORMAL STRESS VERSUS VOLUME CHANGE

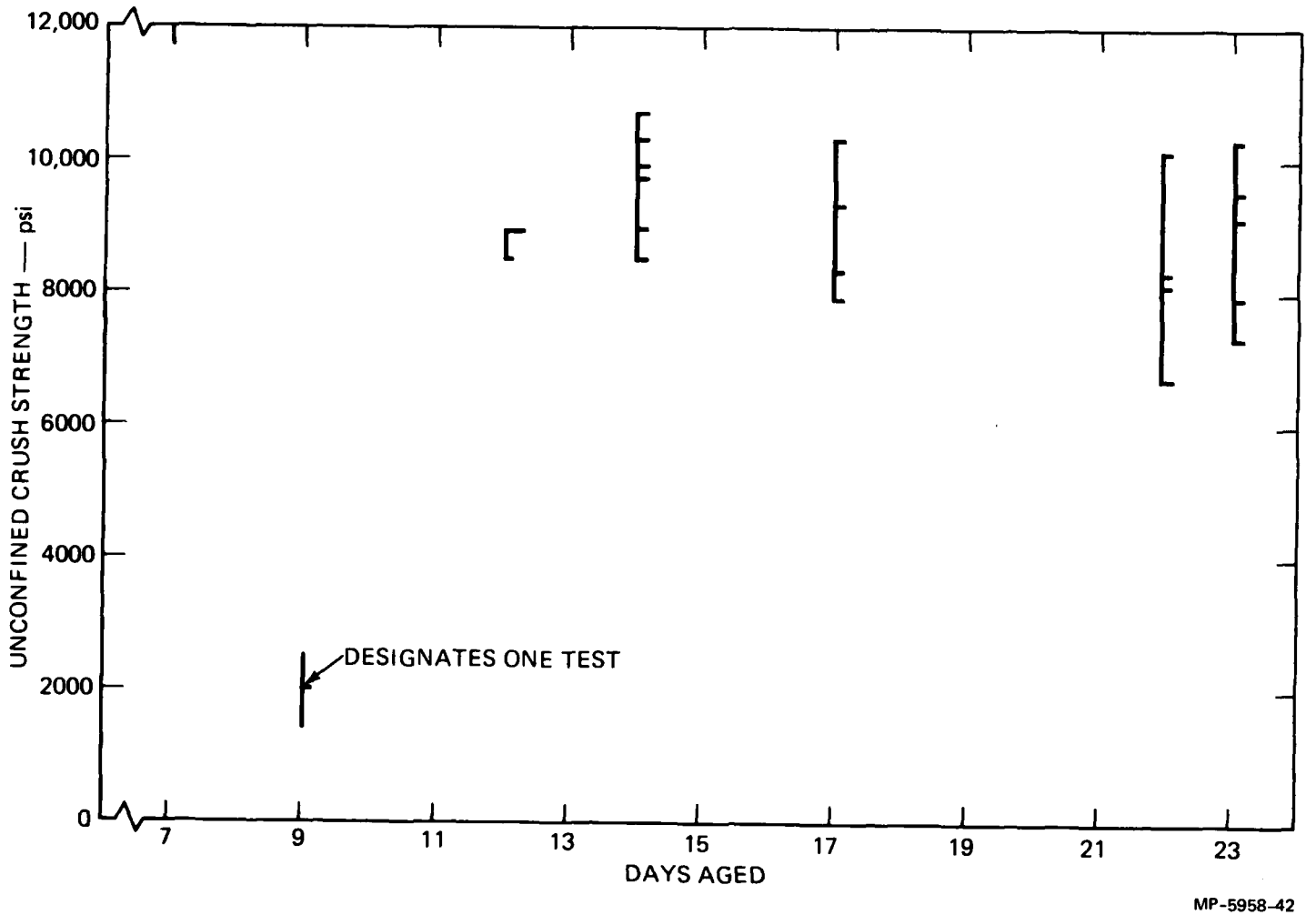

FIGURE 2.10 UNCONFINED CRUSH STRENGTH OF THE MODIFIED GRANITE SIMULANT GS3

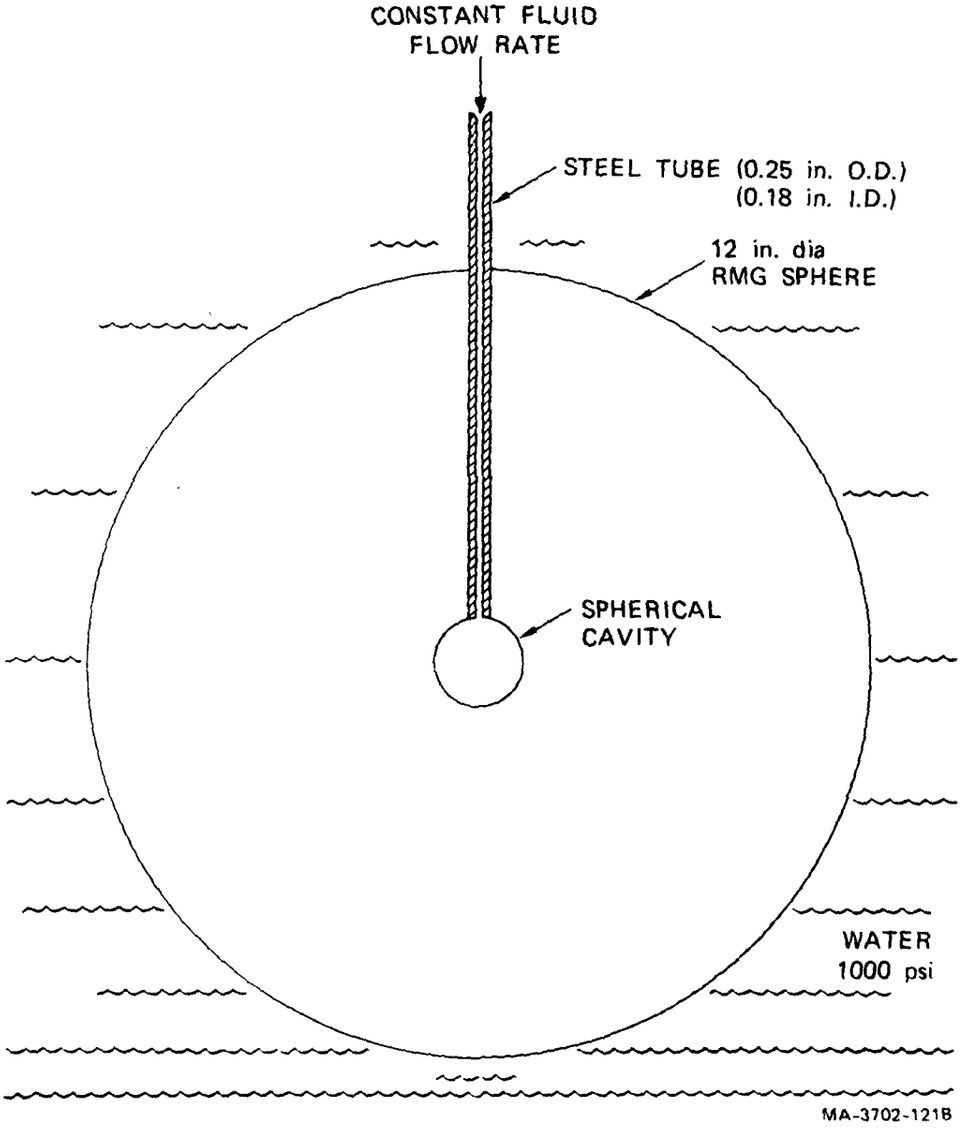

FIGURE 2.11 BASIC CONFIGURATION FOR UNEXPLODED CAVITY TESTS

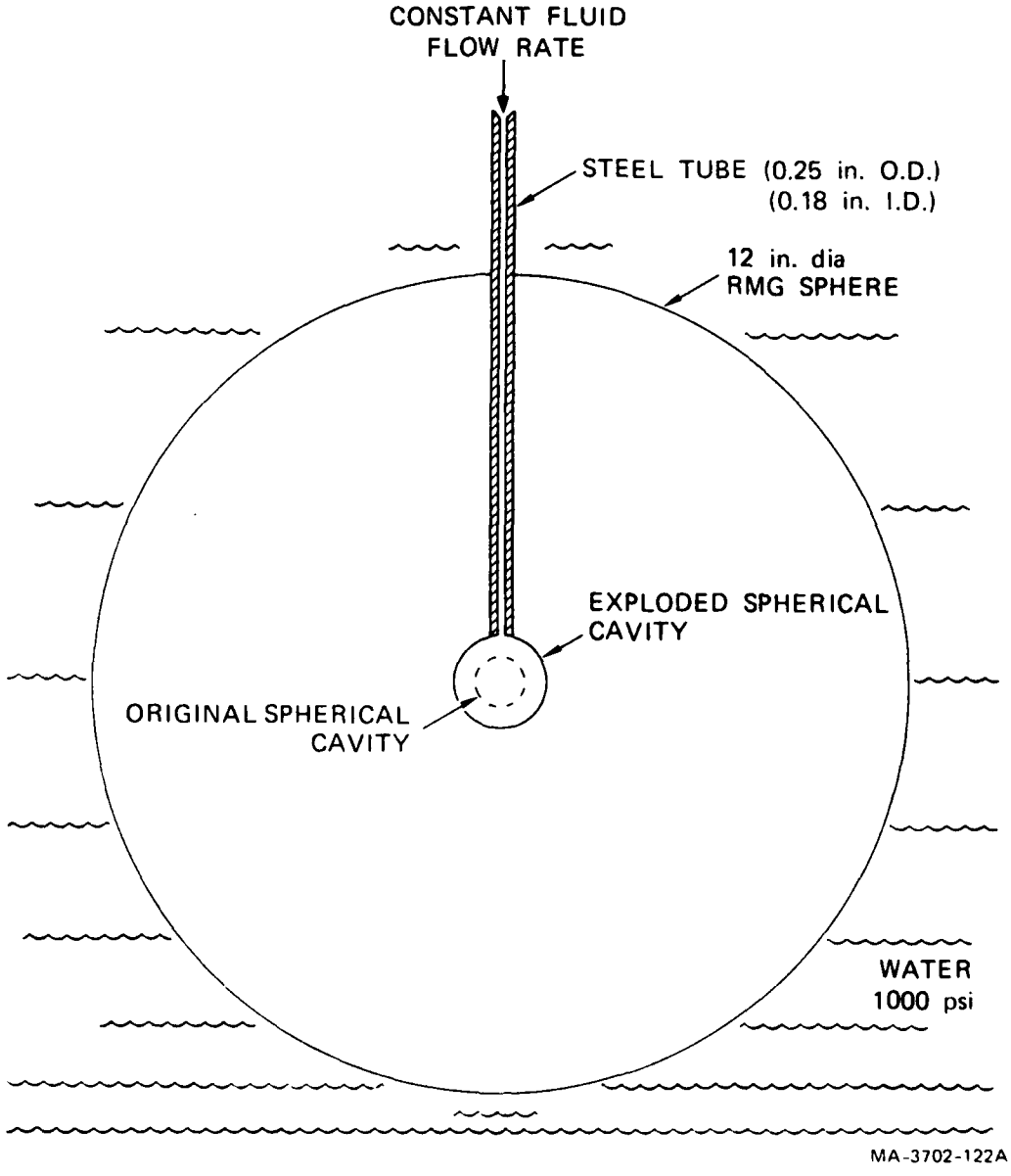

FIGURE 2.12 BASIC CONFIGURATION FOR EXPLODED CAVITY TESTS

of PETN were designed. Figure 2.13 shows one of the 1/2-gram designs. A 9/16-inch-O.D. Lucite* case was used in early tests, but the thicker wall introduced unnecessary inert material. For the 1/4-gram charges, 3/8- and 7/16-inch-O.D. Lucite cases with a 0.308-inch I.D. were designed. Machining of the Lucite produced charge holders with inside diameters slightly different from thsoe specified, and the amount of PETN required to yield a desired explosive density of 1 g/cm^3 was used. Hence, 1/2-gram and 1/4-gram are nominal figures with the actual weight of explosive varying slightly from charge to charge. The charges were assembled by pressing PETN to a density of 1 g/cm^3 into a pair of mating Lucite hemispheres. The bridgewire assembly was then positioned as shown in Figure 2.13 using a notch in one of the hemispheres as a guide, and the hemispheres were snapped together and sealed. Several methods of sealing were investigated, and Homalite,† an epoxy that cures to form a substance similar in properties to acrylic, was found to provide the best protection against intrusion of water from the grout into the charge holder. The charge was positioned by drawing the lead wires through the access tube and adding epoxy to the space between the charge holder and the tube. Venting of the explosive gases was prevented by filling the access tube with epoxy. In later tests a wide-angled ferule was attached near the end of this tube to compress explosively expanding grout and prevent leak paths to the overburden from developing.

The 1/4- and 1/2-gram charges produced exploded cavity diameters of 11/16 and 1 inch, respectively.

*Trade name, Rohm and Haas Corporation.

†Homalite Corporation, Wilmington, Delaware.

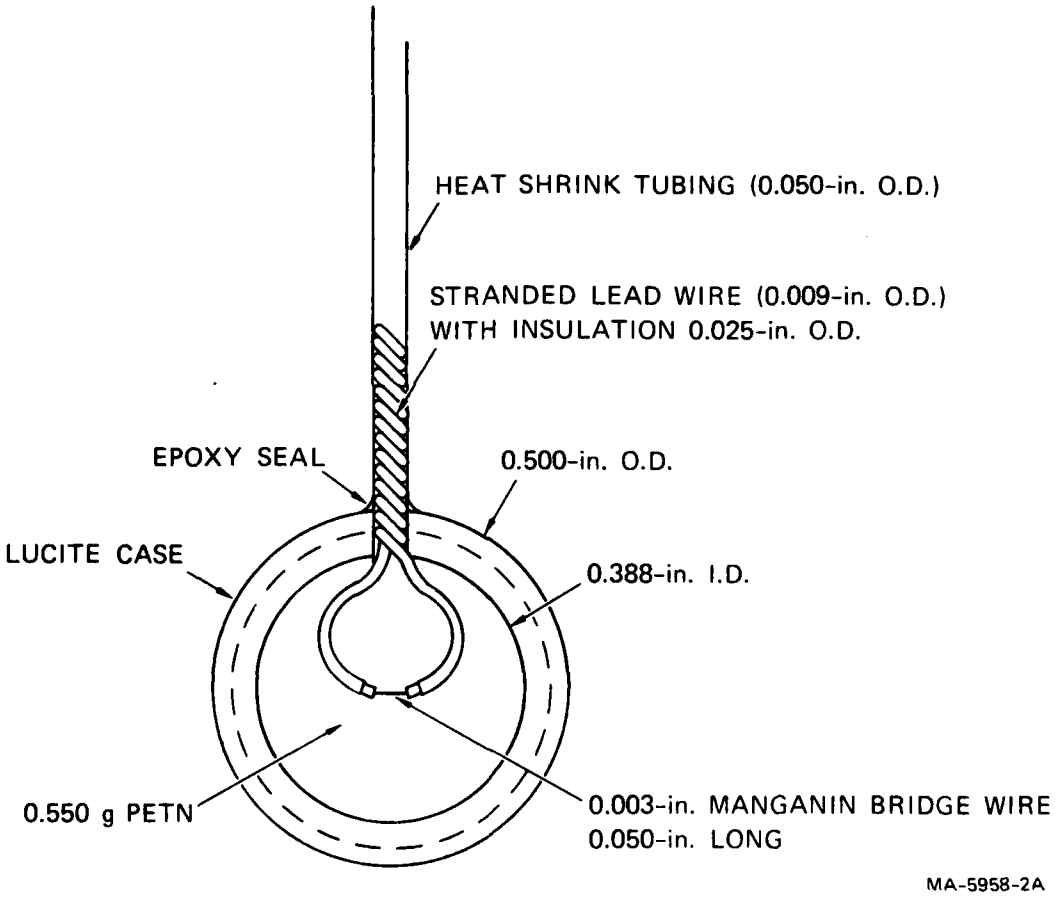

FIGURE 2.13 EXPLOSIVE CHARGE DETAILS

3. EXPERIMENTAL RESULTS

3.1 EXPERIMENTAL SERIES

Table 3.1 summarizes the hydrofracture experiments performed on the 12-inch-diameter spheres. The tests are grouped according to the purpose of the test or the parameter under investigation. Series 1 through 11 are unexploded cavity tests; series 12 through 19 are exploded cavity tests. The reproducibility tests of Series 1 and 12 provide the comparison basis for the following areas of investigation:

- Overburden. In an underground nuclear test, overburden is governed by the depth at which the test is conducted and is typically 1000 psi. Overburden pressure in the range 0-2000 psi was simulated in the laboratory.

- Viscosity. Fluid flow along a fracture surface is related to fluid viscosity, with less viscous fluids producing greater pressure near the crack tip. Hence the dependence of crack growth on fluid pressure gradients was studied by conducting hydrofracture tests with fluids representative of a wide range of viscosities. Dyed glycerol and dyed water, with viscosities of 660 and 1 centipoise, respectively, were chosen.

- Flow rate. During hydrofracture, fluid pressure gradients along a fracture surface are related to the flow rate. The influence of pressure gradients on crack growth was studied by performing hydrofracture tests at the rates of 0.71 and 4.26 cm^3/min.

- Cavity size. Unexploded cavity diameters of 11/16 and 1 inch were chosen since they correspond to exploded cavity diameters produced by 1/4- and 1/2-gram charges of PETN respectively. Additionally, a 2-inch-diameter cavity was selected to provide further data. These sizes simulate an underground test since they closely approximate spherical voids in an infinite medium. Cavity size studies therefore relate to the effect of imperfections in the cavity wall.

Table 3.1

SUMMARY OF CONTAINMENT INVESTIGATIONS
Part A
UNEXPLODED CAVITY EXPERIMENTS

Series	Glycerol (G) or Water (W) Hydrofracture	Overburden Pressure (psi)	Flow Rate (cm^3/min)	Cavity Diameter (in)	Material	Number of Tests	Purpose or Parameter	Observations
1	G	1000	4.26	11/16	2C4	4	Reproducibility	Reasonably reproducible - fracture initiation pressures within 15% of average for each group.
				1	2C4	6		
				1	2C3	4		
				1	GS2	1		
				1	GS3	2		
2	G	60	4.26	1	2C3	1	Overburden (Glycerol)	Fracture initiation pressure increases with overburden using high viscosity fluid.
		500				2		
		1000				4		
		1500				1		
		2050				1		
		1000			2C4	6		
		2000				1		
		2040				1		
3	W	1000	4.26	11/16	2C4	2	Overburden (Water)	Fracture initiation pressure increases with overburden using low viscosity fluid.
		1500				2		
4	G	1000	4.26	11/16	2C4	4	Viscosity	Lower viscosity fluid reduces fracture initiation pressure (2265, 1945 psi).
	W					2		
5	G	1000	4.26	11/16	2C4	4	Flow rate	Slower flow rate reduces fracture initiation pressure (2265, 1780 psi).
			0.71			1		

Table 3.1 (Continued)

SUMMARY OF CONTAINMENT INVESTIGATIONS
Part A
UNEXPLODED CAVITY EXPERIMENTS

Series	Glycerol (G) or Water (W) Hydrofracture	Overburden Pressure (psi)	Flow Rate (cm^3/min)	Cavity Diameter (in)	Material	Number of Tests	Purpose or Parameter	Observations
6	G	1000	4.26	11/16 1 2	2C4 2C3 2C4 2C4	4 4 6 1	Cavity size	Fracture initiation pressure decreases with increasing cavity size.
7	G	1000	4.26	1	2C4 GS2 GS3	6 1 2	Material strength	Fracture initiation pressure increases with increasing material strength (1960 psi for 2C4, 3260 psi for GS3).
8	G	1000	4.26	11/16 1	2C4 GS3/2C4	1 1	Geology	Fracture surface intersects fault plane. Material interface retards crack growth.
9	G	1000	4.26	11/16	2C4	2	Imperfection sensitivity	Cavity imperfections reduce hydrofracture pressures.
10	G	1000	4.26	25/32 1	2C3	3 2	Cavity lining	Cavity lining increases fracture initiation pressure for 1-inch-diameter cavity (2225, 1838 psi).
11	G	1000	4.26	1	2C3	7	Fracture initiation and growth	Spike on pressure record indicates fracture initiation. Crack growth is stable.

Table 3.1 (Concluded)

SUMMARY OF CONTAINMENT INVESTIGATIONS
Part B
EXPLODED CAVITY EXPERIMENTS

Series	Glycerol (G) or Water (W) Hydrofracture	Overburden Pressure (psi)	Flow Rate (cm^3/min)	Charge Size (g)	Material	Number of Tests	Purpose or Parameter	Observations
12	G	1000	4.26	1/4 1/2 1/2	2C4 2C3 2C4	9 3 1	Reproducibility	Reasonably reproducible fracture initiation pressures. Spectrum of hydrofracture records for 1/4 g tests.
13	G	1000 1500	4.26	1/2	2C3	3 1	Overburden	Increase in overburden has no effect on hydrofracture record.
14	G W	1000	4.26	1/4	2C4	9 3	Viscosity	Lower viscosity produces lower and more reproducible hydrofracture pressures.
15	G	1000	4.26 0.71	1/4	2C4	9 3	Flow rate	Slower flow rate produces lower and more reproducible hydrofracture pressures.
16	G	1000	4.26	1/4	2C4	2	Creep	Hydrofracture pressures after 97 hr creep period are at lower end of 1/4 g test spectrum.
17	G	1000	4.26	1/4 1/2	2C4 2C3	2 6	Geology	Fracture surface intersects fault plane. Material interface retards crack growth. Tunnels ruptured by explosion. Nearby cavities have no effect on hydrofracture.
18	G	1000	4.26	1/2	2C3	4	Cavity lining	Insoluble dye lines cavity and raises pressures.
19	G	1000	4.26	1/2	2C3	4	Fracture initiation and growth	Spike on pressure record indicates fracture initiation. Crack growth is unstable.

- Material strength. Four different materials were used in casting the spheres: two similar rock-matching grouts 2C3 and 2C4 and two similar granite simulants GS2 and GS3. The grouts closely match the tuff surrounding a cavity in a nuclear test, and the stronger granite simulants provide data relating fracture initiation and growth to material strength.

- Geology. Natural man-made features in the vicinity of a test cavity may significantly influence containment. Simulation of a fault plane was achieved by casting a Mylar sheet in a rock-matching grout sphere. A material interface was formed by casting a composite sphere of rock-matching grout and granite simulant. Experiments were performed with tunnels and cavities cast at various distances from the explosive charge to provide data relating to tunnel closure, release of cavity gases to nearby structures, and the influence of these structures on fracture initiation and growth.

- Creep. If material relaxation occurs, the explosively formed residual stress field surrounding an exploded cavity would be degraded. Laboratory creep tests of 17- and 97-hour duration were conducted to study the significance of relaxation in rock-matching grout.

- Imperfection sensitivity. Imperfections in a cavity wall probably reduce fracture initiation pressure. They may also determine the number and orientation of the cracks that form. Unexploded cavity experiments without wire hoops embedded in the cavity wall provided comparison data for the effects of imperfections.

- Cavity lining. Experiments in which porous flow is restricted by lining the cavity walls with an impermeable material provide data relating fracture initiation and growth to the pressure in pores and to the pressure distribution along cracks. Glass lining was used in several unexploded cavity tests; however, the glass cracked early in the hydrofracture process and allowed a restricted but unknown amount of fluid to flow into the surrounding material. A second method of restricting flow was the use of an insoluble dye that filtered out of the hydrofracture fluid at the surface of the cavity and along the fracture surface.

- Fracture initiation and growth. The physical occurrences associated with points on a pressure record were studied by performing tests in which the hydrofracture process was terminated at various stages of development. This type of testing is suitable for studying fracture initiation and the subsequent rate of crack growth.

3.2 UNEXPLODED CAVITY TESTS

Series 1 - Reproducibility

Before a meaningful parametric investigation can be performed, experimental reproducibility must be demonstrated. Reproducibility testing included glycerol and water hydrofracture, 11/16- and 1-inch-diameter cavities, and spheres of rock matching grout and granite simulant. In these tests external pressure was fixed at 1000 psi since this represents the hydrostatic pressure in nuclear tests typically conducted at a depth of 1100 feet in tuff with a density of 2.1 g/cm^3.

Pressure records for hydrofracture Tests 73, 75, 83, and 84, performed on RMG 2C4 spheres with an 11/16-inch-diameter cavity, are shown in Figure 3.1. Dyed glycerol was pumped into the cavities at the rate of 4.26 cm^3/min. The results are typical of unexploded cavity tests in that pressure increased smoothly and rapidly to a well-defined peak, dropped sharply, and finally decayed slowly to a value well above overburden. Peak cavity pressures, which are a measure of reproducibility, were 2060, 2110, 2420, and 2470 psi, with an average of 2265 psi. Maximum deviation from this average is 9%. The fracture initiation tests of Series 11 reveal that the pronounced pressure spike represents initiation of a macroscopic crack, with the subsequent sharp pressure drop indicating crack propagation. Further testing is required, however, to firmly establish the rate of crack growth and the volume of fluid required to propagate a crack to the surface of the sphere.

After each hydrofracture test, release of internal pressure was followed by release of overburden. The sphere was removed from the pressure vessel, and in each case the extent of visible surface cracking was approximately half the circumference. The sphere was tapped apart with a broad chisel revealing a partially dyed fracture plane as shown in Figure 3.2 for Test 84.

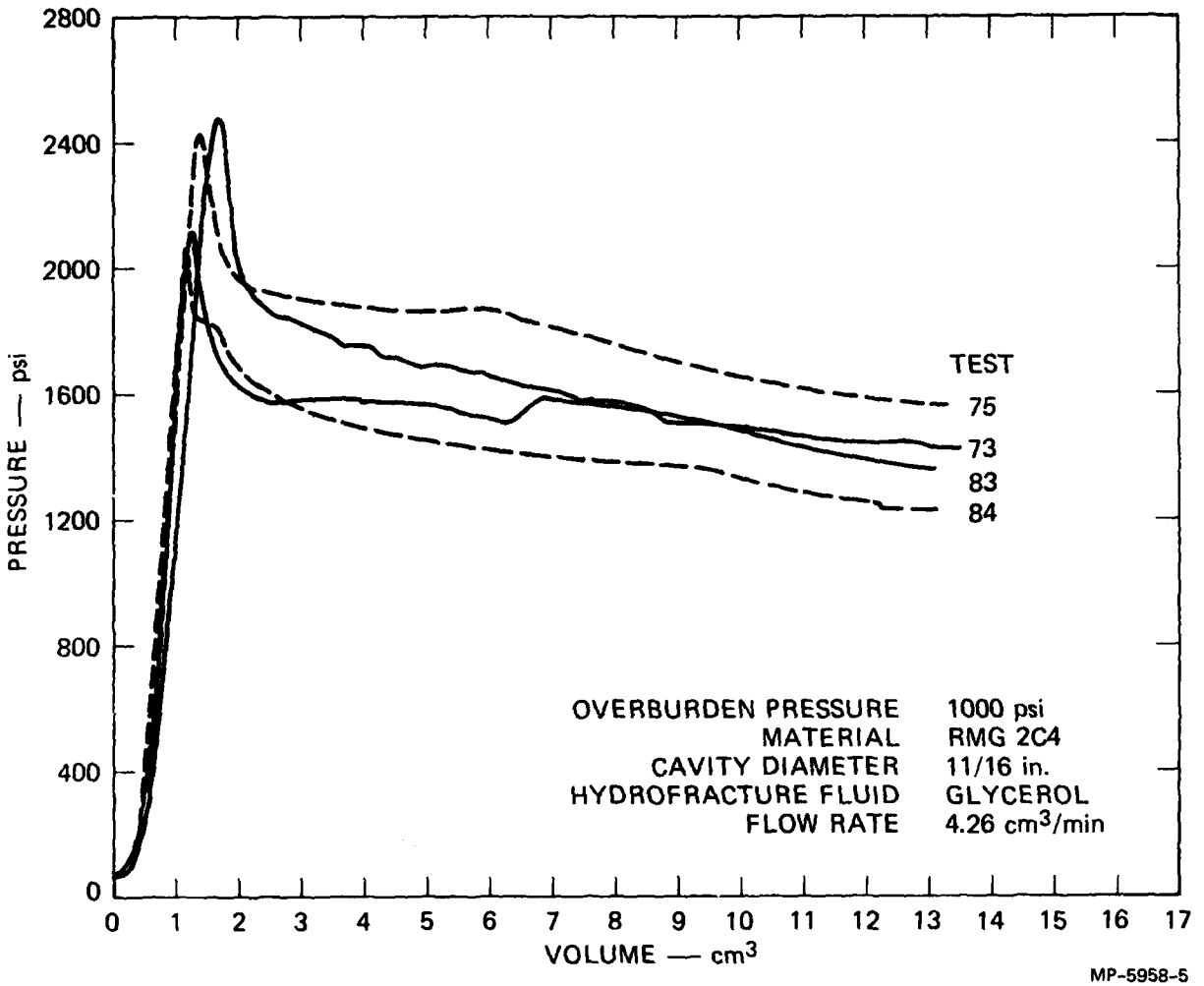

FIGURE 3.1 HYDROFRACTURE PRESSURES FOR UNEXPLODED CAVITY TESTS 73, 75, 83, AND 84—REPRODUCIBILITY

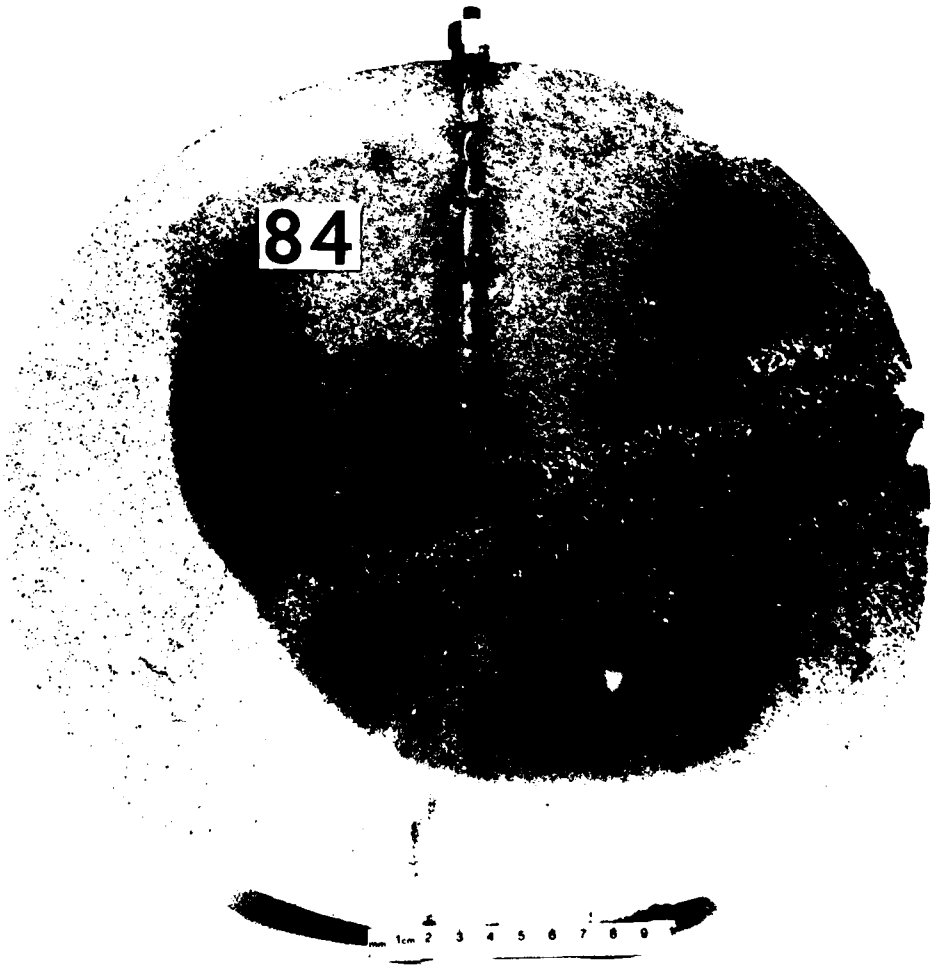

FIGURE 3.2 HYDROFRACTURE FROM UNEXPLODED CAVITY TEST 84

The orientation of the fractured surface was determined by the wire cage used in casting the cavity. This observation applies, in general, to all tests using the wire cage: Tests of Series 1 through 8 as well as Tests 30 and 31 of Series 11.

Similar reproducibility tests were performed on spheres with a 1-inch-diameter cavity. Hydrofracture records for Tests 55, 65, and 66 are shown in Figure 3.3, and records for Tests 56, 59, and 60 are shown in Figure 3.4. The results are again typical except that the latter group exhibits a gradual increase in pressure following the pressure spike. This pressure rise suggests increasing resistance to crack growth and/or increasing resistance to flow along an existing crack. The extent of surface cracking in the six tests ranges from 60 degrees in Test 59 to 240 degrees in Test 65. The pressure records show that after 11 cm^3 of flow the highest and lowest cavity pressures, 1610 and 1180 psi, occurred in Tests 59 and 65, respectively. Hence there is a correspondence here between cavity pressure and the extent of the sectorial crack in the fracture plane. Peak pressures for the six tests were 1720, 1770, 1890, 1980, 2160, and 2240 psi with an average of 1960 psi. Maximum deviation from this average is 14%.

A third group of reproducibility tests was performed on RMG 2C3 spheres with a 1-inch-diameter cavity. Hydrofracture records for Tests 19 through 22 are shown in Figure 3.5. Fracture initiation pressures were 1650, 1750, 1950, and 2000 psi with an average of 1838 psi. Maximum deviation from this average is 10%. The extent of dye penetration along the fracture plane is similar to that shown in Figure 3.2.

A fourth group of tests was performed on spheres of the modified granite simulants GS2 and GS3 having a 1-inch-diameter cavity. Use of these stronger materials resulted in the substantially greater fracture initiation pressures of 3100, 3420, and 3520 psi as shown by the hydrofracture records for Tests 49, 71, and 72 in Figure 3.6. Maximum deviation from the average value of 3347 psi is 7%. With volume measured from the pressure spike, the hydrofracture records for the three tests show that

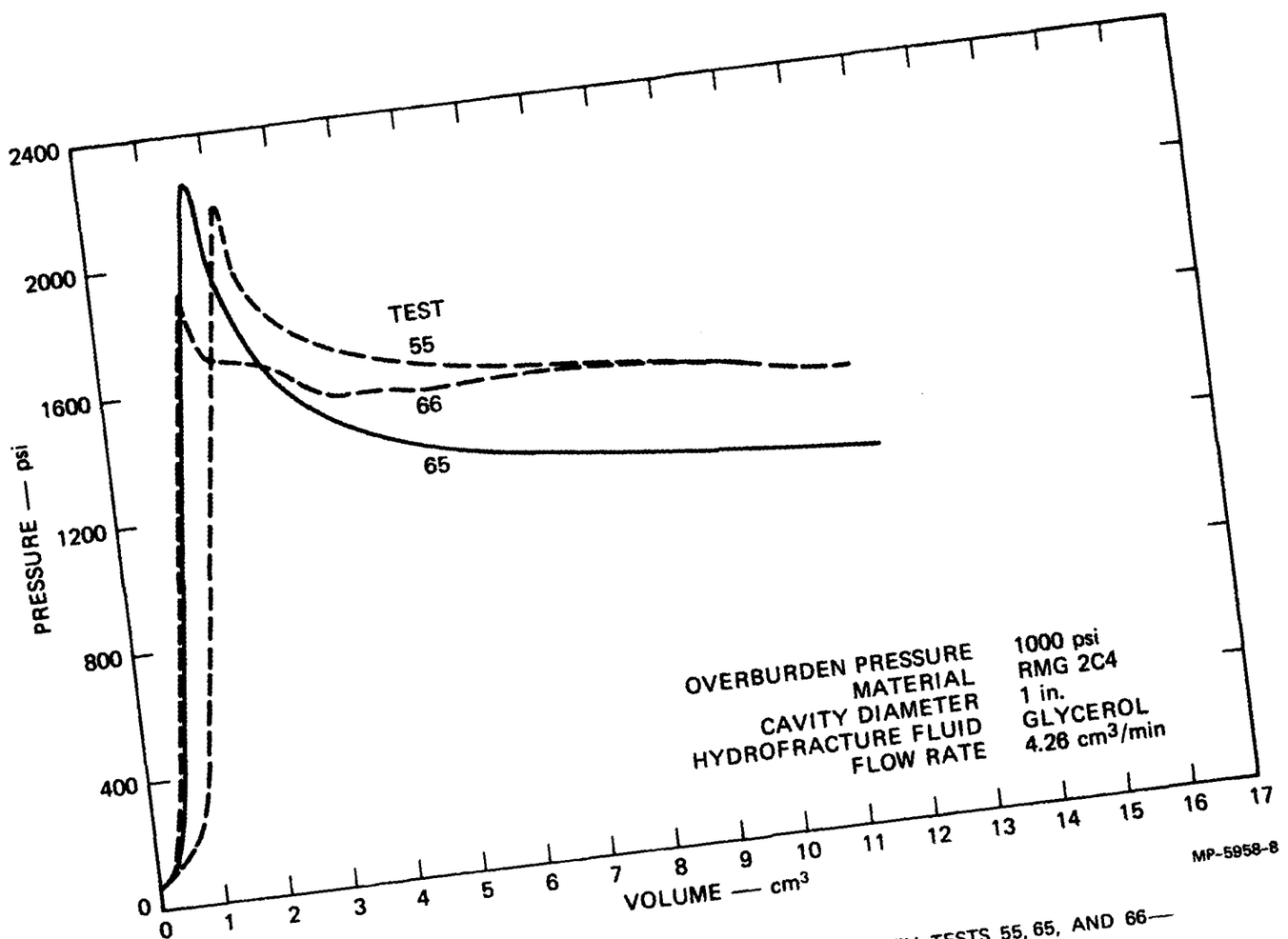

FIGURE 3.3 HYDROFRACTURE PRESSURES FOR UNEXPLODED CAVITY TESTS 55, 65, AND 66—REPRODUCIBILITY

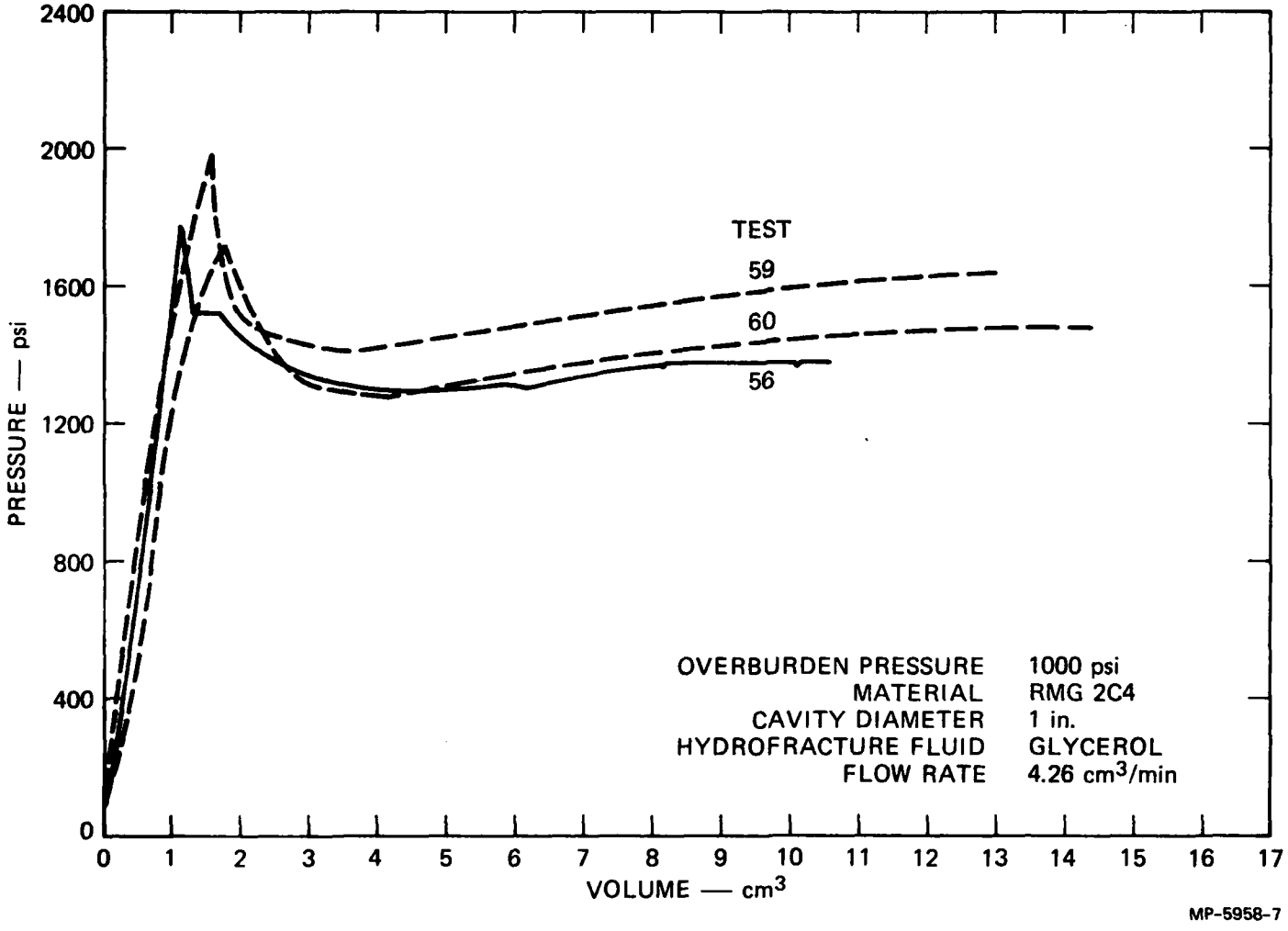

FIGURE 3.4 HYDROFRACTURE PRESSURES FOR UNEXPLODED CAVITY TESTS 56, 59, AND 60—REPRODUCIBILITY

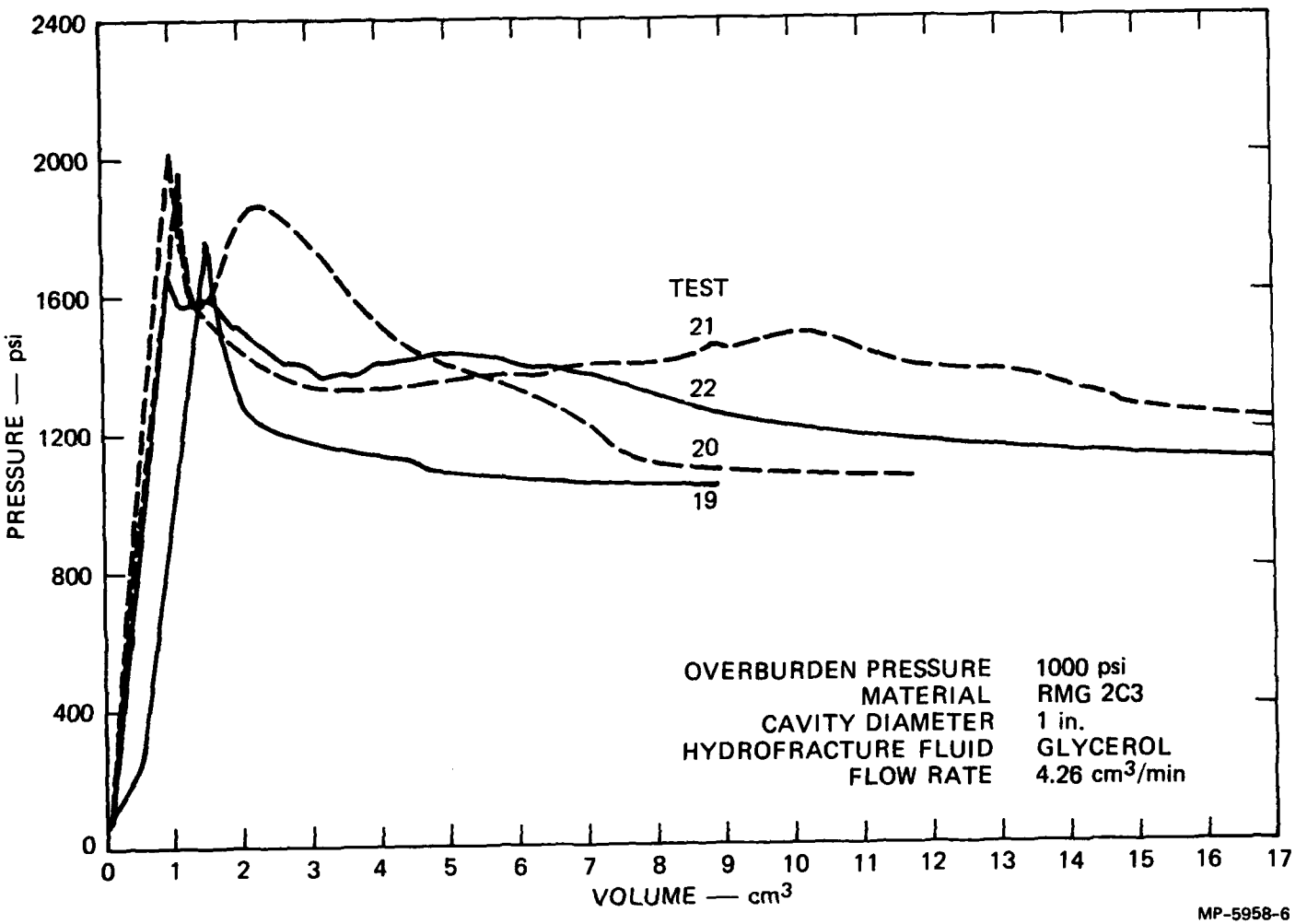

FIGURE 3.5 HYDROFRACTURE PRESSURES FOR UNEXPLODED CAVITY TESTS 19, 20, 21, AND 22 — REPRODUCIBILITY

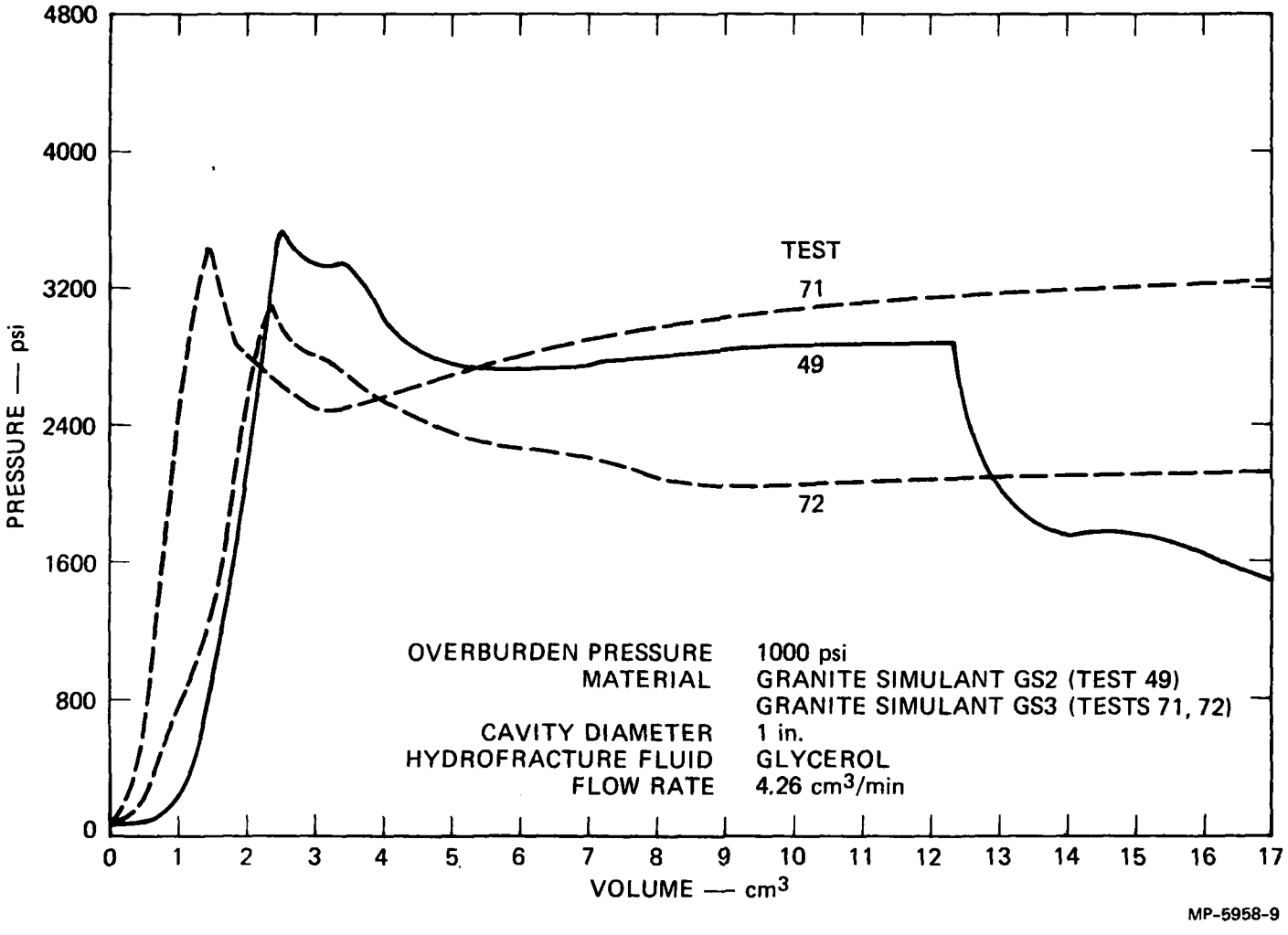

FIGURE 3.6 HYDROFRACTURE PRESSURES FOR UNEXPLODED CAVITY TESTS 49, 71, AND 72 — REPRODUCIBILITY

9 cm^3 of pump displacement resulted in a range of cavity pressures from 2120 to 3150 psi. The fracture pattern for Tests 49 and 71 at the upper end of this range consists of two distinct fracture planes, resulting in the three-piece sphere shown in Figure 3.7. The fracture pattern for Test 72 at the bottom of the range is the typical single plane of fracture, resulting in two hemispherical pieces. Also, a surface crack extending nearly 360 degrees resulted from hydrofracture in Test 72, a result associated with low cavity pressure in a fractured sphere.

Summarizing, average fracture initiation pressure for a sphere with a 1-inch-diameter cavity was 1838 psi for RMG 2C3, 1960 psi for RMG 2C4, and 3347 psi for the granite simulants. For an 11/16-inch cavity the average was 2265 psi for RMG 2C4. Also, high cavity pressures late in the hydrofracture process indicate a small sectorial crack or the development of multiple fractures planes.

Series 2 - Overburden (Glycerol)

Tests with external pressure ranging from 60 to 2050 psi were performed on RMG 2C3 spheres with a 1-inch-diameter cavity. Hydrofracturing was performed by pumping dyed glycerol into the cavities at the rate of 4.26 cm^3/min. Results reveal an increase in fracture initiation pressure with increased overburden as shown in Figure 3.8. Further benefit of overburden to containment is shown by the difference between peak cavity pressure and overburden: 520 psi for Test 41 performed at 60 psi overburden, 740 and 780 psi for Tests 37 and 34 at 500 psi, 750 psi for Test 19 at 1000 psi, 940 psi for Test 38 at 1500 psi, and 1480 psi for Test 46 at 2050 psi. Hence, in general, an increase in overburden results in an even greater increase in the cavity breakdown pressure.

Overburden tests also represent a possible source of data for establishing a fracture criterion. Figure 3.9 shows the pressure required to initiate fracture for the unexploded cavity tests described in Table 3.1. The overburden tests described above are indicated by the symbol □. For a given overburden, cavity pressures that yield zero tangential stress and

MP-5958-44

FIGURE 3.7 HYDROFRACTURE FROM UNEXPLODED CAVITY TEST 71

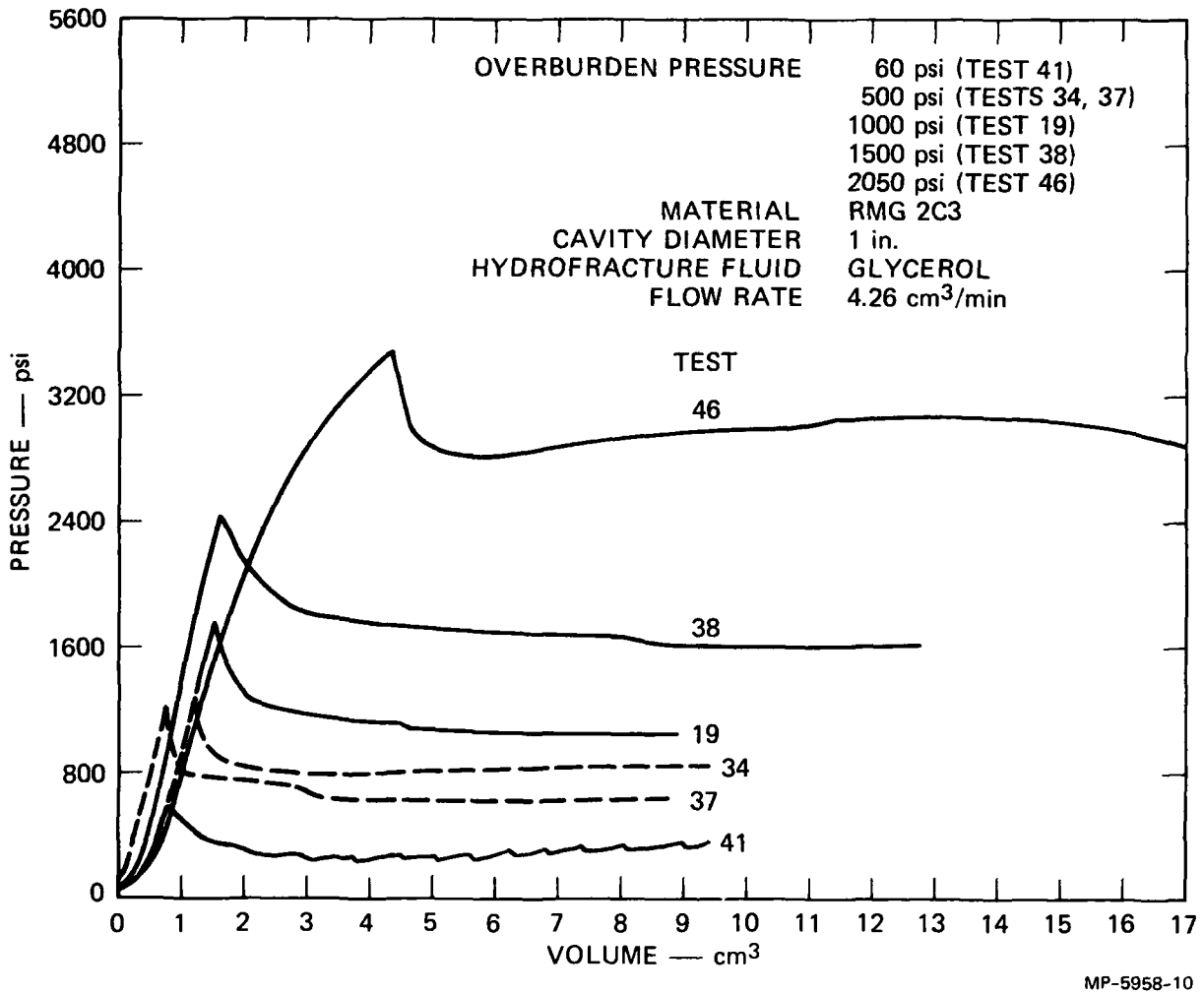

FIGURE 3.8 HYDROFRACTURE PRESSURES FOR UNEXPLODED CAVITY TESTS 19, 34, 37, 38, 41, AND 46 — OVERBURDEN EFFECT

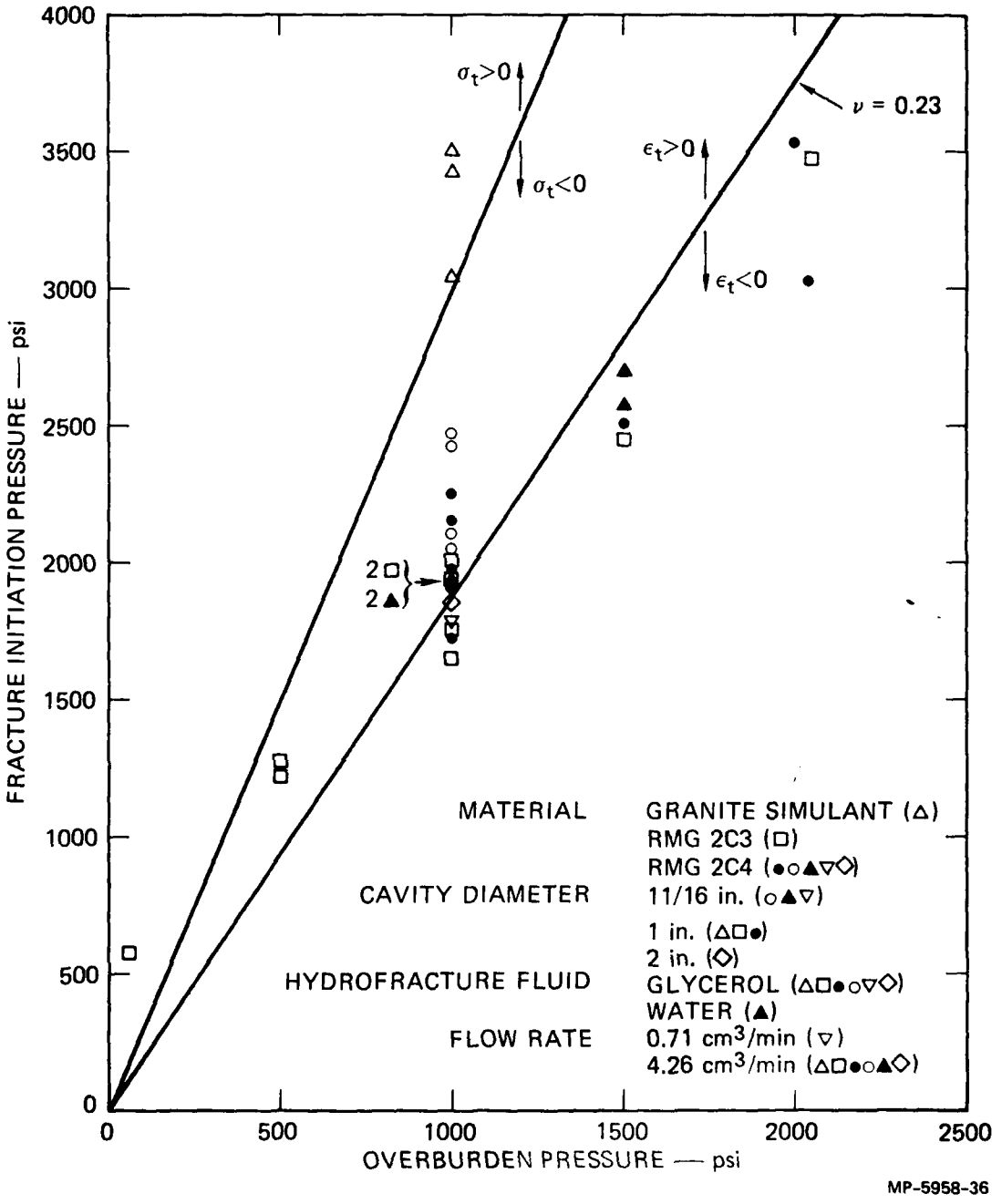

FIGURE 3.9 FRACTURE INITIATION PRESSURE VERSUS OVERBURDEN PRESSURE FOR UNEXPLODED CAVITIES

strain at the wall of a cavity in an infinite medium lie along the paths shown in the figure. A zero tangential stress criterion is seen to be conservative only for overburden pressures well above 1000 psi. Zero tangential strain was determined for a Poisson's ratio (ν) of 0.23, which is a typical value for the materials tested.

Similar tests with external pressure ranging from 1000 to 2040 psi were performed on RMG 2C4 spheres. Fracture initiation pressure again increased with increasing overburden, as shown in Figure 3.10. Also, the difference between peak cavity pressure and overburden again showed a general increase as external pressure increased: 980 psi for Test 59 performed at 1000 psi, 1000 psi for Test 82 at 1500 psi, 1520 psi for Test 91 at 2000 psi, and 880 psi for Test 90 at 2040 psi. These tests are indicated by the symbol ● on Figure 3.9. The zero tangential strain criterion for fracture initiation is again seen to be conservative only for external pressures well above 1000 psi.

Series 3 - Overburden (Water)

A second series of overburden tests was performed on RMG 2C4 spheres with an 11/16-inch cavity. Hydrofracturing was performed with dyed water pumped at the rate of 4.26 cm^3/min. The pressure records shown in Figure 3.11 reveal excellent reproducibility for the two overburden pressures tested. Differences between fracture initiation pressure and overburden followed the pattern of the previous series of overburden tests and increased with increasing external pressure: 940 and 950 psi for Tests 93 and 94 performed at 1000 psi and 1080 and 1200 psi for Tests 106 and 107 performed at 1500 psi. Results of these four tests, indicated by the symbol ▲ in Figure 3.9, follow the zero tangential strain criterion for cavity breakdown more closely than any other series of tests.

Tests 95 and 96 were additional 1500 psi overburden tests in this series. The hydrofracture records, shown in Figure 3.12, do not show the general decay of pressure following the pressure spike that is typical of unexploded cavity tests. Furthermore, the 1880 and 1900 psi fracture

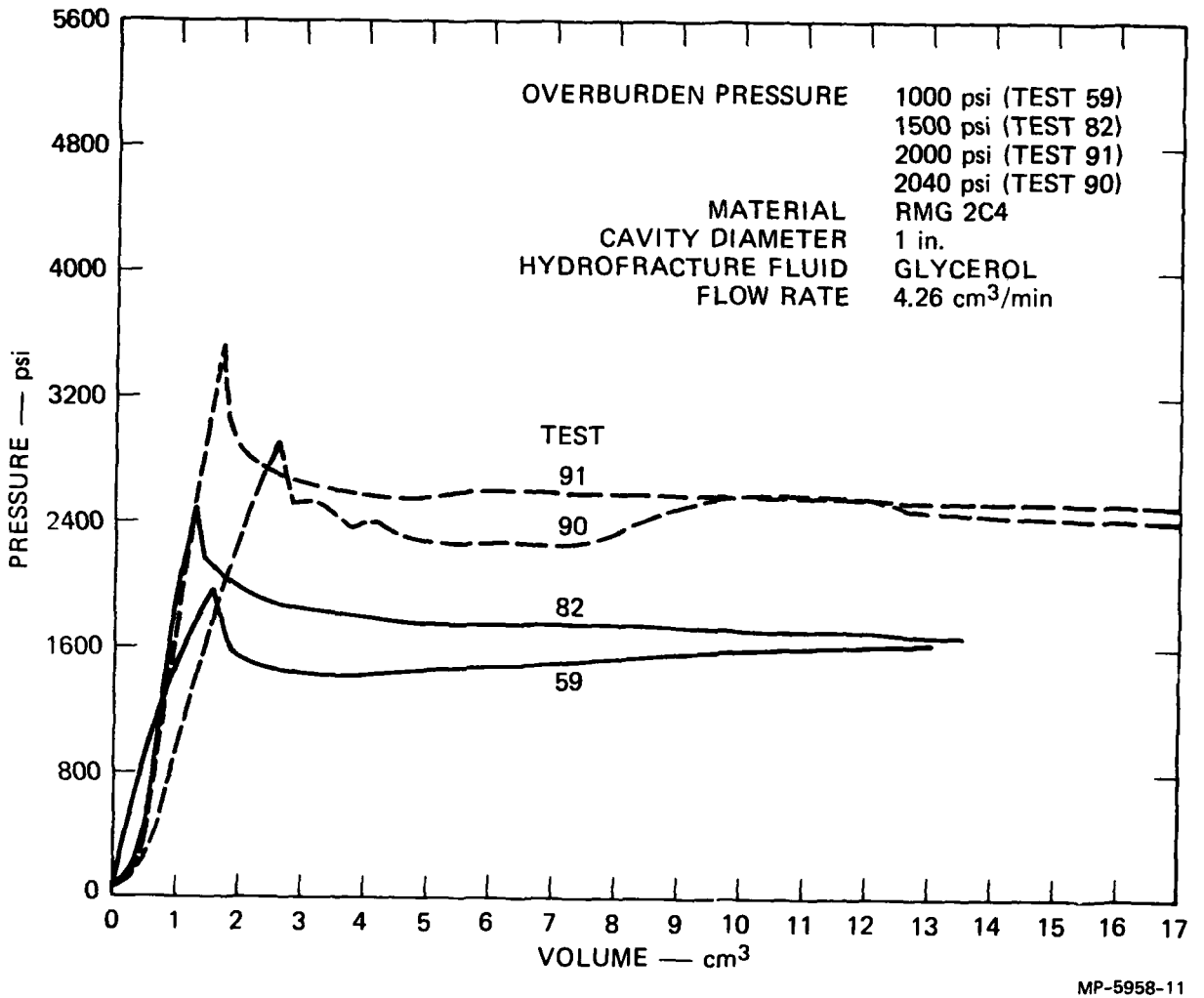

FIGURE 3.10 HYDROFRACTURE PRESSURES FOR UNEXPLODED CAVITY TESTS 59, 82, 90, AND 91— OVERBURDEN EFFECT

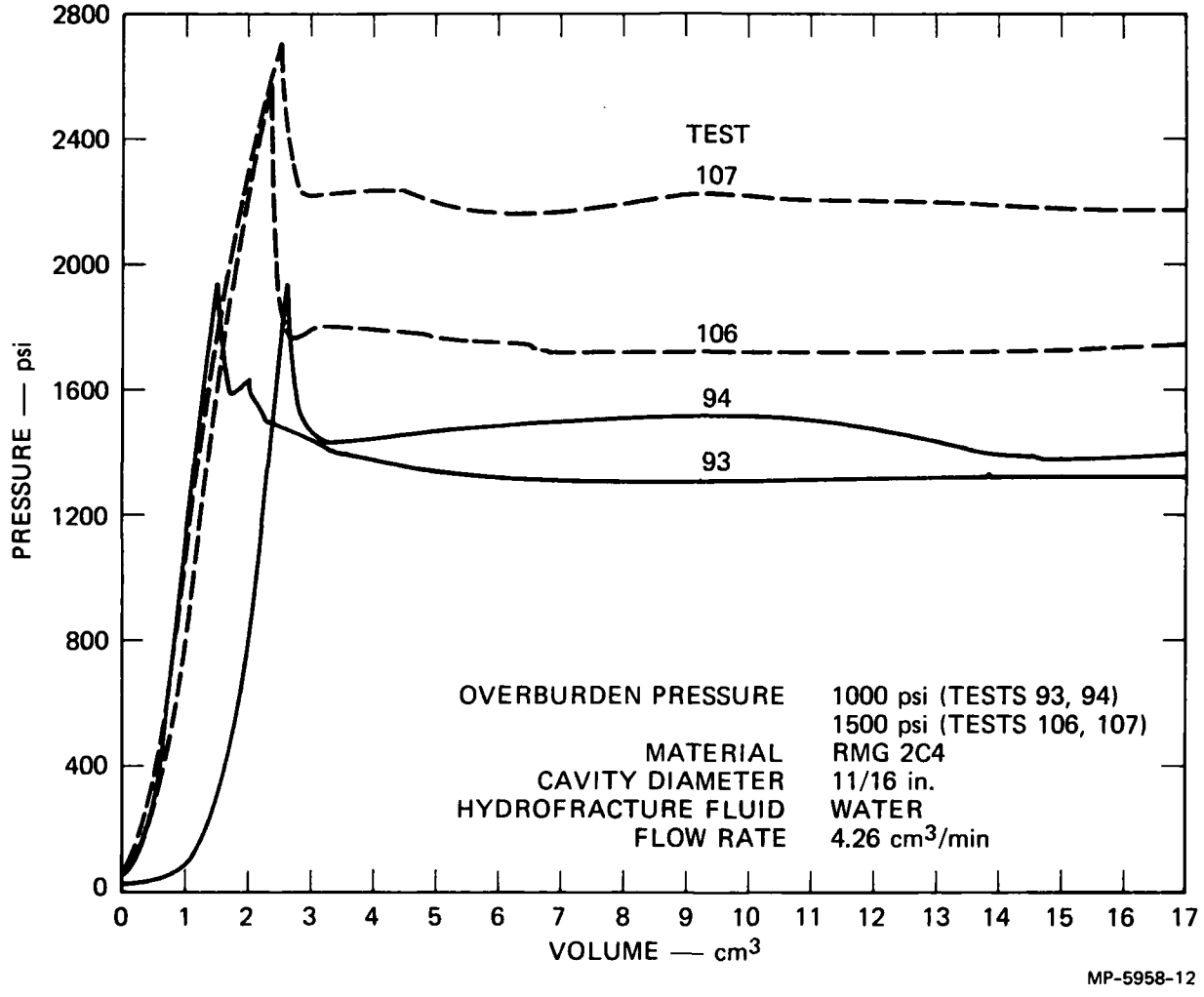

FIGURE 3.11 HYDROFRACTURE PRESSURES FOR UNEXPLODED CAVITY TESTS 93, 94, 106, AND 107—OVERBURDEN EFFECT

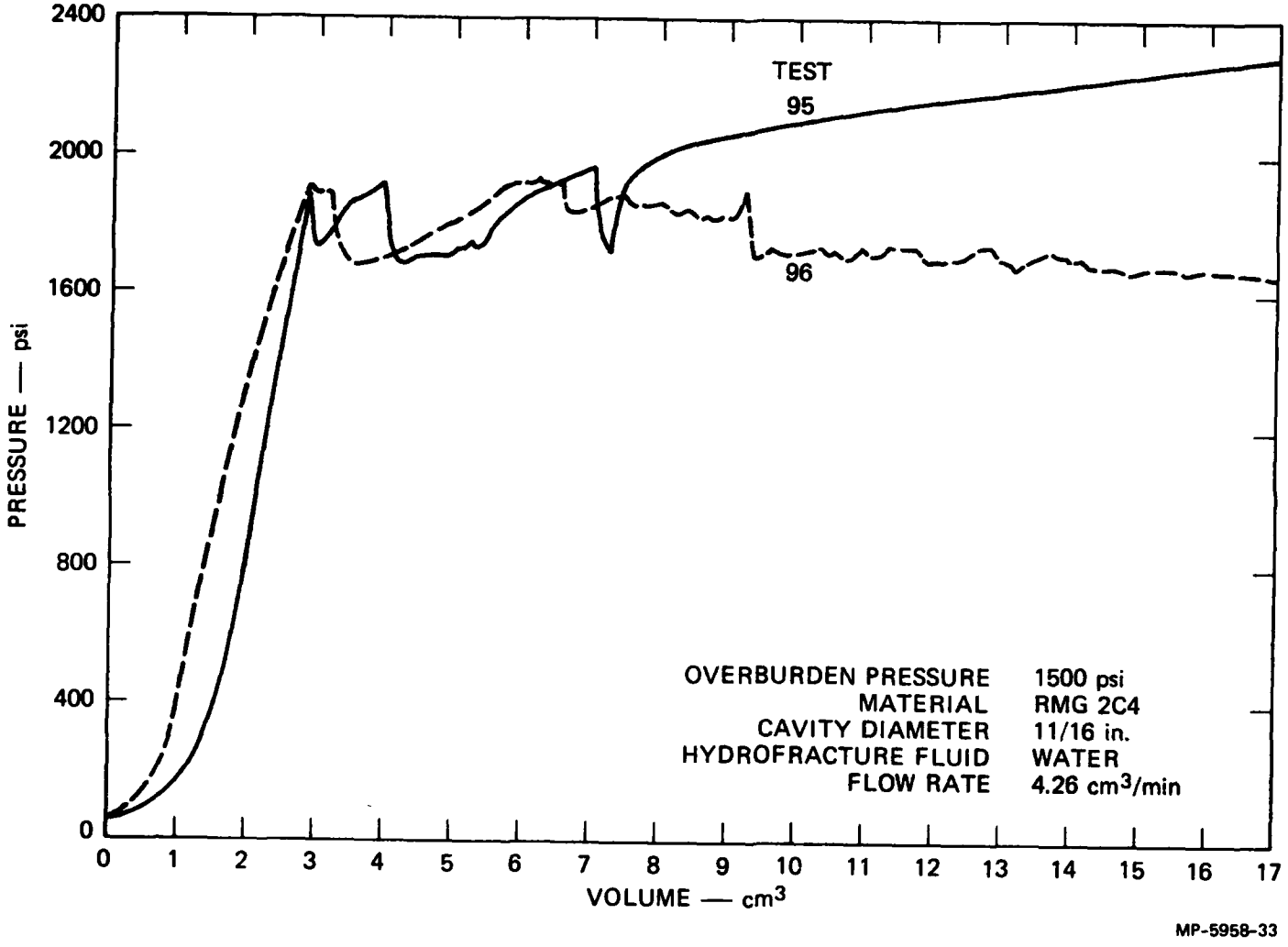

FIGURE 3.12 HYDROFRACTURE PRESSURES FOR UNEXPLODED CAVITY TESTS 95 AND 96—OVERBURDEN EFFECT

initiation pressures are less than the breakdown pressures for the 1000 psi overburden tests. The unusual pressure records reflect the fracture patterns developed. Figure 3.13 shows a horizontal cross section of the sphere used in Test 95. The small dyed areas result from vertical filaments of dyed water that extend throughout the grout. Since the mechanism producing this unusual mode of fracture is unknown, the tests point out the value of extensive reproducibility testing.

Series 4 - Viscosity

Pressure records for tests involving hydrofracture fluids of different viscosity are shown in Figure 3.14. The spheres were RMG 2C4 with an 11/16-inch-diameter cavity. External pressure was 1000 psi and the flow rate was 4.26 cm^3/min. Fracture was initiated in water hydrofracture Tests 93 and 94 at 1950 and 1940 psi. Dyed water viscosity was 1 centipoise. Fracture was initiated in glycerol hydrofracture Tests 75 and 84 at 2420 and 2060 psi. Dyed glycerol viscosity was 660 centipoise. Hence, increased fluid viscosity raises the fracture initiation pressure. However, after pressure gradients from cavity to overburden have stabilized, average cavity pressures for the two groups of tests are the same (Figure 3.14).

Cracking of the spheres by hydrofracture was less extensive with water than with glycerol. Figure 3.15 for Test 93 and Figure 3.2 for Test 84 show typical results. The less viscous fluid thus requires a smaller fractured area to accommodate the imposed volumetric flow rate and pressure gradient.

Series 5 - Flow Rate

Hydrofracture Test 103 was performed on a RMG 2C4 sphere with an 11/16-inch-diameter cavity. Dyed glycerol was pumped into the cavity at the rate of 0.71 cm^3/min. The pressure record is shown in Figure 3.16. For comparison, hydrofracture results for Tests 75 and 84, conducted at a six times greater flow rate of 4.26 cm^3/min, are also shown. The increase in flow rate raised fracture initiation pressure from 1780 psi to an average of 2265 psi. Cavity breakdown may be preceded by the formation of microcracks, which coalesce to form a major fracture plane. Evidence of such

MP-5958-45

FIGURE 3.13 HYDROFRACTURE FROM UNEXPLODED CAVITY TEST 95

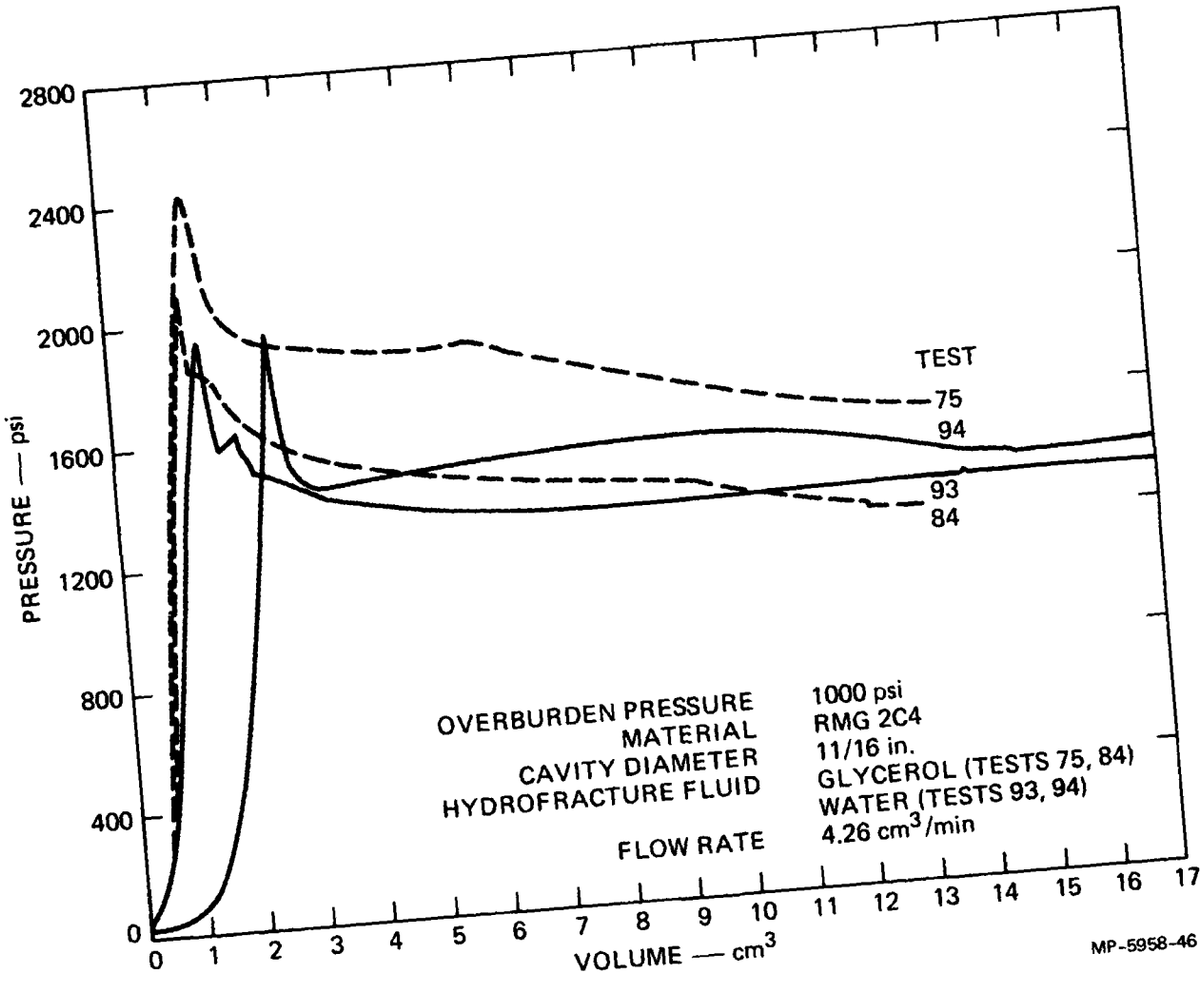

FIGURE 3.14 HYDROFRACTURE PRESSURES FOR UNEXPLODED CAVITY TESTS 75, 84, 93, AND 94—VISCOSITY EFFECT

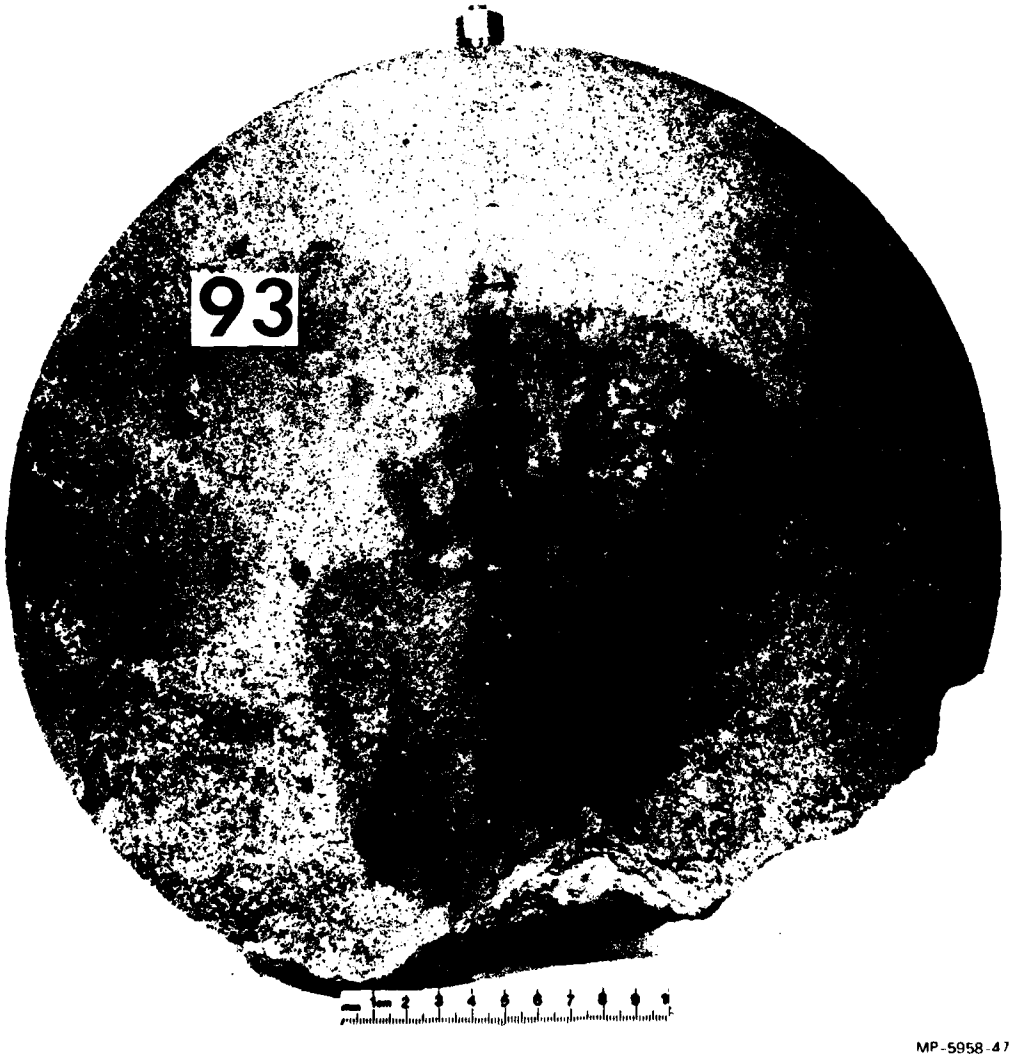

FIGURE 3.15 HYDROFRACTURE FROM UNEXPLODED CAVITY TEST 93

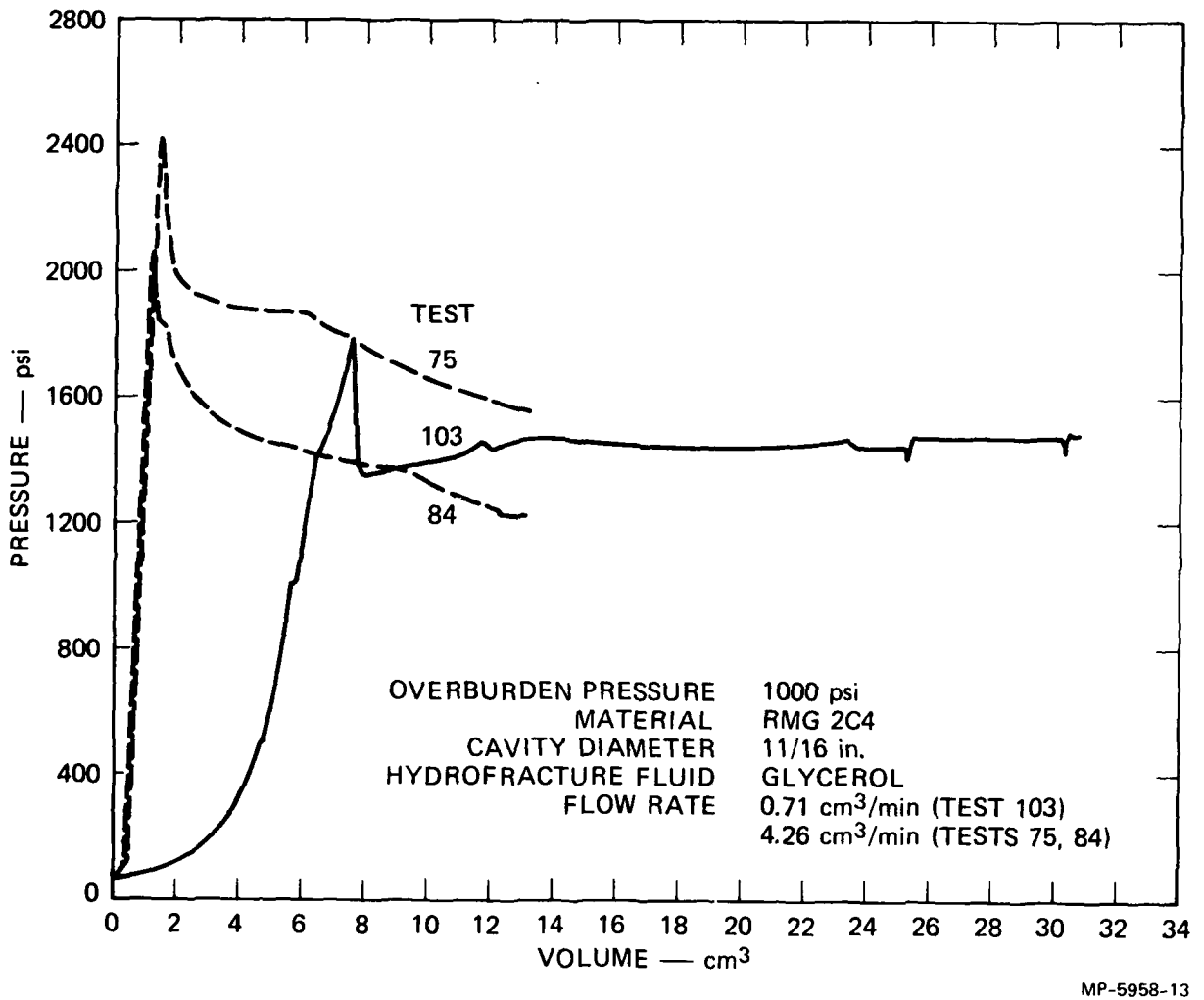

FIGURE 3.16 HYDROFRACTURE PRESSURES FOR UNEXPLODED CAVITY TESTS 75, 84, AND 103 — FLOW RATE EFFECT

microcracking is seen in Figure 3.16 where the smooth pressure rise of Test 103 is interrupted several times.

Figure 3.16 shows the quantity of fluid required to initiate fracture to be seven times greater at the slower flow rate. However, since calculations have shown that loss of fluid due to porous flow is negligible in these tests, this apparent increase is attributed to the compression of air trapped in the system.

Series 6 - Cavity Size

Results of hydrofracture tests on RMG 2C4 spheres with cavities of various diameter are shown in Figures 3.17 and 3.18. In all cases dyed glycerol was pumped into the cavities at a rate of 4.26 cm^3/min. Figure 3.17 shows complete pressure records for the 11/16-inch cavity Tests 75 and 84, the 1-inch cavity Tests 60 and 65, and the 2-inch cavity Test 92. Results of additional 11/16- and 1-inch cavity tests are shown in Figures 3.1, 3.3, and 3.4.

In Figure 3.18 fracture initiation pressures for all cavity size tests are plotted against the ratio of cavity to sphere radius. The average of these breakdown pressures decreases as cavity size increases: 2265, 1960, and 1850 psi for 11/16-, 1-, and 2-inch diameters, respectively. Figure 3.9 shows that a zero tangential strain criterion predicts fracture initiation most accurately for the 2-inch cavity test. However, for given internal and external pressures, static stress analyses indicate that, as cavity size varies, changes in the state of strain at the cavity wall are negligible. Hence, lower breakdown pressure for a larger cavity may be a statistical problem involving the number of flaws in a cavity wall.

Series 7 - Material Strength

Effects of material strength on containment can be seen by comparing hydrofracture results obtained using rock-matching grout and granite simulant. Material properties are shown in Figures 2.4 through 2.10. Pressure records are shown in Figures 3.3 through 3.6. The results of these

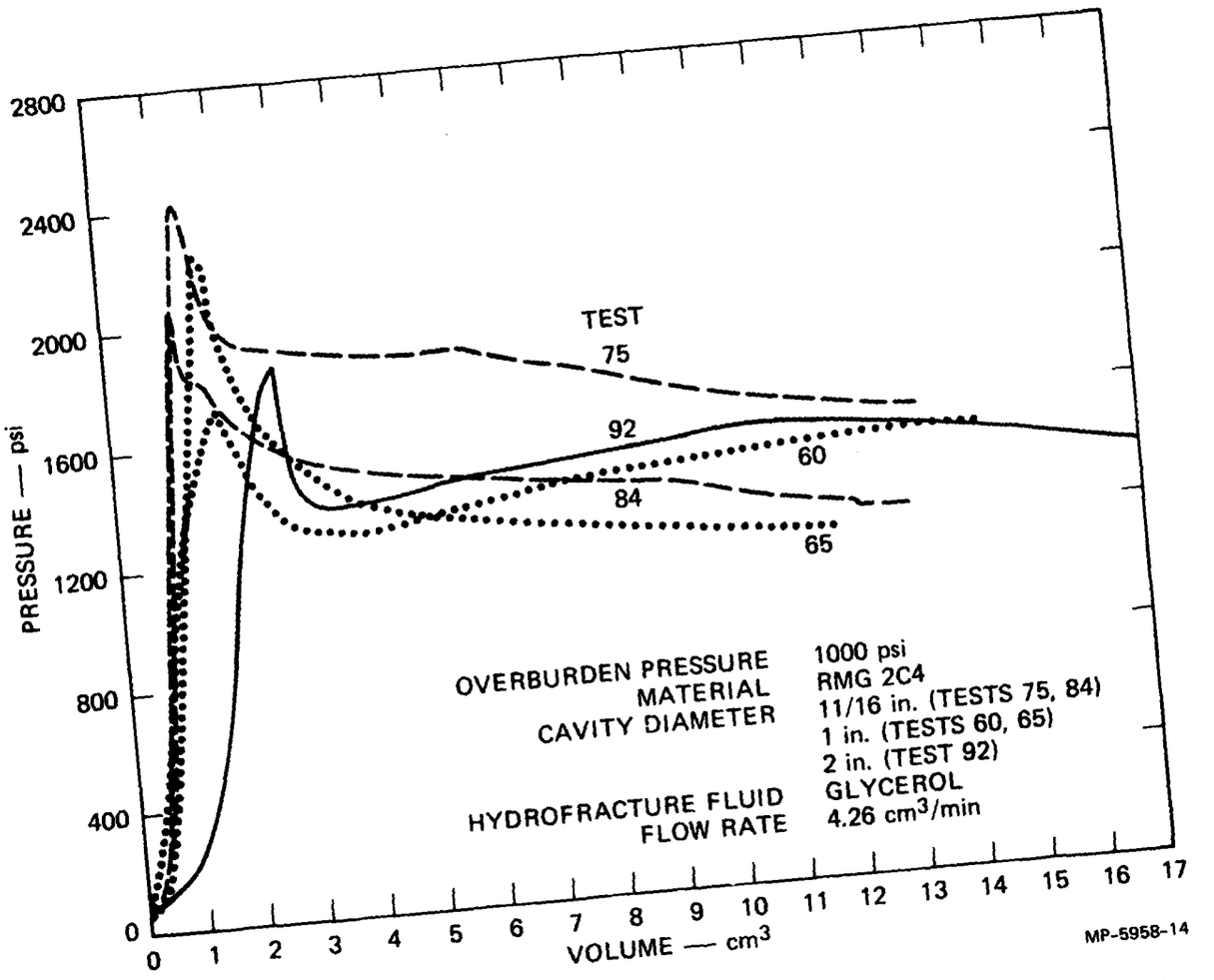

FIGURE 3.17 HYDROFRACTURE PRESSURES FOR UNEXPLODED CAVITY TESTS 60, 65, 75, 84, AND 92 — CAVITY SIZE EFFECT

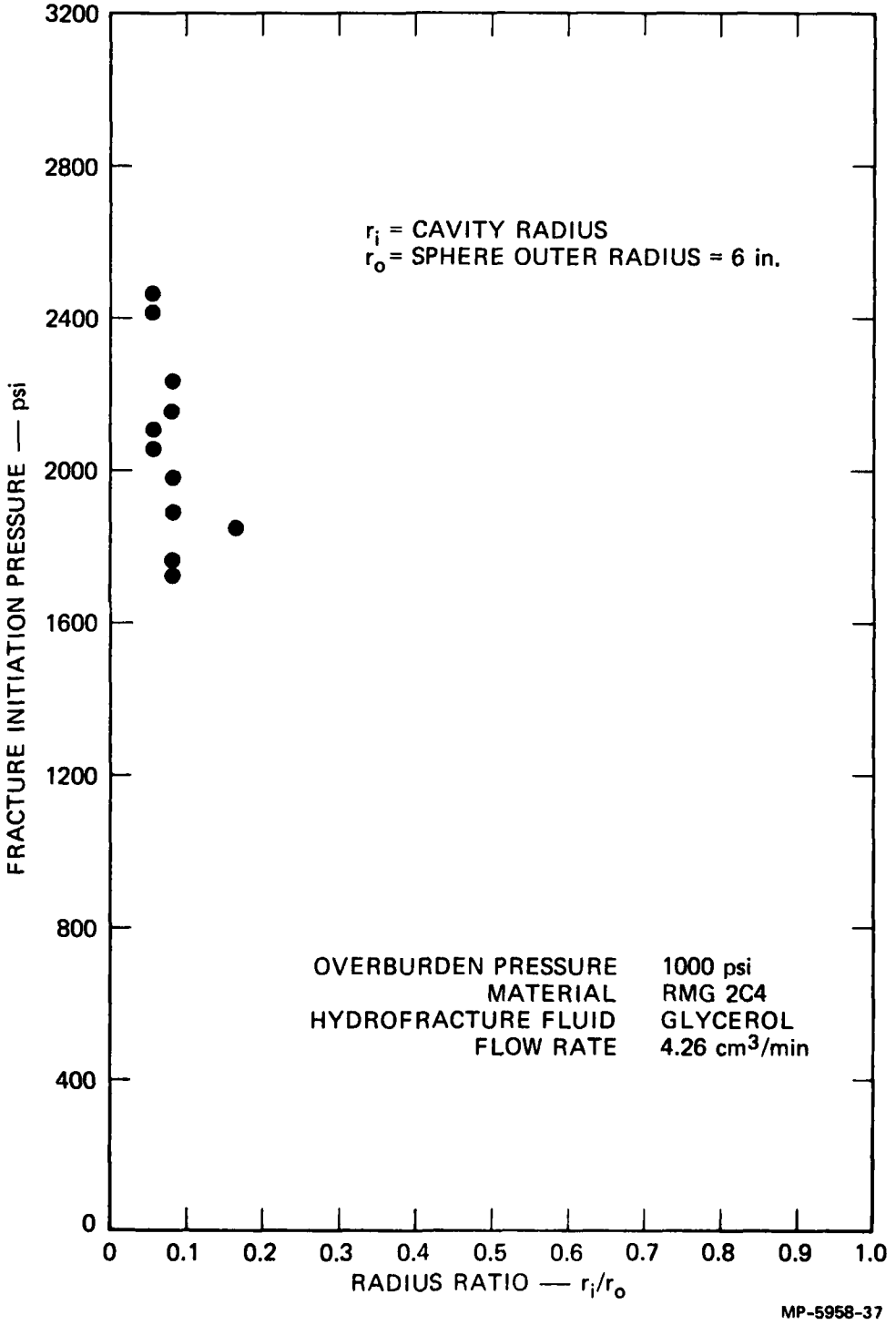

FIGURE 3.18 FRACTURE INITIATION PRESSURE VERSUS CAVITY SIZE FOR UNEXPLODED CAVITIES

1-inch-diameter cavity tests were described in Series 1. Average fracture initiation occurred at 1838 psi for RMG 2C3, 1960 for RMG 2C4, and 3347 psi for the granite simulants. As shown in Figure 3.9, only the granite simulant spheres were able to sustain a tensile circumferential stress at the cavity wall without fracturing.

Series 8 - Geology

Simulated Fault. A fault plane was simulated by casting a 3-inch-diameter sheet of 5-mil Mylar in a RMG 2C4 sphere as shown sketched in Figure 3.19. The fracture initiated in the 11/16-inch-diameter cavity at 1750 psi as shown in Figure 3.19 for Test 80. Average fracture initiation pressure for the tests of Figure 3.1 without the fault was 2265 psi, indicating a degradation of the containment capacity of the sphere with the Mylar sheet. However, as shown in Figure 3.19, after 7 cm^3 of fluid flow, measured from fracture initiation, the sphere with a fault sustains a higher cavity pressure than spheres without this feature. This may be explained by the shape of the fracture surface in Test 80, as seen in Figure 3.20. The irregular pattern provides greater resistance to flow than the planar fracture surfaces developed in the tests without the fault.

Material Interface. A second type of geological feature investigated was the plane interface between dissimilar materials. Figure 3.21 shows the position of the simulated surface between RMG 2C4 and GS3. The hydrofracture record of such a composite sphere with a 1-inch-diameter cavity is also shown in Figure 3.21. For comparison, typical pressure records for RMG 2C4 and GS3 spheres without an interface are included. Fracture initiation of the composite sphere, at 2560 psi, is bounded by the average values of 1960 psi for RMG 2C4 spheres and 3347 psi for granite simulant spheres.

Surface cracking of the composite sphere by hydrofracture was confined to the weaker RMG 2C4 as shown in Figure 3.22. Cracking of the GS3 was limited to a small region near the interface.

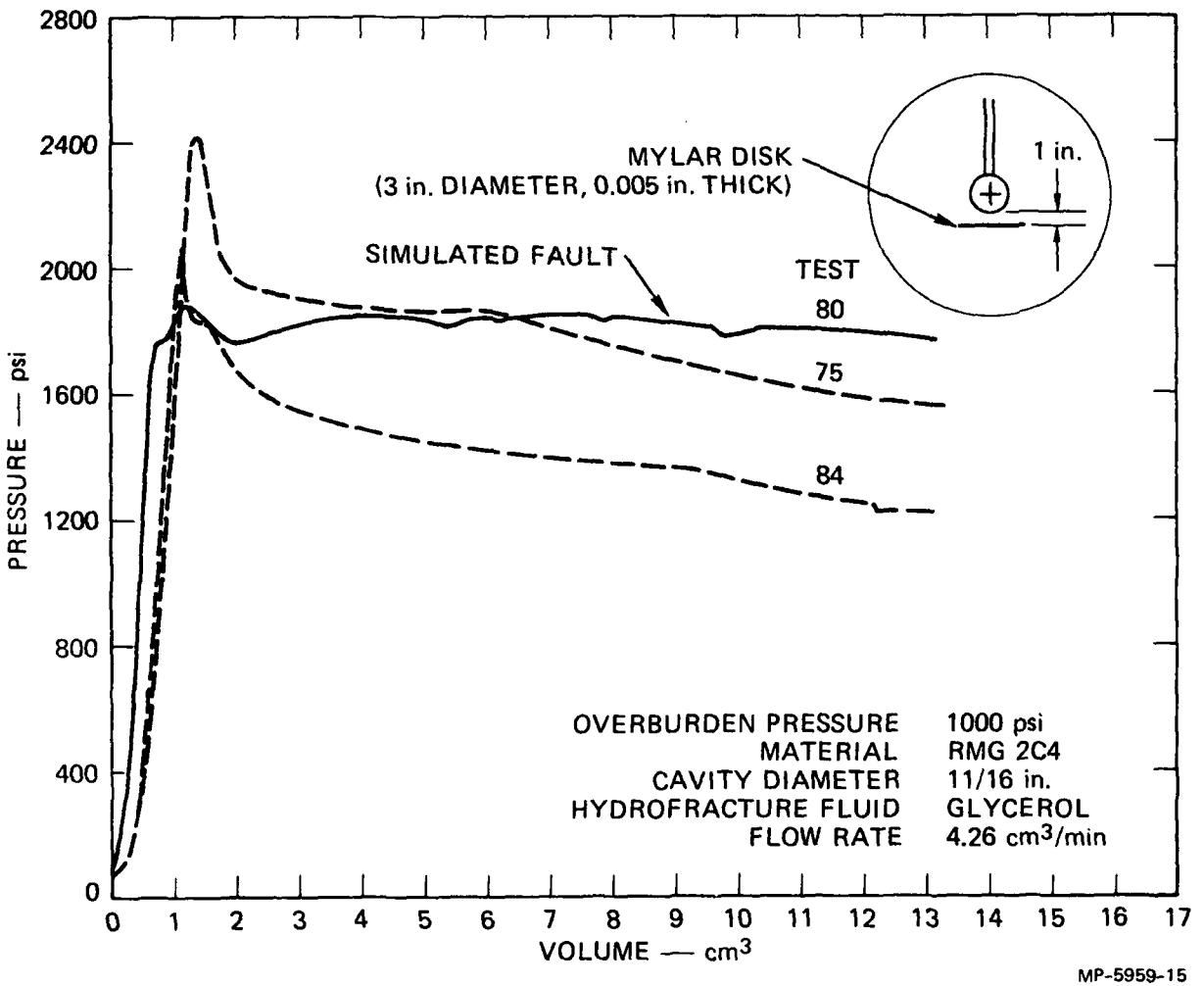

FIGURE 3.19 HYDROFRACTURE PRESSURES FOR UNEXPLODED CAVITY TESTS 75, 80, AND 84 — SIMULATED FAULT EFFECT

FIGURE 3.20 HYDROFRACTURE FROM UNEXPLODED CAVITY TEST 80

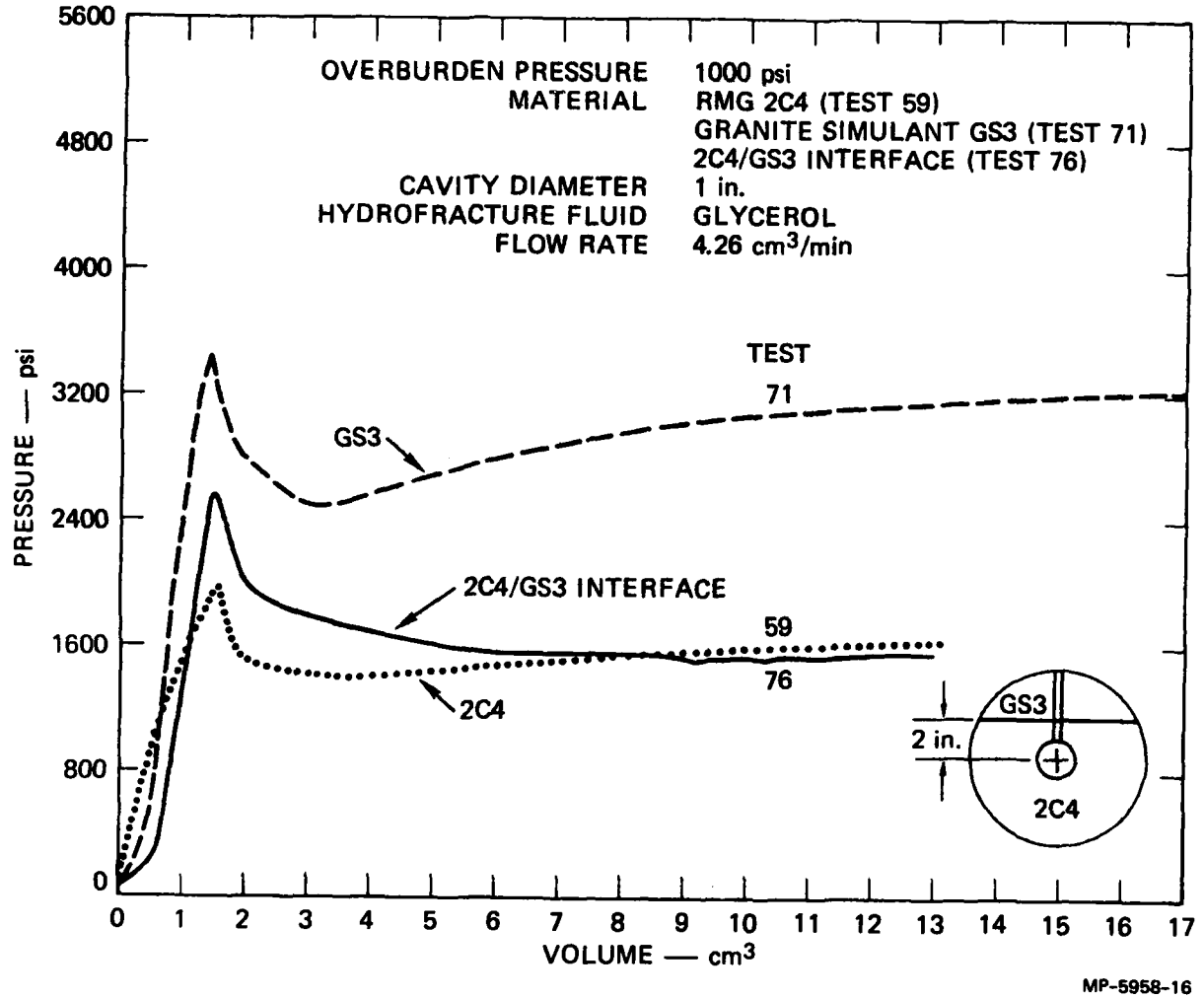

FIGURE 3.21 HYDROFRACTURE PRESSURES FOR UNEXPLODED CAVITY TESTS 59, 71, AND 76 — MATERIAL INTERFACE EFFECT

FIGURE 3.22 HYDROFRACTURE FROM UNEXPLODED CAVITY TEST 76

Series 9 - Imperfection Sensitivity

The wire hoops used in the reproducibility tests of Series 1 to aid in forming the spherical cavity induce imperfections in the cavity wall. Resulting hydrofracture records for RMG 2C4 spheres with an 11/16-inch-diameter cavity are shown in Figure 3.1. Similar experiments, Tests 104 and 105, were performed on spheres without the imperfections. Pressure records for these tests are shown in Figure 3.23 along with typical results from Figure 3.1. Average fracture initiation pressure increased from 2265 to 2530 psi as a result of removing the wire hoops. Also, with fluid volume measured from fracture initiation, cavity pressure after 11 cm^3 of flow increased from 1400 to 2124 psi. While these imperfections degraded the containment capacity of a cavity, they may represent a means of simulating the surface condition of an excavated cavity.

Series 10 - Cavity Lining

The cavity in Tests 51 and 52 was formed by casting RMG 2C3 around a 1-inch-diameter glass sphere. Hydrofracture was performed by pumping dyed glycerol into the cavity at the rate of 4.26 cm^3/min. Pressure records are shown in Figure 3.24. Also shown are the records for Tests 19 and 21, in which cavities were formed with a balloon in a wire cage. Tests 19 and 21 are typical results taken from Figure 3.5. Interruption of the smooth initial pressure rise in Tests 51 and 52 indicates cracking of the glass sphere. However, as shown in Figure 3.25, the glass lining remains nearly intact. Also, contact between undamaged sections of glass and the grout is sufficient to restrict fluid flow in these areas. The major differences between the two groups of tests are: (1) imperfections induced by the wire cage are eliminated using the glass sphere and (2) spherical symmetry of the porous flow is disturbed in the glass-lined tests. Fracture initiation pressures in the glass-lined cavity tests were 2150 and 2300 psi, an average of 2225 psi. This average is reduced to 1838 psi in the wire cage tests. Since porous flow is negligible in both groups of tests, imperfection sensitivity becomes the dominant parameter. Addition of a wire cage in these 1-inch cavity tests resulted in a 387 psi decrease in fracture

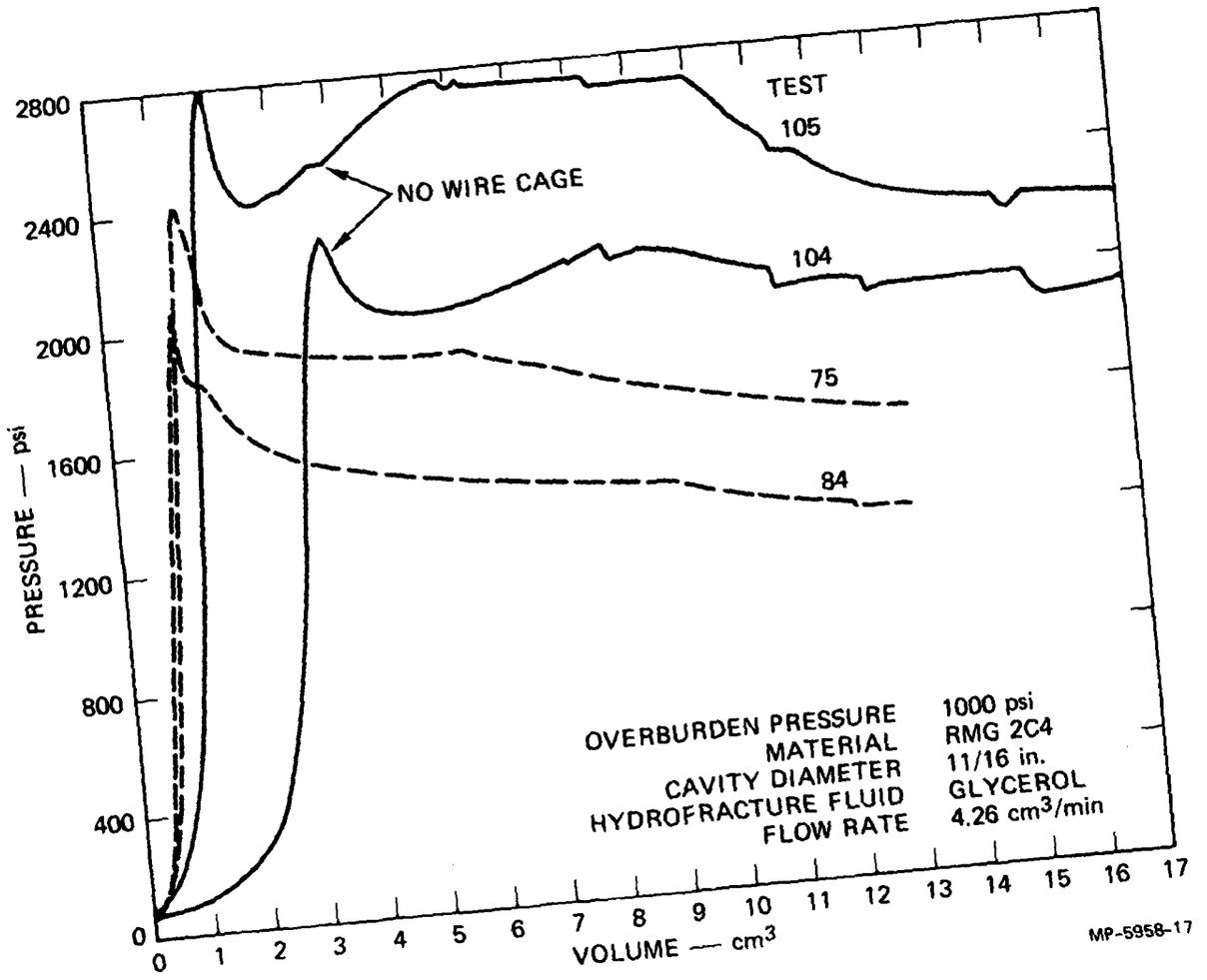

FIGURE 3.23 HYDROFRACTURE PRESSURES FOR UNEXPLODED CAVITY TESTS 75, 84, 104, AND 105 — IMPERFECTION SENSITIVITY EFFECT

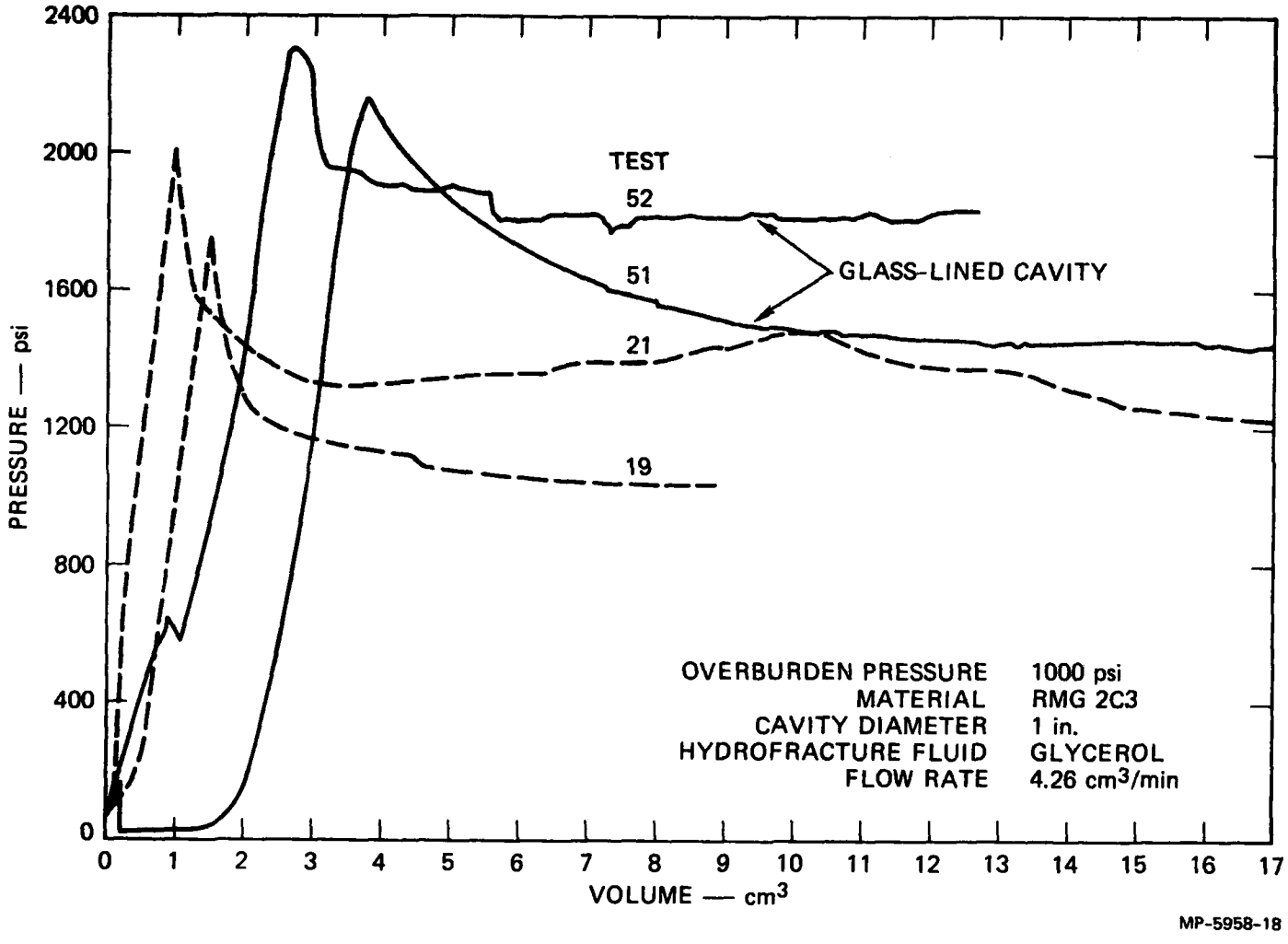

FIGURE 3.24 HYDROFRACTURE PRESSURES FOR UNEXPLODED CAVITY TESTS 19, 21, 51, AND 52— CAVITY LINING EFFECT

MP-5958-50

FIGURE 3.25 HYDROFRACTURE FROM UNEXPLODED CAVITY TEST 51

initiation pressure. In the 11/16-inch cavity tests of Series 9, addition of a wire cage resulted in a 265 psi decrease in fracture initiation pressure.

Tests 2, 3, and 4 represent another group of glass-lined cavity experiments. Hydrofracture records for these 25/32-inch-diameter cavity tests are shown in Figure 3.26. An added feature was the presence of a second dye in the glycerol hydrofracture fluid. Being insoluble, the new dye filtered out at the surface of the cavity and in the plane of the fracture as shown in Figure 3.27. The soluble dye was able to flow along the fracture plane nearer to the crack tip.

An unusual feature of Tests 2 and 3 is the high cavity pressure following fracture initiation. Since the fracture initiation pressures of 1760 and 1790 psi are low compared with the 2610 psi value for Test 4, smaller cracks may have formed. A subsequent slow rate of crack growth and clogging of the crack by the insoluble dye would result in high cavity pressures. Fracture initiation in Test 4 was followed by a general decay in cavity pressure.

Series 11 - Fracture Initiation and Growth

Tests were conducted on RMG 2C3 spheres with a 1-inch-diameter cavity to correlate initiation and growth of a macroscopic crack with points on a pressure-volume curve. Pressures were produced by pumping dyed glycerol at a rate of 4.26 cm^3/min. Cavities in Tests 10 through 14 were glass-lined. Cavities in Tests 30 and 31 were formed with a balloon in a wire cage.

In Tests 13, 14, and 30 pumping was stopped before peak cavity pressure was reached, as shown in Figure 3.28 for Test 30. While subsequent sectioning of the spheres failed to reveal any cracking, fluid penetration along the access tube was evident.

In Tests 10 through 12 and 31, pumping was stopped soon after peak cavity pressure was reached, as shown in Figure 3.28. Sectioning of the spheres from Tests 12 and 31 revealed a small fracture extending from the

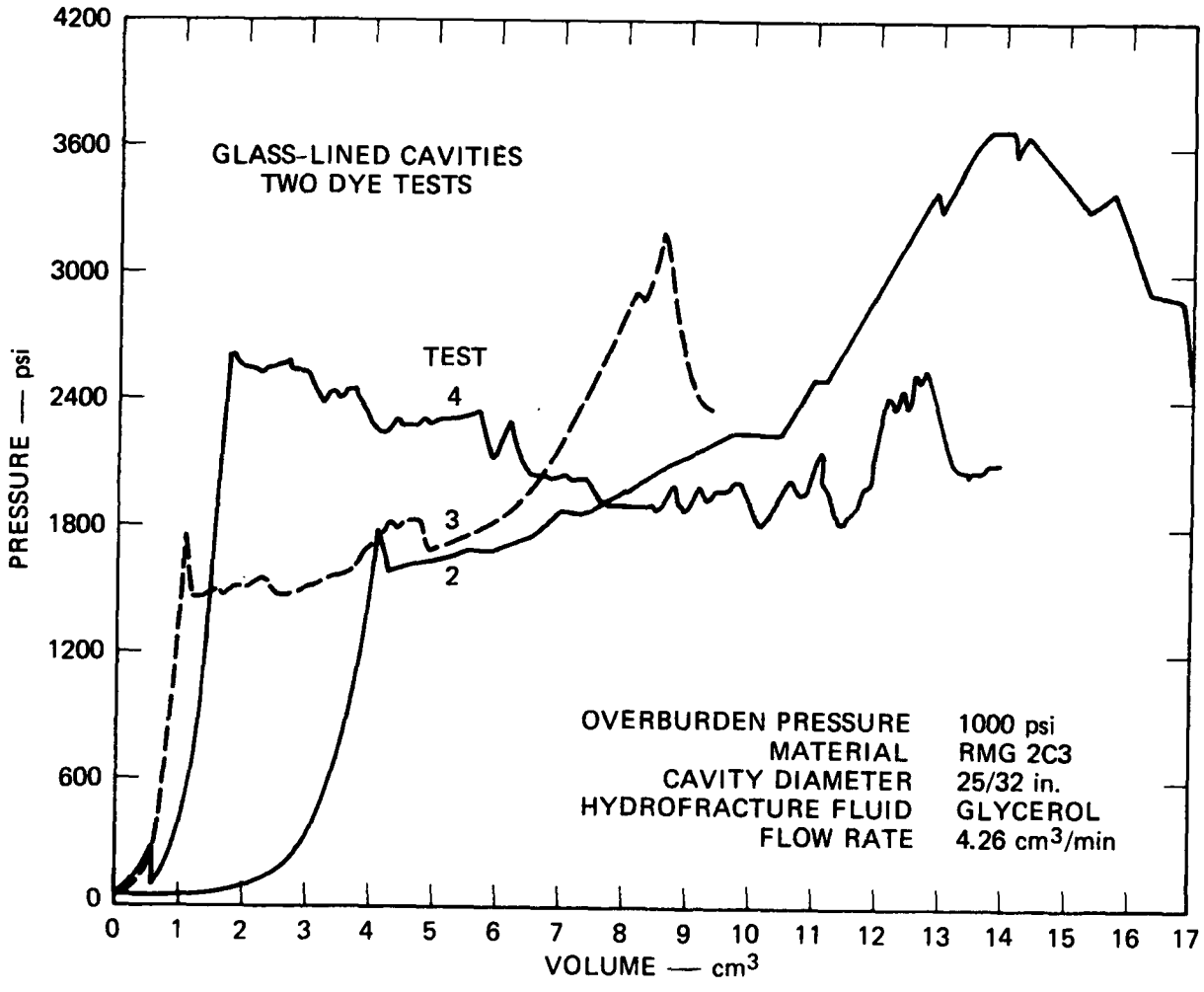

FIGURE 3.26 HYDROFRACTURE PRESSURES FOR UNEXPLODED CAVITY TESTS 2, 3, AND 4—CAVITY LINING EFFECT

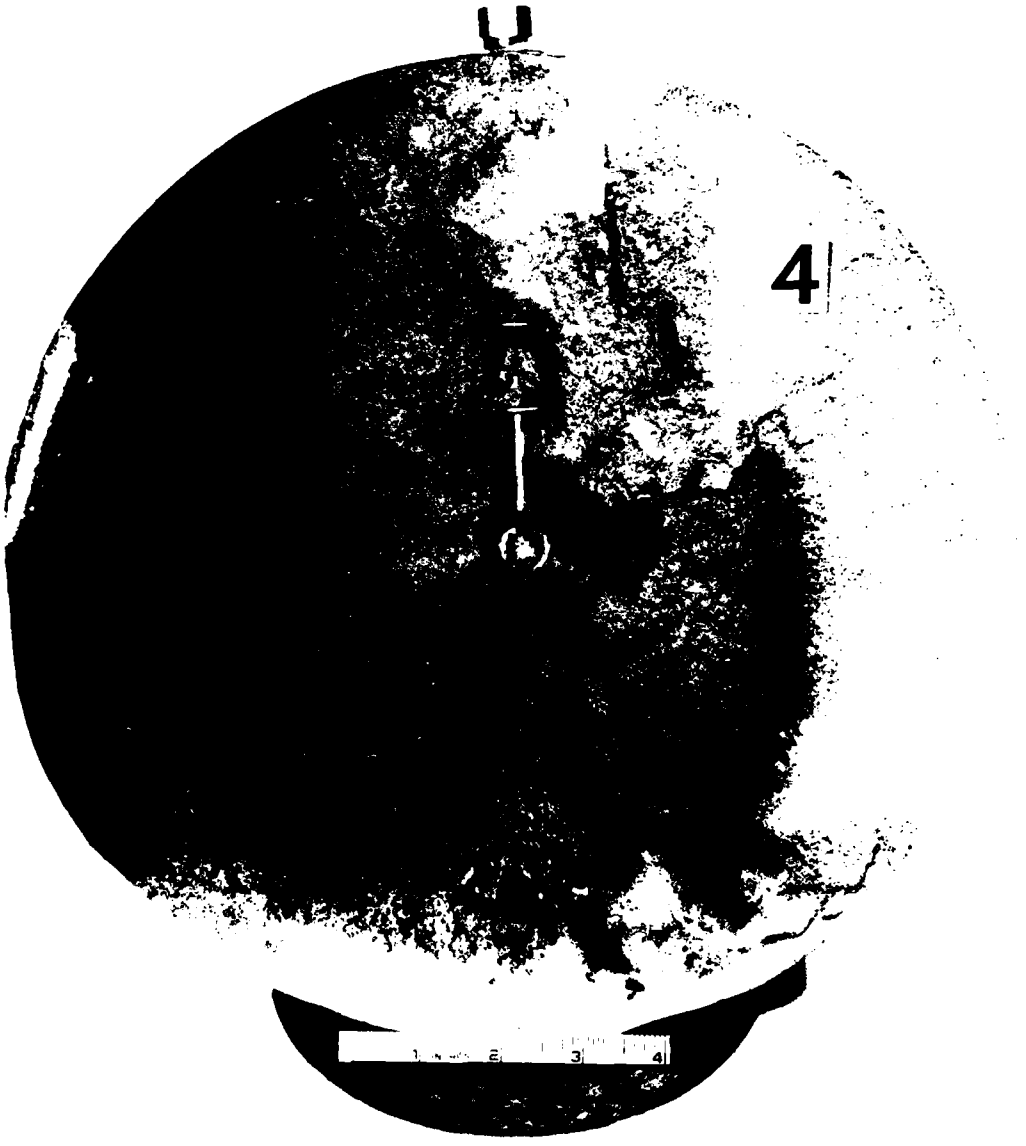

MP-5958-51

FIGURE 3.27 HYDROFRACTURE FROM UNEXPLODED CAVITY TEST 4

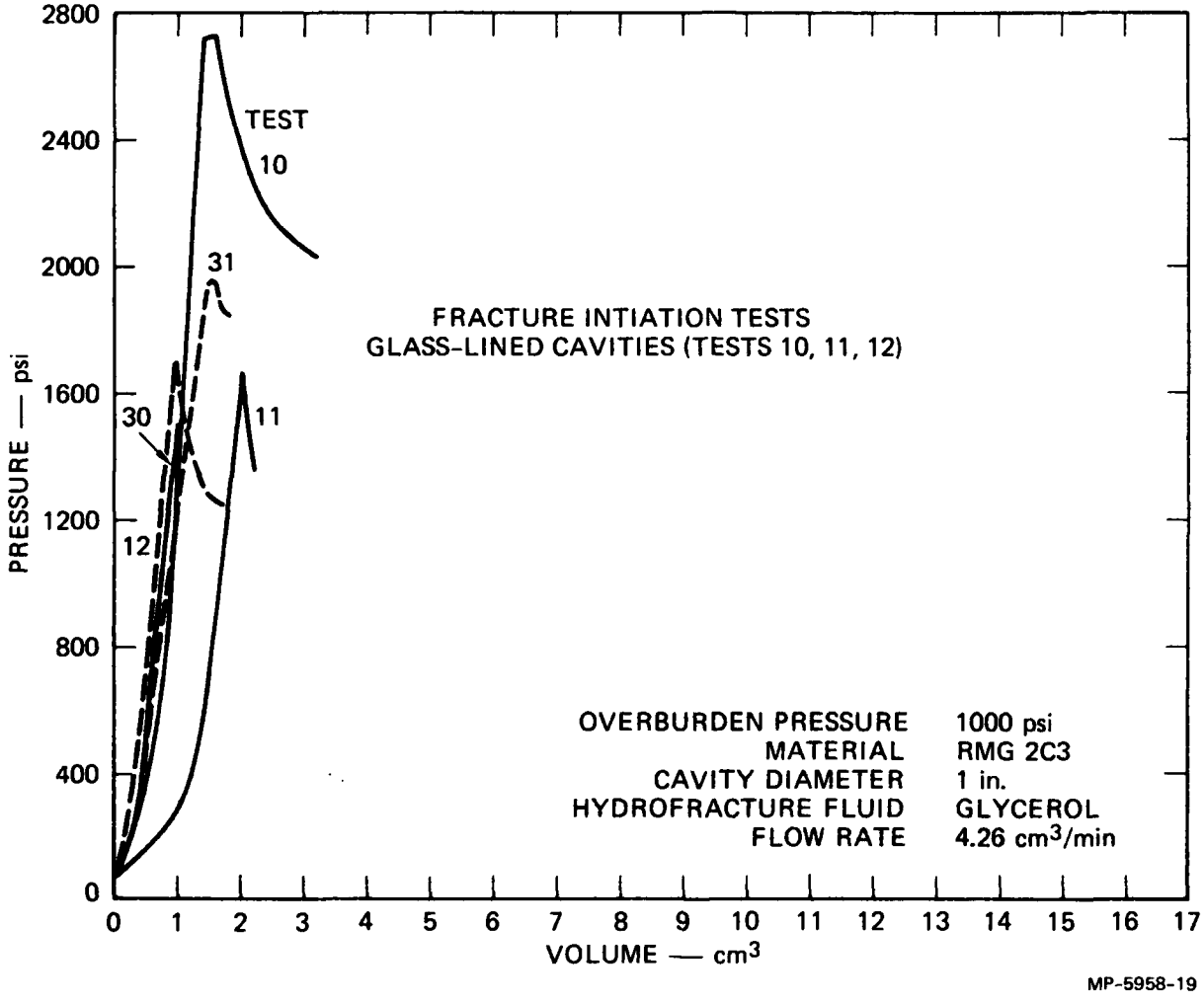

FIGURE 3.28 HYDROFRACTURE PRESSURES FOR UNEXPLODED CAVITY TESTS 10, 11, 12, 30, AND 31 — FRACTURE INITIATION

cavity. The fracture pattern in Test 10 was more extensive, as shown in Figure 3.29. Surface cracking was evident in Test 11 and the sphere tapped apart with a chisel.

Hence, while the pressure spike is indicative of fracture initiation, the subsequent rate of crack growth varied considerably from test to test.

3.3 EXPLODED CAVITY TESTS

Series 12 - Reproducibility

Testing of exploded cavity reproducibility included nominal 1/4- and 1/2-gram charges of PETN cast in RMG 2C3 and RMG 2C4. Hydrofracture was performed by pumping dyed glycerol into the vented exploded cavities at the rate of 4.26 cm^3/min. Overburden was held constant at 1000 psi.

Tests 15, 23, and 25 were conducted on spheres of RMG 2C3. Pressure records for these 1/2-gram charge tests are shown in Figure 3.30. The results are typical of exploded cavity tests in that cavity pressure first increased smoothly and rapidly, then dropped sharply to form a pressure peak or spike, increased gradually but erratically to a maximum, and finally decayed to a value above overburden. Results of Series 19 tests confirm that the spike represents fracture initiation. Increase of cavity pressure following this breakdown indicates a resistance to flow due to the explosively generated residual stress field surrounding the cavity. Fracture initiation pressures were 2340, 2360, and 2760 psi, with an average of 2487 psi. Maximum deviation from the average is 11% and represents reproducibility comparable to that found in the unexploded cavity tests shown in Figure 3.5 which produced an average fracture initiation pressure of 1838 psi. Hence, the residual stress field increased this breakdown pressure by 35%.

The fracture surface in Test 23 is shown in Figure 3.31. The intensely dyed region surrounding the cavity confirms the calculated nature of the residual stress field. Analyses[5,6] have shown that annular regions of residual tensile and compressive circumferential stress surround the explosively developed cavity. In the tensile region a large gap between the fracture surfaces develops and allows for the development of an

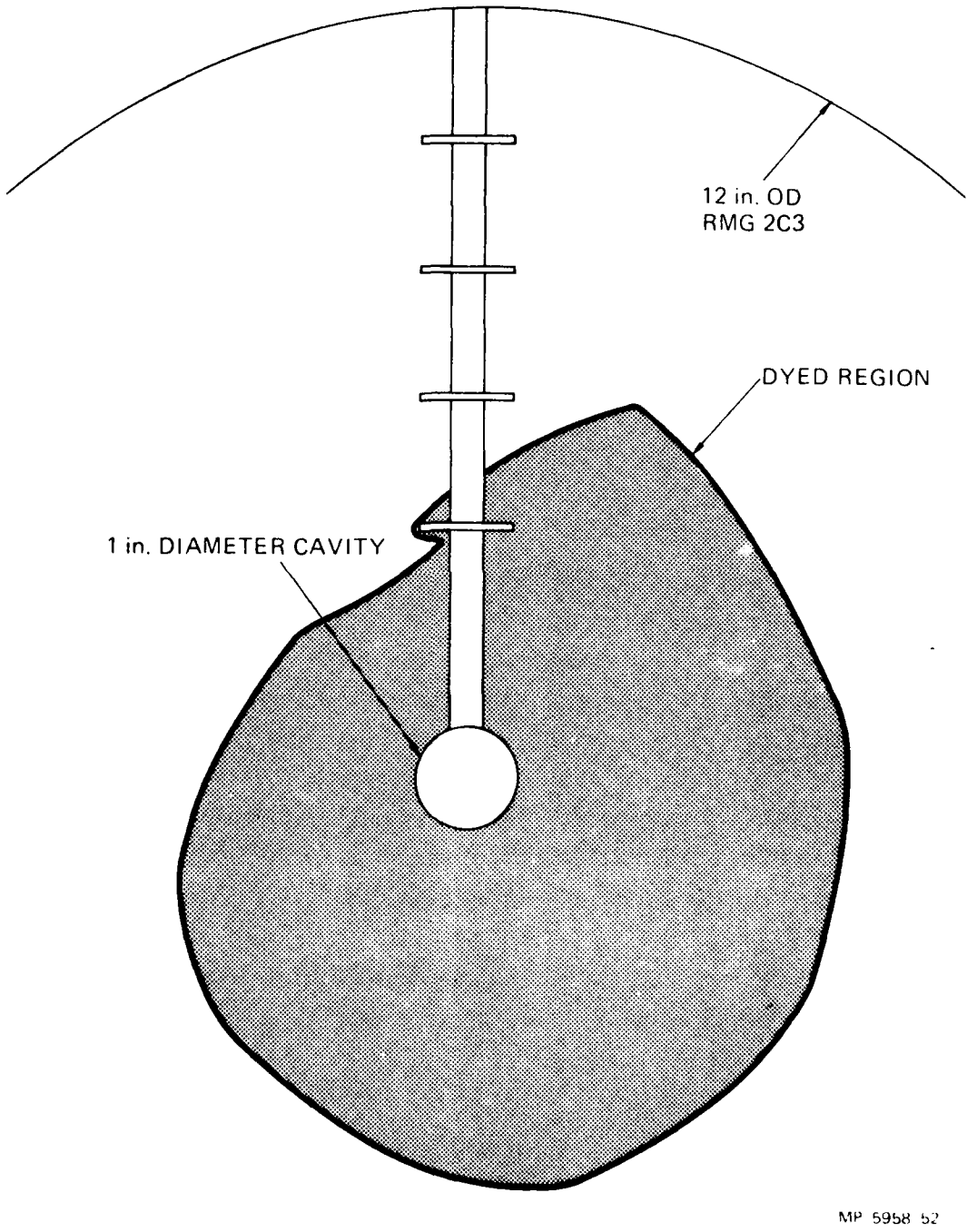

FIGURE 3.29 HYDROFRACTURE FROM UNEXPLODED CAVITY TEST 10

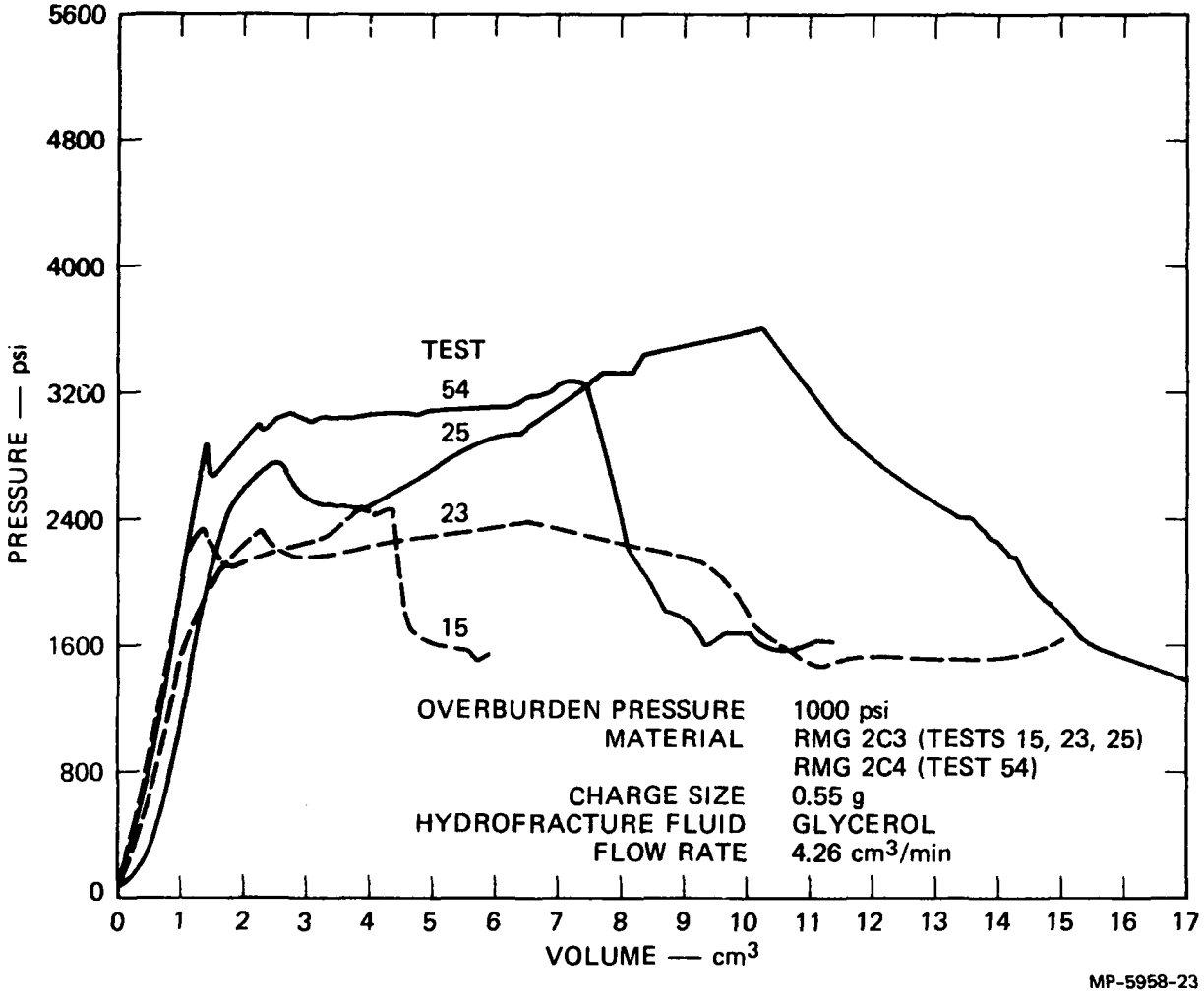

FIGURE 3.30 HYDROFRACTURE PRESSURES FOR EXPLODED CAVITY TESTS 15, 23, 25, AND 54—REPRODUCIBILITY

FIGURE 31 HYDROFRACTURE FROM EXPLODED CAVITY TEST 23

intensely dyed region. In the surrounding compressive region a smaller gap develops, reduces fluid pressure and flow, and results in a less intensely dyed region.

Test 54 was performed on a RMG 2C4 sphere. The pressure record for this 1/2-gram charge test is shown in Figure 3.30. Since this is the only test of a 1/2-gram charge in RMG 2C4, reproducibility is not demonstrated. However, the 2880-psi fracture initiation pressure represents a 47% increase over the average value for the corresponding 1-inch-diameter unexploded cavity tests of Figures 3.3 and 3.4.

Hydrofracture records for nine 1/4-gram charge tests performed on RMG 2C4 spheres are shown in Figures 3.32, 3.33, and 3.34. Fracture initiation pressures were 2070, 2080, 2200, 2200, 2230, 2270, 2470, 2520, and 3440 psi. The 2387-psi average represents a 5% increase over the 2265-psi average for the corresponding 11/16-inch-diameter unexploded cavity tests of Figure 3.1, and a 6% decrease from the 2530-psi average for the imperfection-free cavity tests of Figure 3.23. Hence, the residual stress field generated by the 1/4-gram charge does not siginficantly increase fracture initiation pressure.

Following fracture initiation the pressure records for the 1/4-gram tests reveal a spectrum of results, with maximum cavity pressures ranging from 1900 to 6650 psi. The spectrum of pressures reflects the variety of fracture patterns developed. Figure 3.35 shows the single plane of fracture developed in Test 67 where cavity pressure reached a maximum of 4600 psi. Figure 3.36 shows the network of cracks developed in Test 77 where flow was stopped when cavity pressure reached 5000 psi. Sawing was required to expose the fracture pattern in Test 77 since none of the cracks propagated to the surface of the sphere.

Series 13 - Overburden

Test 40 was similar to 1/2-gram charge tests 15, 23, and 25 except that overburden pressure was 1500 instead of 1000 psi. The hydrofracture records for Tests 15 and 40 are shown in Figure 3.37. Fracture initiation pressure decreased slightly from an average of 2487 psi for the three

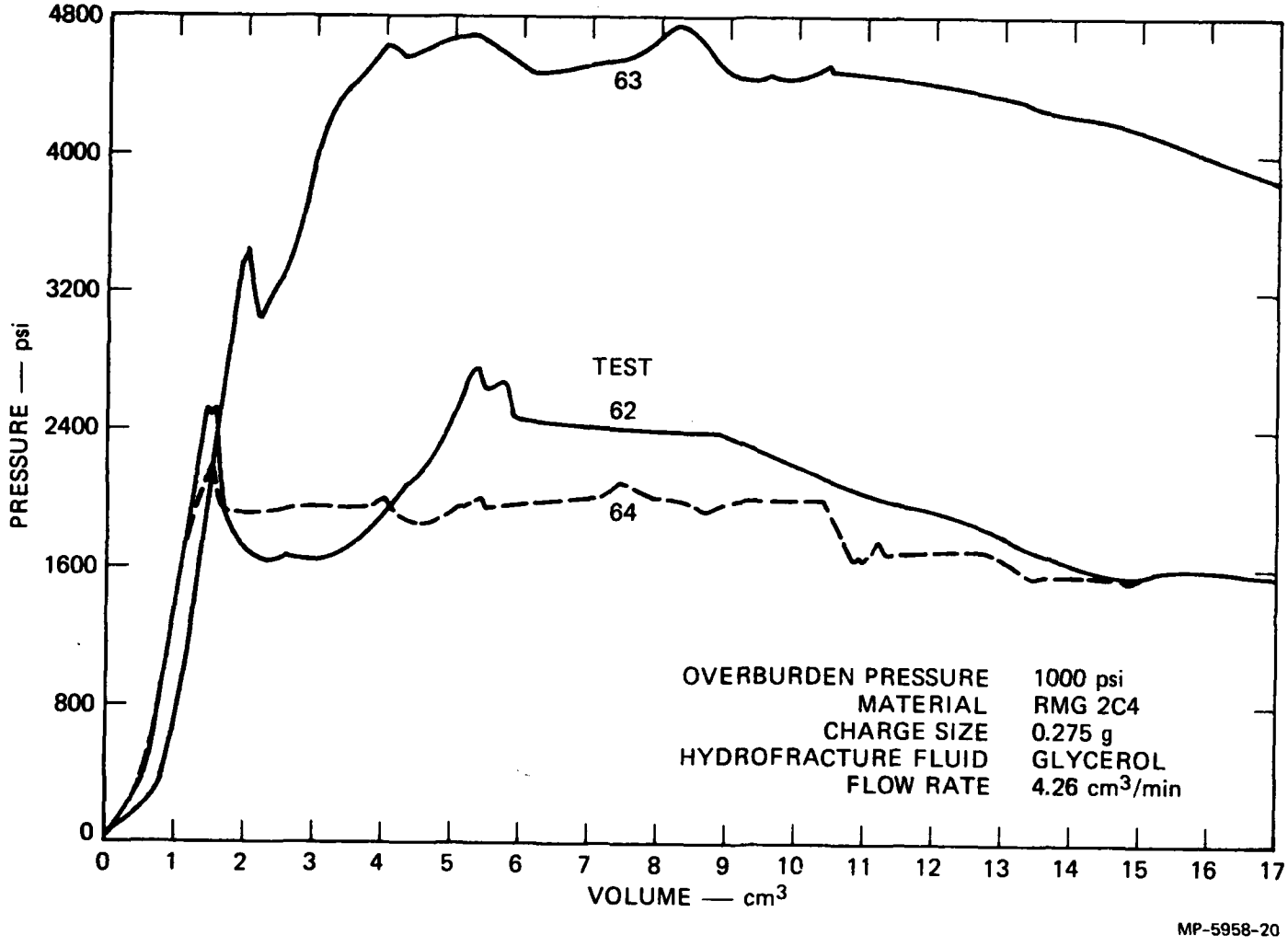

FIGURE 3.32 HYDROFRACTURE PRESSURES FOR EXPLODED CAVITY TESTS 62, 63, AND 64— REPRODUCIBILITY

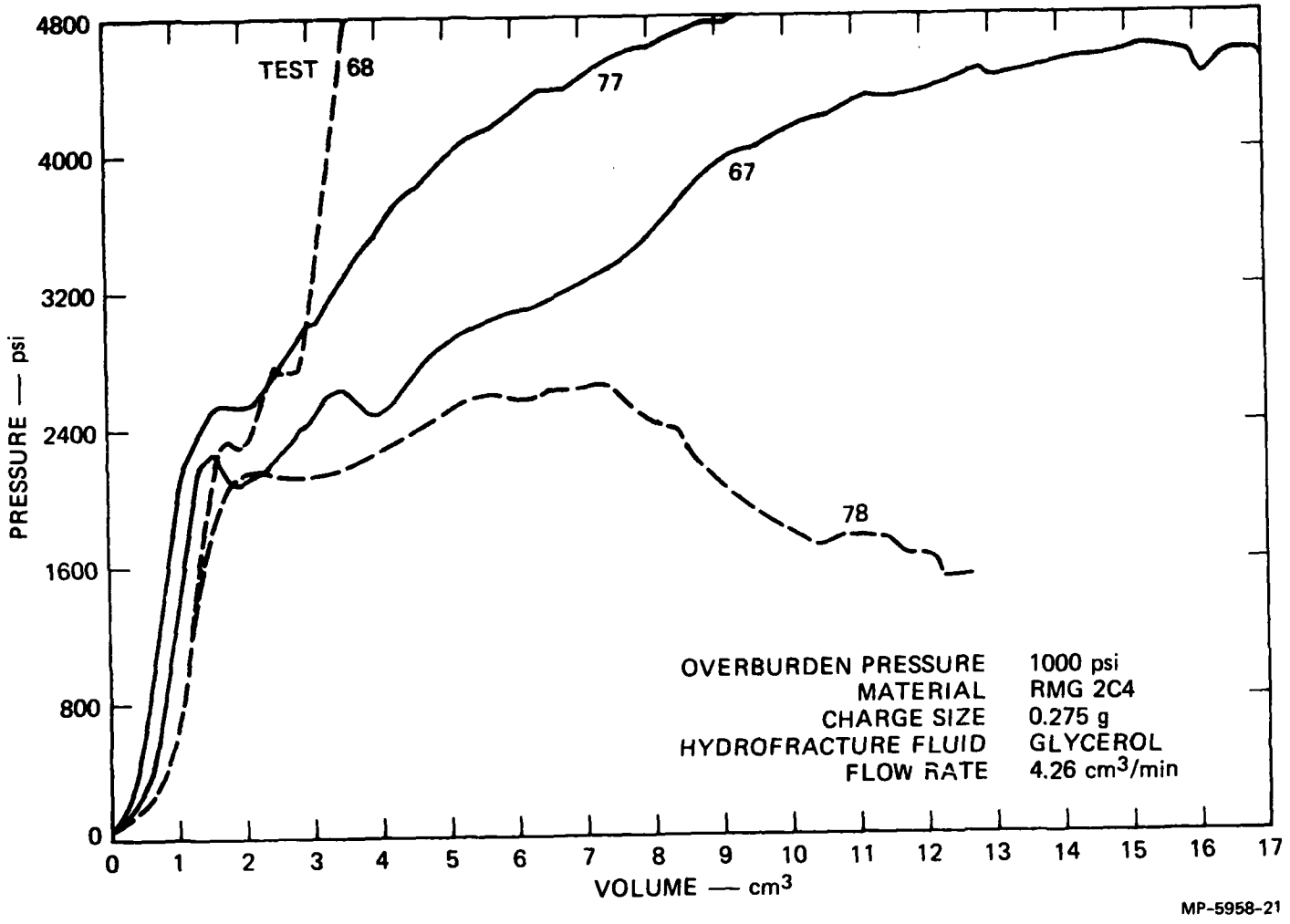

FIGURE 3.33 HYDROFRACTURE PRESSURES FOR EXPLODED CAVITY TESTS 67, 68, 77, AND 78—REPRODUCIBILITY

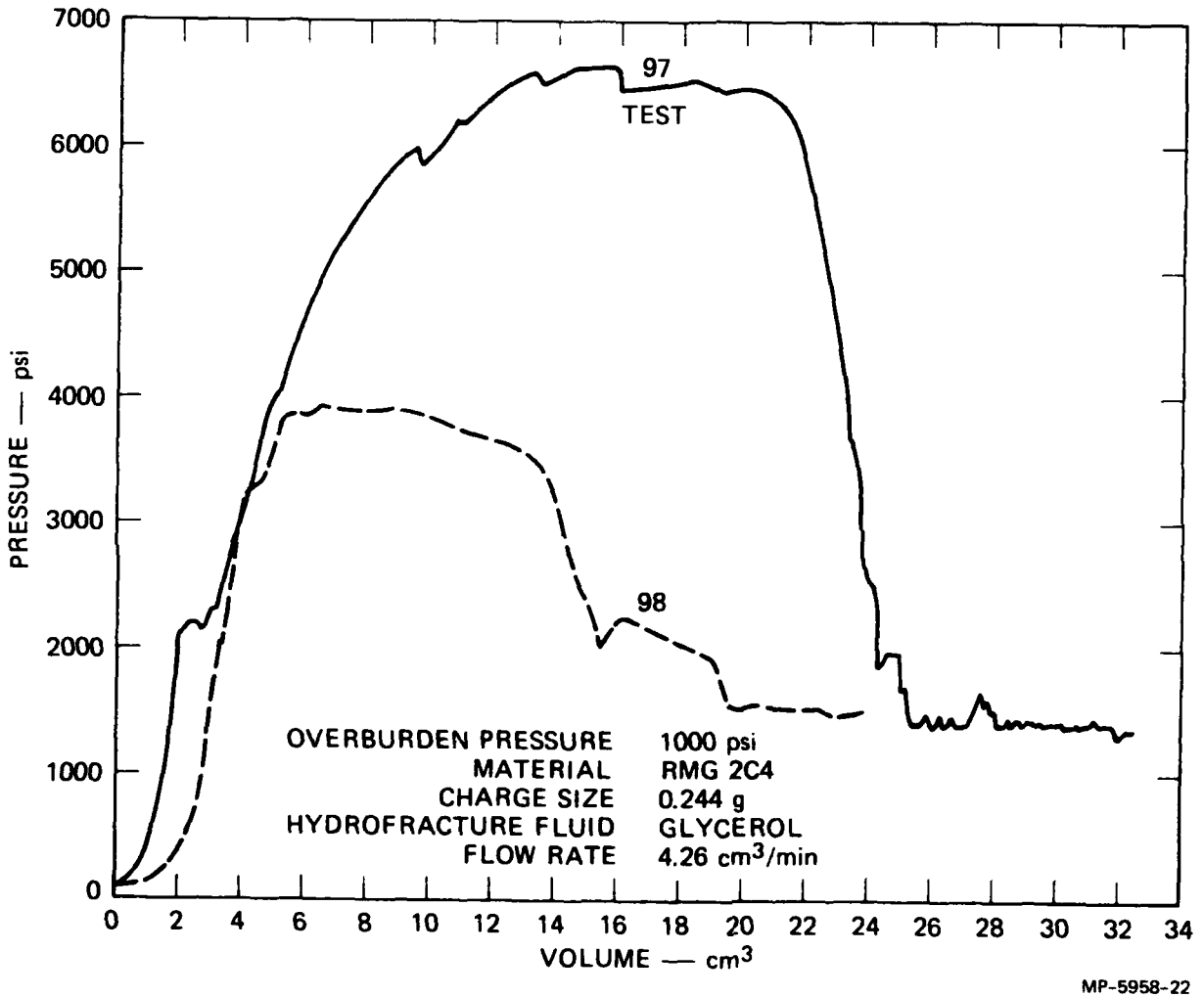

FIGURE 3.34 HYDROFRACTURE PRESSURES FOR EXPLODED CAVITY TESTS 97 AND 98— REPRODUCIBILITY

MP-5958-54

FIGURE 3.35 HYDROFRACTURE FROM EXPLODED CAVITY TEST 67

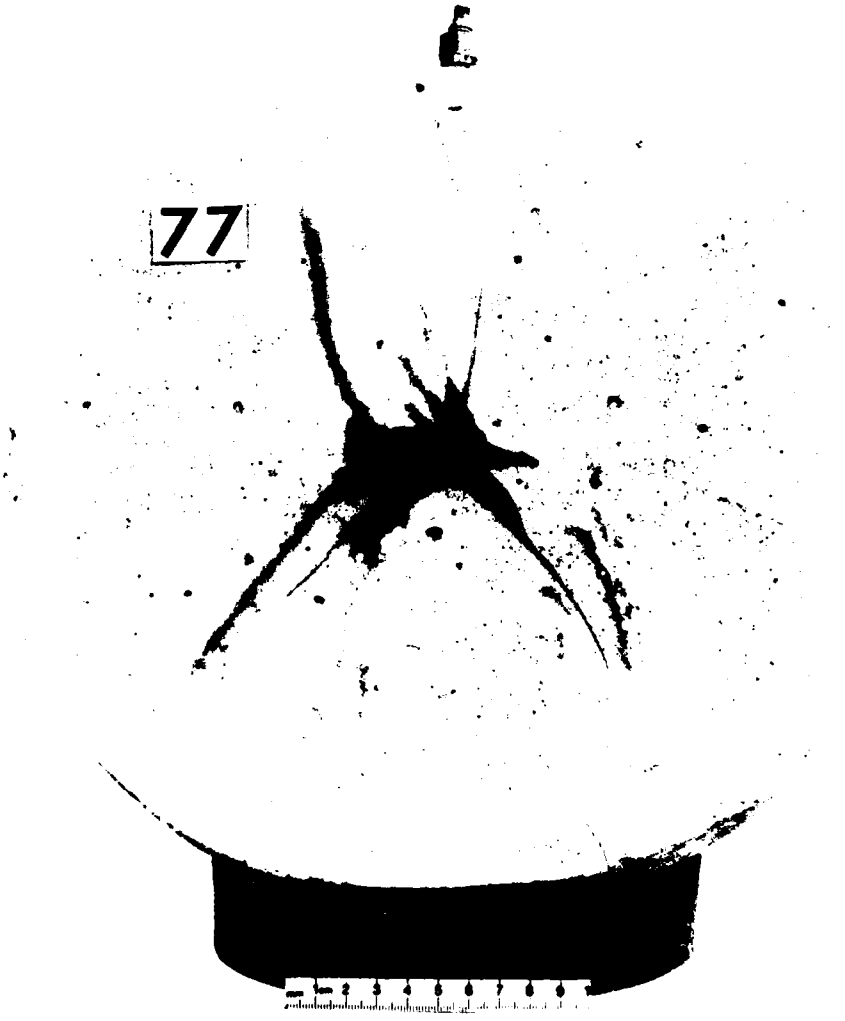

MP 5958 55

FIGURE 3.36 HYDROFRACTURE FROM EXPLODED CAVITY TEST 77

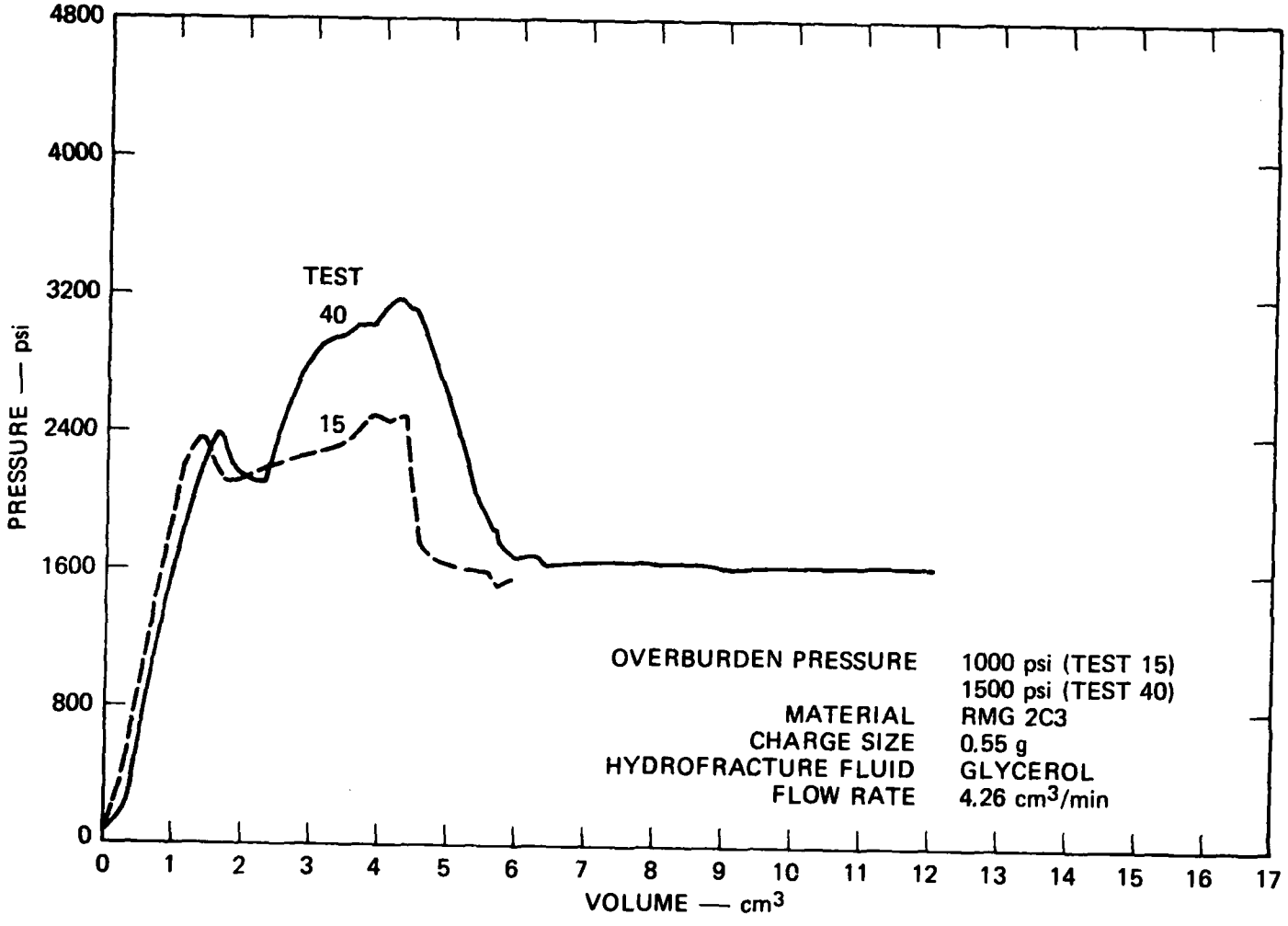

FIGURE 3.37 HYDROFRACTURE PRESSURES FOR EXPLODED CAVITY TESTS 15 AND 40—OVERBURDEN EFFECT

1000 psi tests to 2380 psi for the 1500-psi tests, indicating that the residual stress field surrounding the exploded cavities dominates the added stresses imposed by the increased overburden. Also, the maximum cavity pressure following fracture initiation in Test 40 (3160 psi) is within the range obtained in the 1000-psi tests. Finally, after steady state flow along the fracture surface was achieved, typical cavity pressure was 1600 psi for tests at both levels of overburden, indicating the dominance of residual stresses over external pressure.

While the change in external pressure did not significantly affect the exploded cavity test results, overburden still represents an important factor in containment since the chance of explosive cracking increases with decreasing overburden.

Series 14 - Viscosity

Tests 85, 87, and 108 were similar to the 1/4-gram tests of Figures 3.32, 3.33, and 3.34 except for the hydrofracture fluid. Dyed water, with a viscosity of 1 centipoise, was used in the first group, and dyed glycerol, with a viscosity of 660 centipoise, in the second. Pressure records for the water hydrofracture tests are shown in Figure 3.38. Fracture initiation pressures were 1680, 1840, and 2680 psi. The 2067-psi average represents a decrease of 13% from the 2387-psi average for the glycerol hydrofracture tests. The lower viscosity fluid also reduced the spectrum of cavity pressures obtained in the glycerol tests. Since porous flow calculations show negligible fluid penetration into RMG 2C4 for the water and glycerol hydrofracture tests, the lower cavity pressures associated with a less viscous fluid are attributed to more extensive penetration of water into cavity imperfections and along the fracture plane. However, these effects are not reflected by the fracture surface for Test 85 shown in Figure 3.39, where a typical exploded cavity dye pattern was produced.

Series 15 - Flow Rate

Tests 100, 101, and 102 were similar to the 1/4-gram charge tests of Figures 3.32, 3.33, and 3.34 except for the rate of fluid flow during

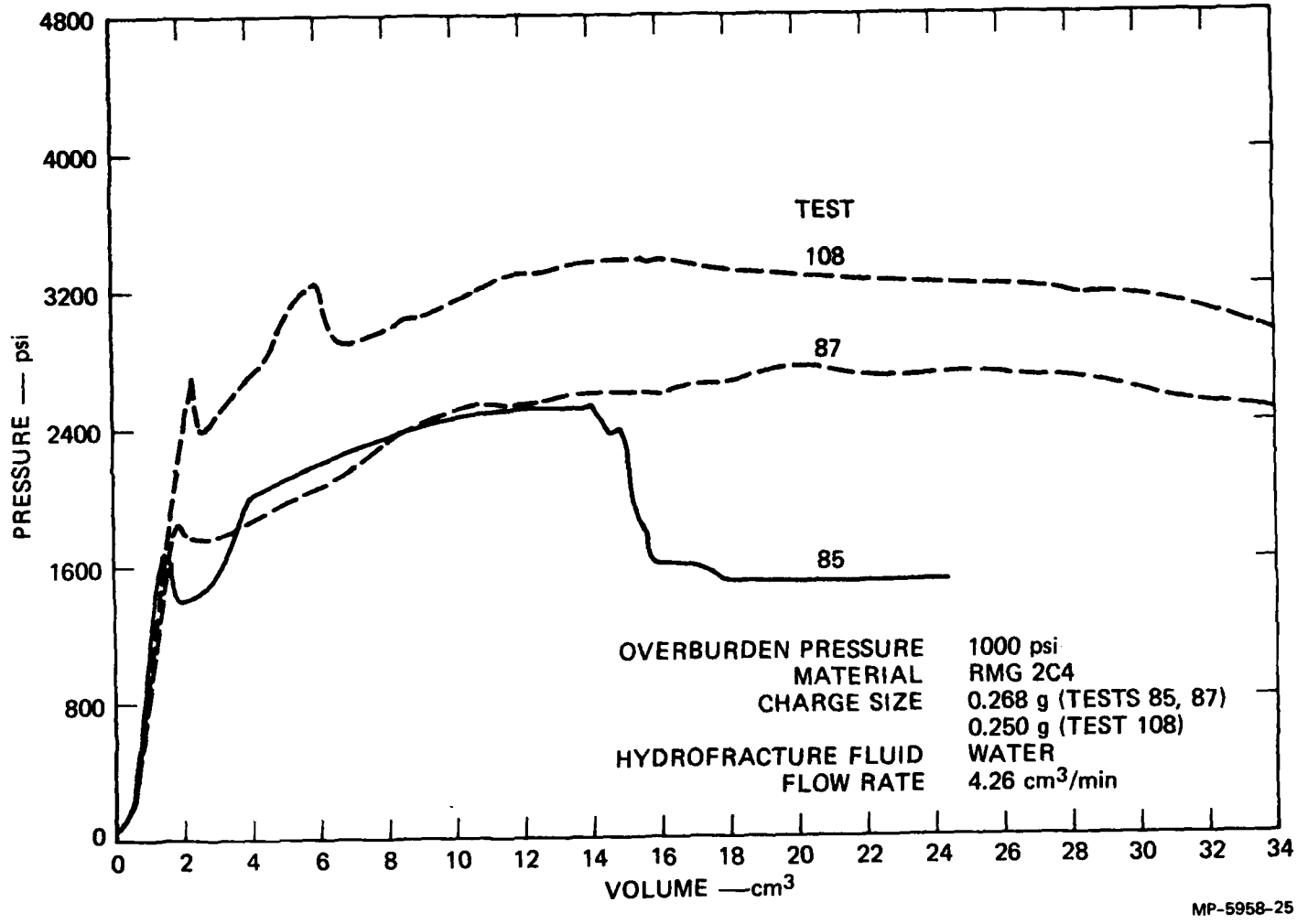

FIGURE 3.38 HYDROFRACTURE PRESSURES FOR EXPLODED CAVITY TESTS 85, 87, AND 108—VISCOSITY EFFECT

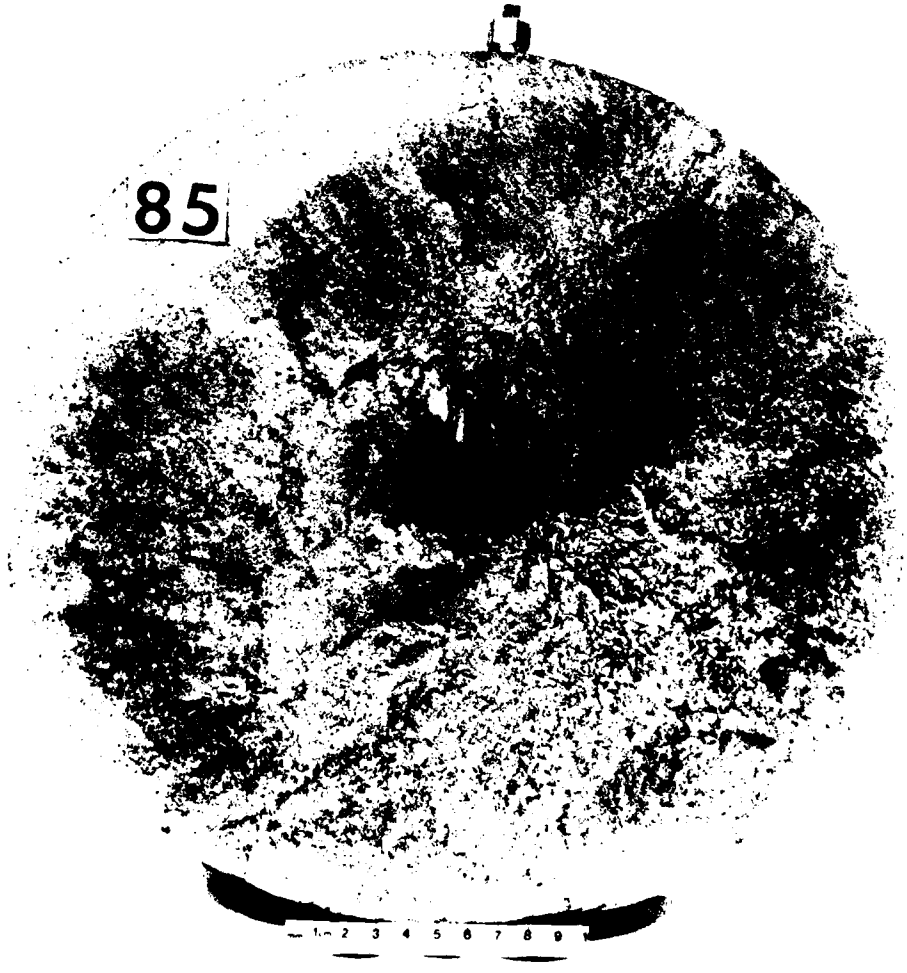

FIGURE 3.39 HYDROFRACTURE FROM EXPLODED CAVITY TEST 85

hydrofracture. A flow rate of 0.71 cm^3/min, one-sixth the normal 4.26 cm^3/min, was used in Tests 100, 101, and 102. Pressure records are shown in Figure 3.40. Fracture initiation pressures were 2200, 2320, and 2600 psi. The 2373-psi average represents a decrease of less than 1% from the 2387-psi average for the faster flow rate tests. Following cavity fracture initiation, the slower flow rate tests produced cavity pressures at the low end of the spectrum associated with the 1/4-gram charge tests of Series 12. Hence, lowering the hydrofracture flow rate improved reproducibility.

The fracture surface of Test 101 is shown in Figure 3.41. The slower flow rate produced the familiar region of intensely dyed grout surrounding the exploded cavity. Surface cracking of the sphere resulted from cracks that initiated on opposite sides of the cavity. The limited extent of cracking near the cavity restricted flow sufficiently to allow for an increase of pressure following feacture initiation--a result typical of exploded cavity tests.

Series 16 - Creep

After detonation of a 1/4-gram charge and release of internal pressure, the RMG 2C4 spheres in Tests 99 and 109 remained in the pressure vessel and subjected to a 1000-psi overburden for 17 and 97 hours, respectively. Subsequent hydrofracture resulted in the pressure records shown in Figure 3.42. Increasing the material relaxation period resulted in a decrease of fracture initiation pressure from 3400 to 2260 psi. However, the average value for the 1/4-gram charge tests of Figures 3.32, 3.33, and 3.34 with no creep period was 2387 psi. Average fracture initiation pressure for the corresponding 11/16-inch-diameter unexploded cavities of Figure 3.1 was 2265 psi and agrees very well with the results for the longer creep test. Also, the general decay of pressure following fracture initiation in the longer creep test is characteristic of unexploded cavity tests. Further evidence of creep is reflected in the fracture surface of Test 109 shown in Figure 3.43. The intensity of the dye in the region surrounding the cavity

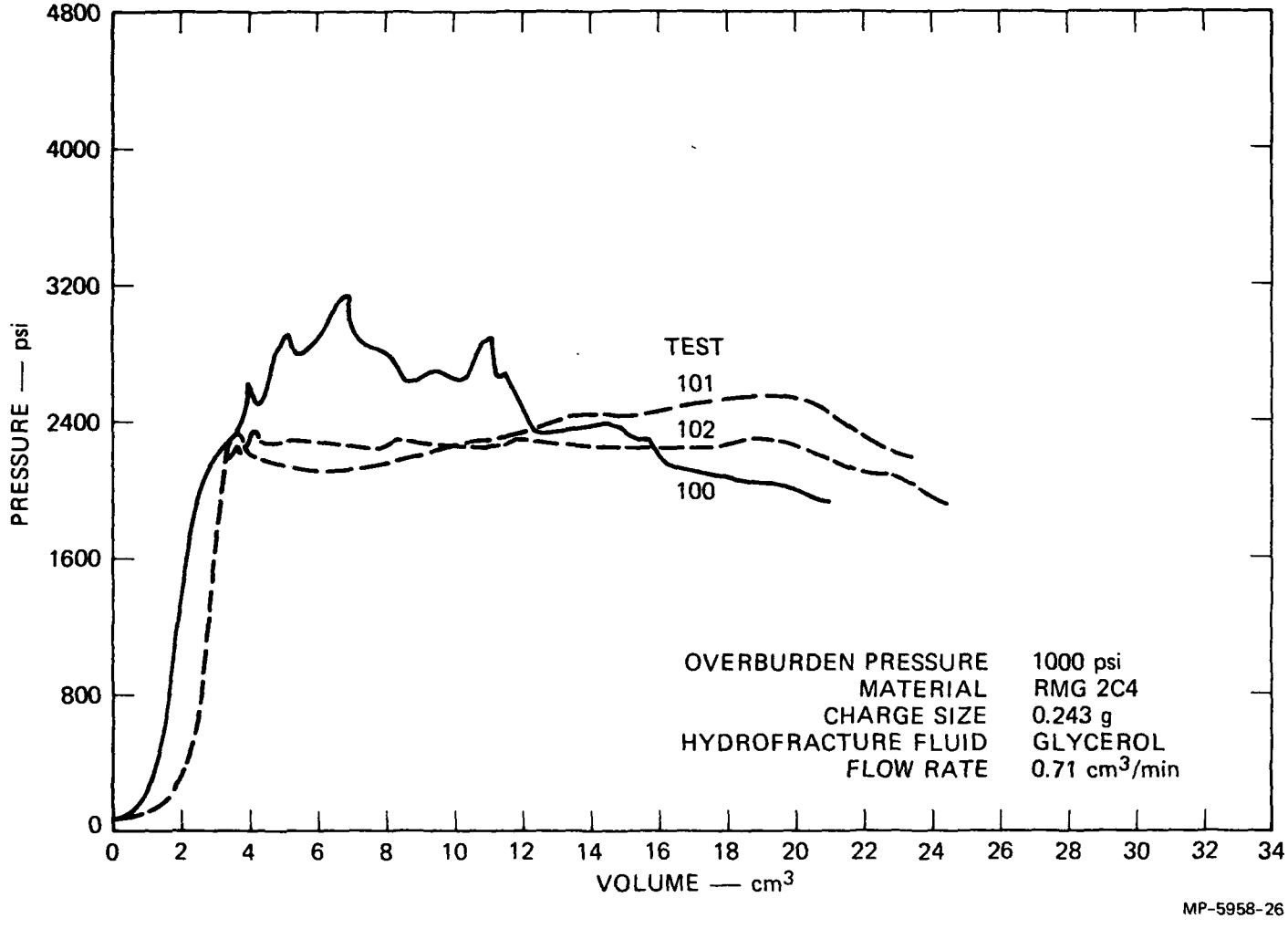

FIGURE 3.40 HYDROFRACTURE PRESSURES FOR EXPLODED CAVITY TESTS 100, 101, AND 102 — FLOW RATE EFFECT

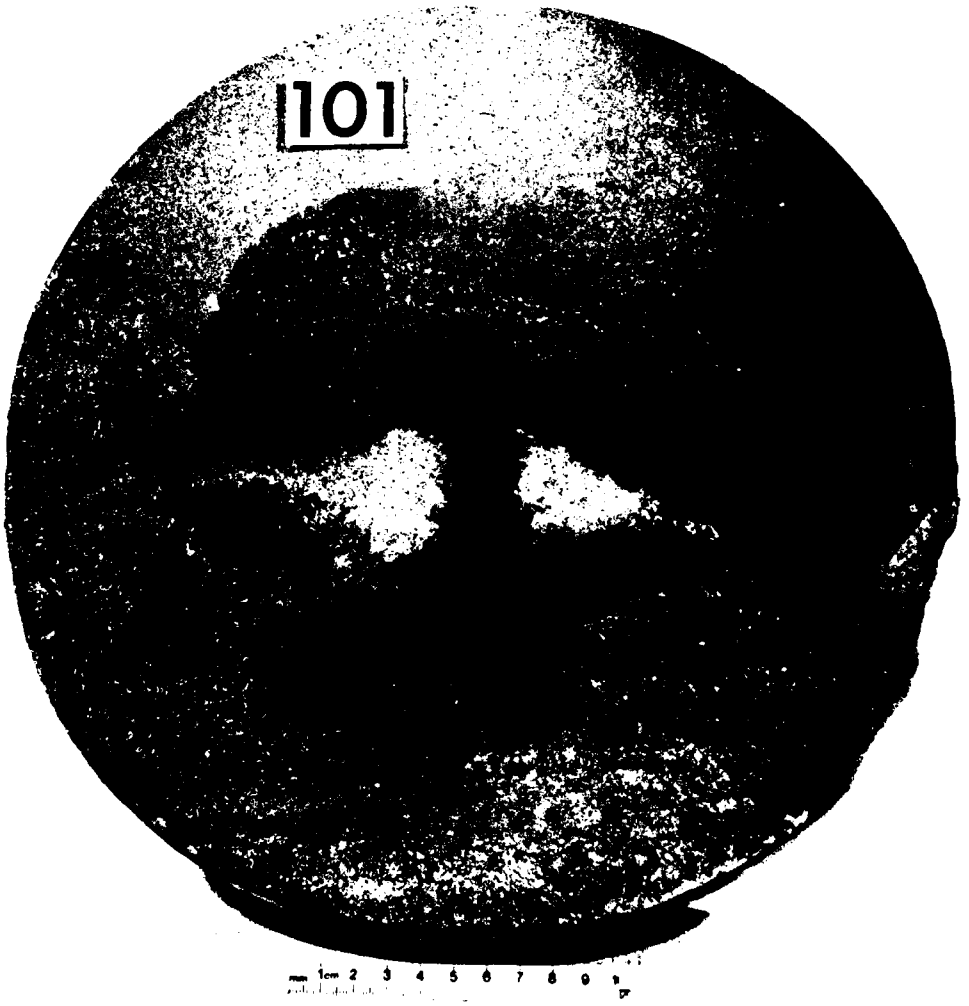

FIGURE 3.41 HYDROFOIL

AD-A084 662 SRI INTERNATIONAL MENLO PARK CA F/G 18/3
LABORATORY INVESTIGATION OF CONTAINMENT IN UNDERGROUND NUCLEAR --ETC(U)
JAN 78 J C CIZEK, A L FLORENCE DNA001-77-C-0025
UNCLASSIFIED DNA-4846F NL

2 OF 2
AD A 084662

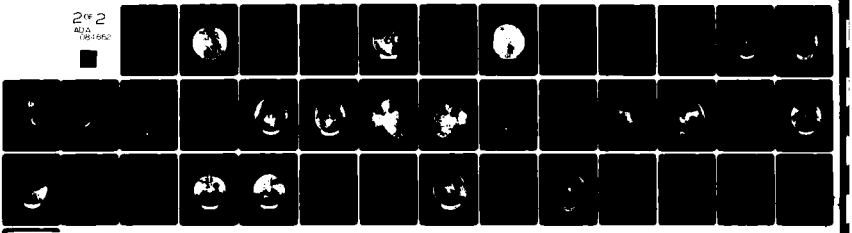

END
DATE FILMED
6-80
DTIC

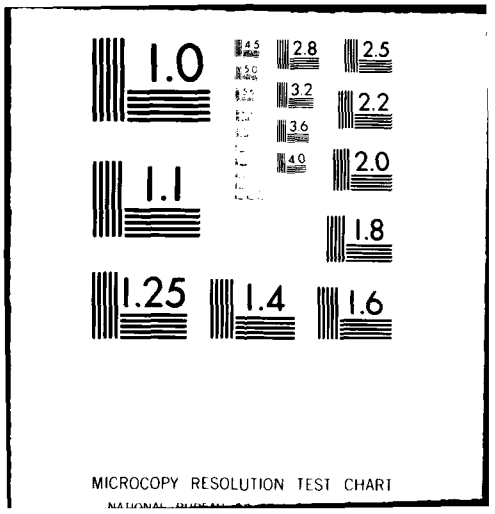
1.0
1.1
1.25
1.4
1.6
1.8
2.0
2.2
2.5
2.8
3.2
3.6
4.0
4.5
5.0
MICROCOPY RESOLUTION TEST CHART

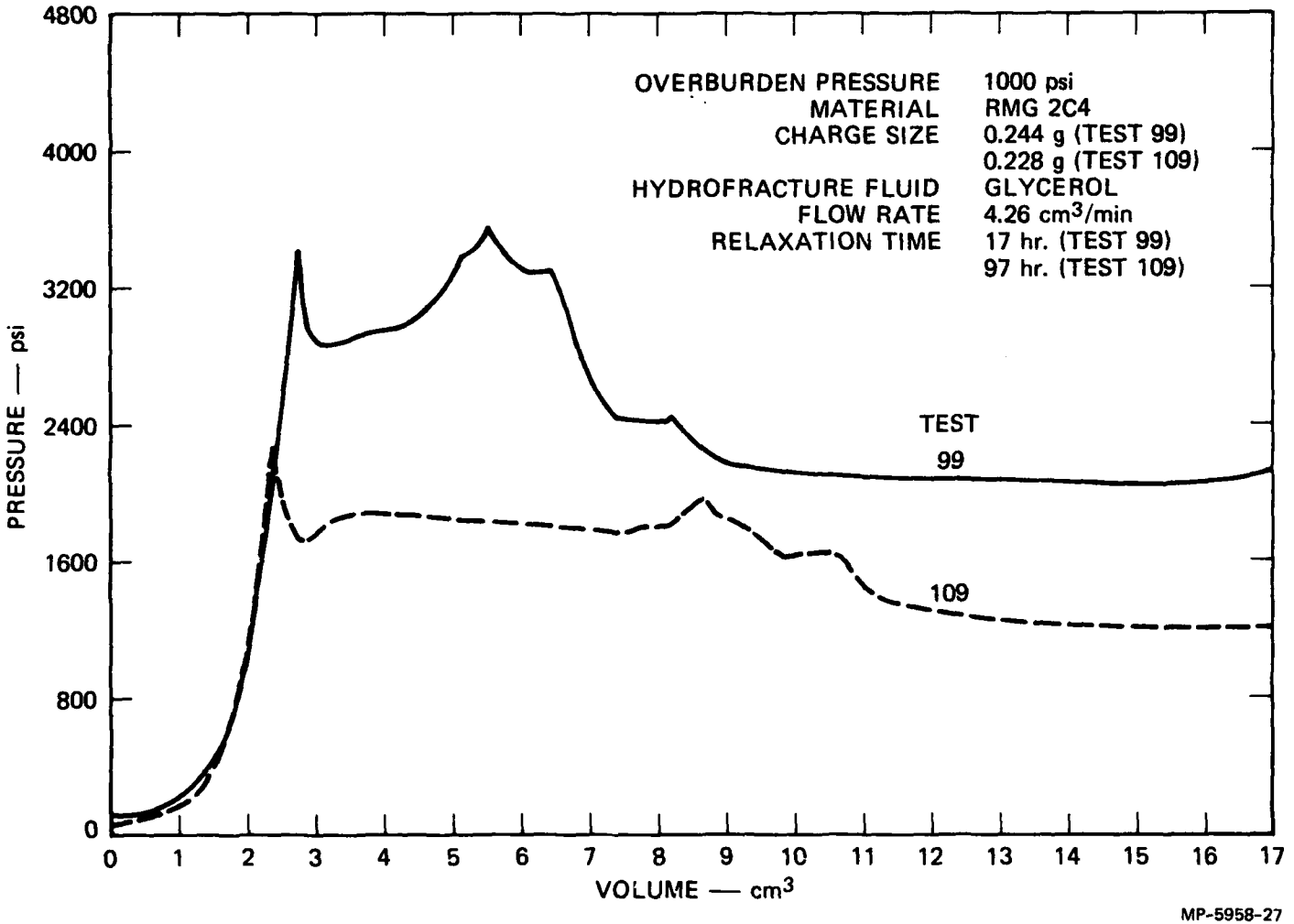

FIGURE 3.42 HYDROFRACTURE PRESSURES FOR EXPLODED CAVITY TESTS 99 AND 109—CREEP EFFECT

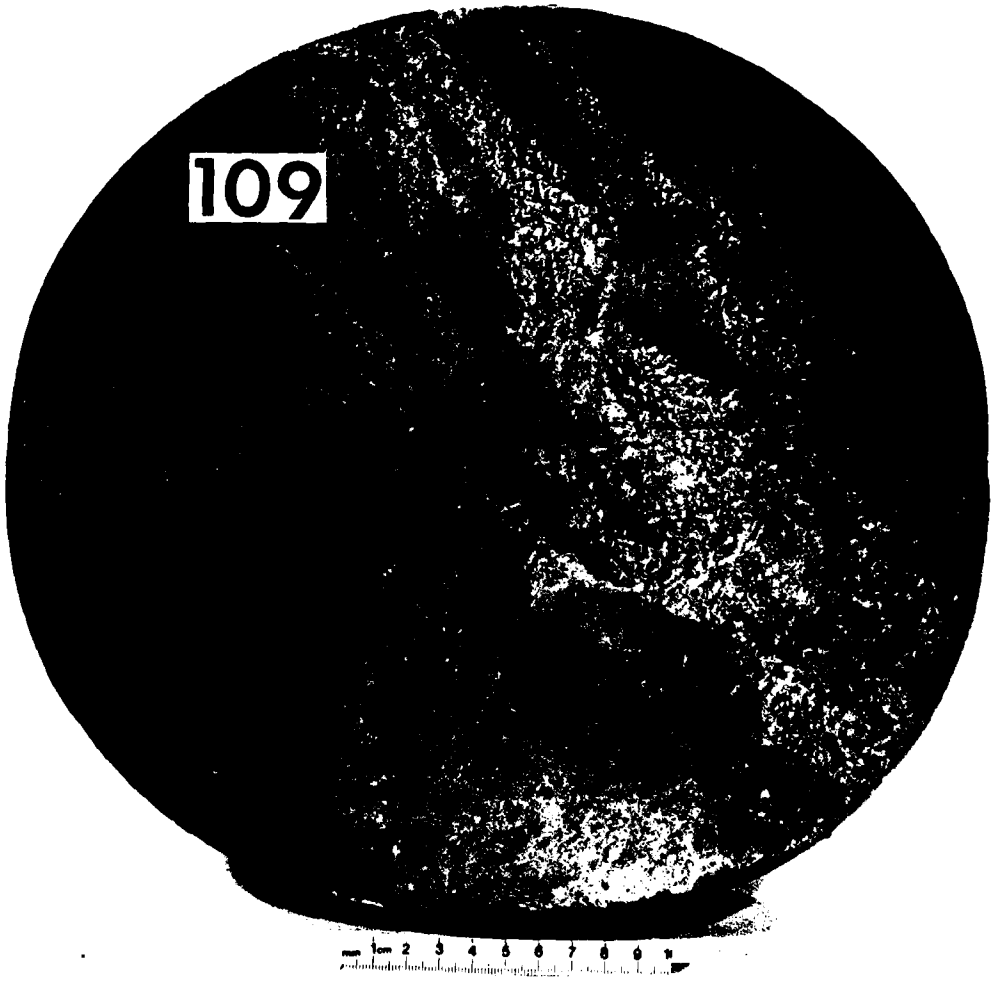

MP-5958-58

FIGURE 3.43 HYDROFRACTURE FROM EXPLODED CAVITY TEST 109

is less than would be experienced in an exploded cavity test with no creep period. Hence, the viscoplastic nature of the RMG 2C4 accounts for degradation of an explosively generated stress field with time.

Since the pressure record for Test 109 borders the lower end of the 1/4-gram test spectrum, complete stress relaxation has not occurred after 97 hours. Residual stress will remain after any creep period, however, because plastic strains are generated in the grout by the explosive.

Series 17 - Geology

Spheres containing the geological features of a simulated fault, a material interface, tunnels, and cavities were hydrofractured by pumping dyed glycerol into the cavities at the rate of 4.26 cm^3/min. External pressure was held constant at 1000 psi.

Simulated Fault. In Test 79 the simulated fault plane sketched in Figure 3.44 was cast in a RMG 2C4 sphere with a 1/4-gram charge of PETN. The hydrofracture record is also shown in Figure 3.44. Lack of a pronounced pressure spike complicates the determination of fracture initiation pressure, but apparently fracture initiation occurred at 2360 psi, which is within 2% of the 2387-psi average for the corresponding 1/4-gram tests without the fault.

Also shown in Figure 3.44 is the pressure record for Test 80, the simulated fault experiment for the corresponding 11/16-inch-diameter unexploded cavity described in Series 8. Although Figure 3.45 shows that orientation of the fracture surface was determined by the Mylar sheet in Test 79, no serious loss of containment capability can be attributed to the presence of the simulated fault.

Material Interface. In Test 89 a simulated interface between RMG 2C4 and GS3, sketched in Figure 3.46, was cast in a sphere with a 1/4-gram charge of PETN. The hydrofracture record, also shown in Figure 3.46, reveals a fracture initiation pressure of 3000 psi, which is 26% greater than the 2387-psi average for 1/4-gram tests conducted on RMG 2C4 spheres. Figure 3.47

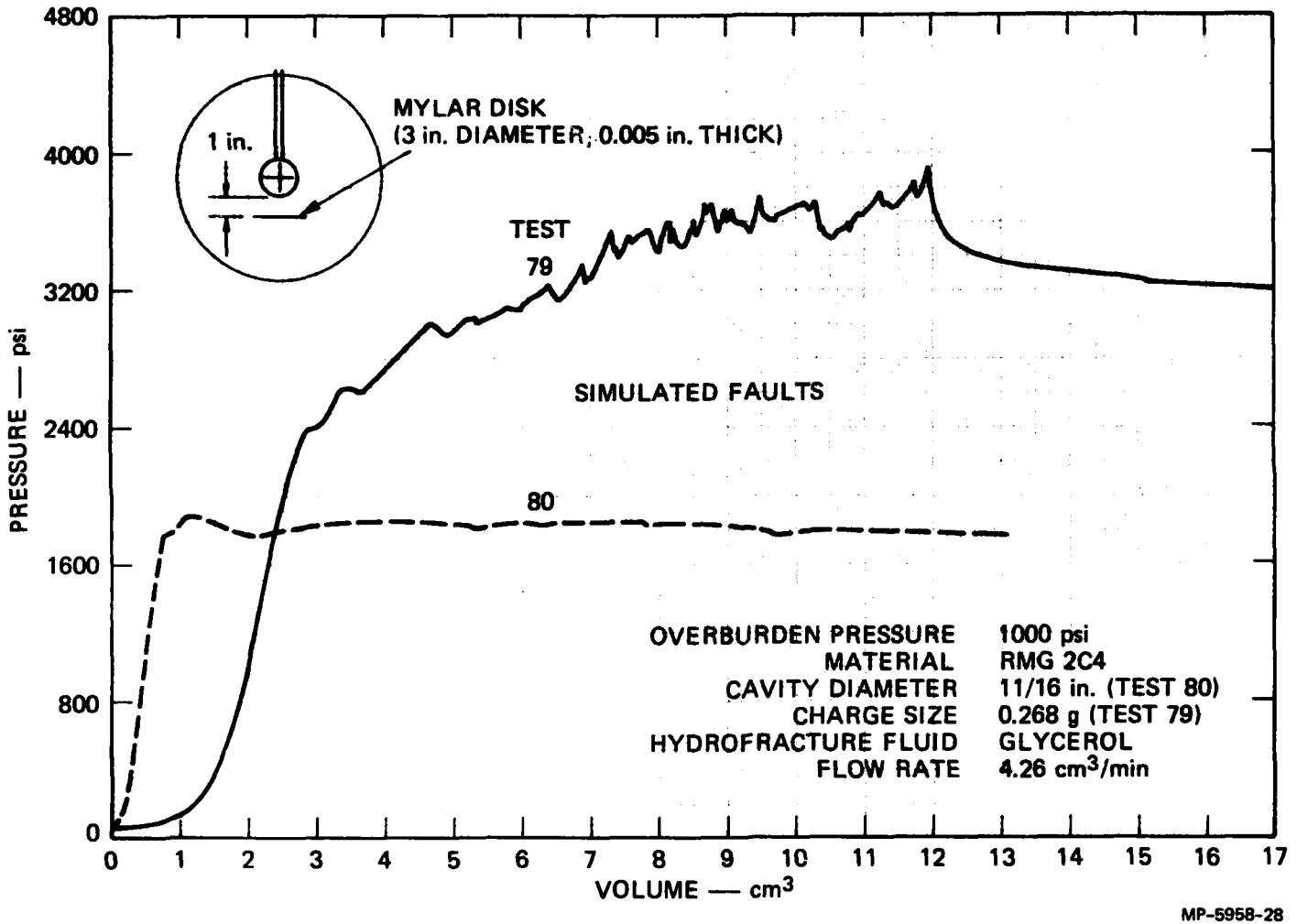

FIGURE 3.44 HYDROFRACTURE PRESSURES FOR UNEXPLODED CAVITY TEST 80 AND EXPLODED CAVITY TEST 79—SIMULATED FAULT EFFECT

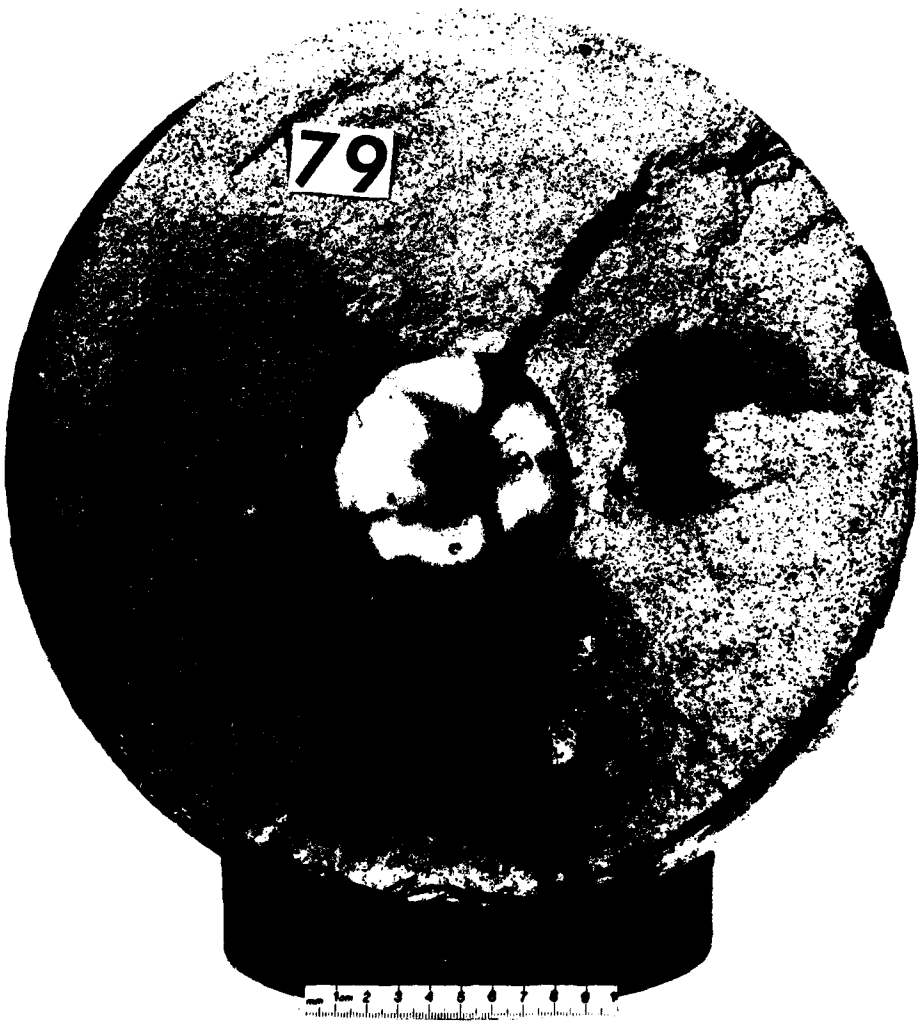

FIGURE 3.45 HYDROFRACTURE FROM EXPLODED CAVITY TEST 79

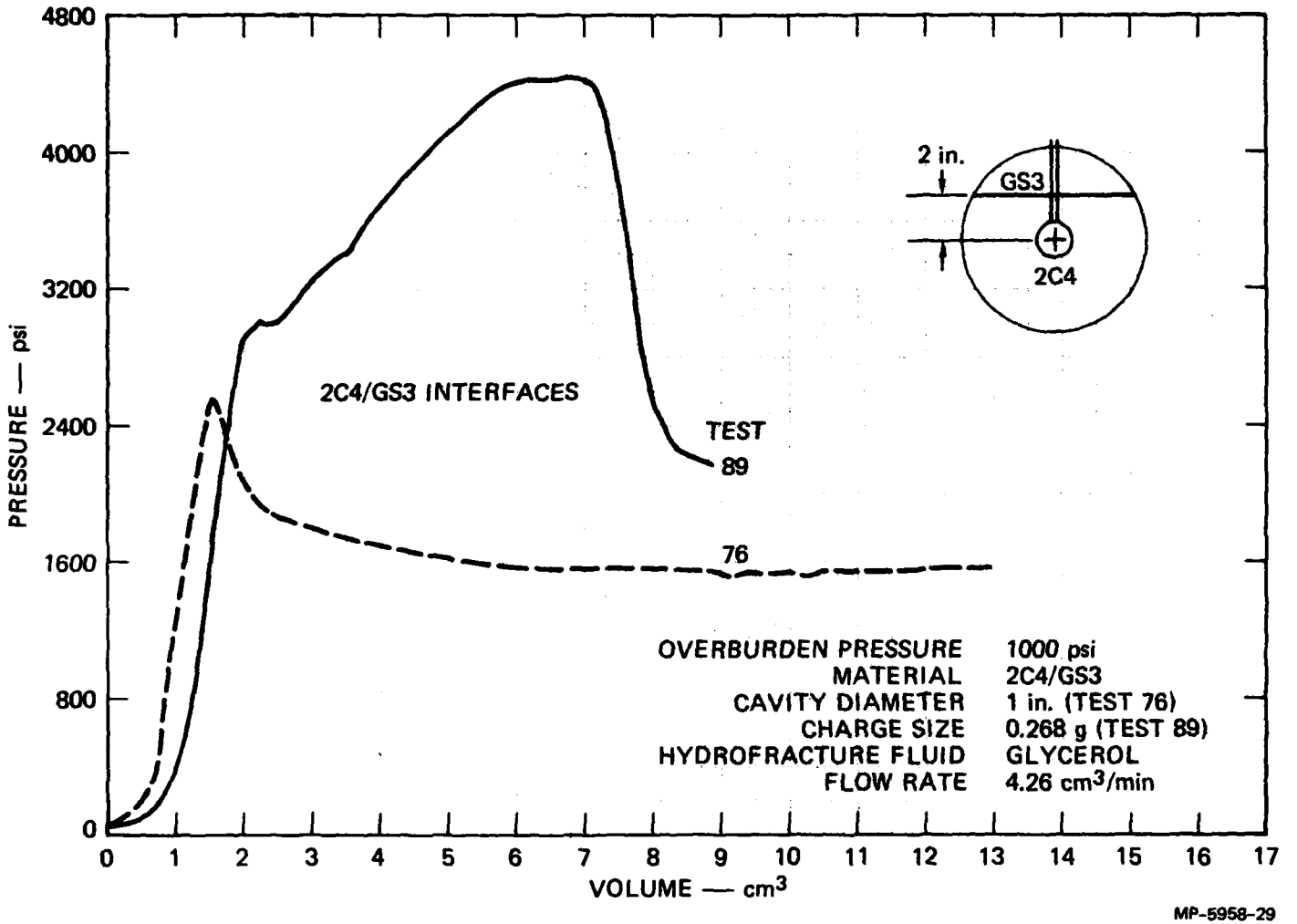

FIGURE 3.46 HYDROFRACTURE PRESSURES FOR UNEXPLODED CAVITY TEST 76 AND EXPLODED CAVITY TEST 89—MATERIAL INTERFACE EFFECT

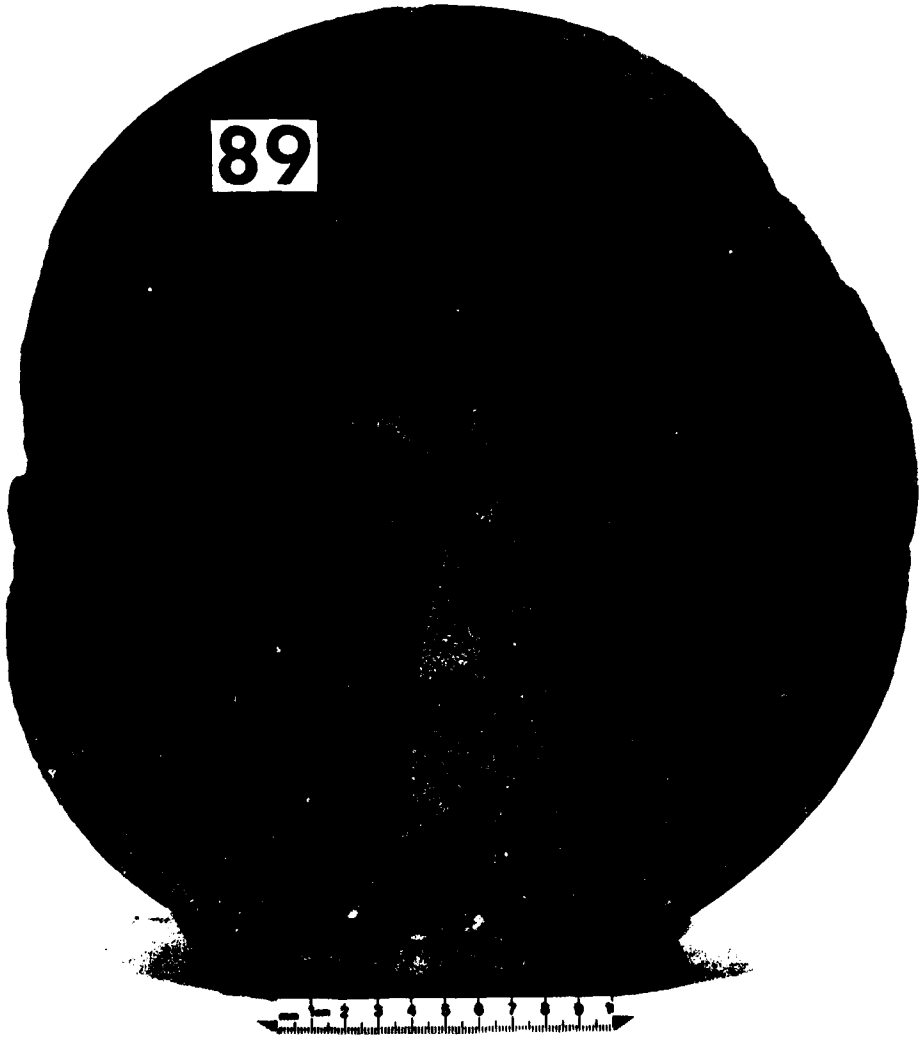

MP-5958-60

FIGURE 3.47 HYDROFRACTURE FROM EXPLODED CAVITY TEST 89

shows that cracking of the composite sphere appeared only in the weaker 2C4 and along the interface. Hence, a surface of discontinuity is a potentially effective means of directing crack growth.

Tunnels. Four tests were conducted on RMG 2C3 spheres containing tunnels in a variety of orientations.

Tests 26 and 27, termed Hybla Gold, were carried out with the overall configuration of Figure 3.48. A tunnel extended from the charge as shown in Figure 3.49. The specially designed charge contained 0.607 gram of PETN packed to a density of 1 g/cm^3.

In Test 26 the grout sphere was cracked to the surface by the explosion, so hydrofracture was not performed. The fracture surface passed through the tunnel axis as shown in Figures 3.50 and 3.51. The darkened areas were formed by deposits from the detonation products after the Lucite tunnel split open. Figures 3.52 and 3.53 are close-up views of the cavity and tunnel regions. Figure 3.54 is a sketch of the exploded cavity, tunnel fracture, and incipient stemming adjacent to the cavity.

In Test 27 the grout sphere was not cracked to the surface by the hydrofracture, so hydrofracture was performed. The pressure record is shown in Figure 3.55. The initial pressure peak is replaced by a smooth rise to a plateau of 1280 psi, which is about half the 2487-psi average fracture initiation pressure for the spherically symmetric 1/2-gram tests of Figure 3.30. The smooth rise in pressure to a plateau indicates that cracks were formed by the explosive gases near the cavity and tunnel. Figures 3.56 and 3.57 reveal a fracture surface similar to that found in Test 26. Similar darkened areas were formed by deposits from the detonation products after the Lucite tunnel split open. Figures 3.58 and 3.59 are close-up views of the cavity and tunnel region. The three areas surrounding the cavity that are not dyed represent the region of greatest residual stress that enhances containment of cavity gases. The region does not completely enclose the cavity because of the strong perturbation of the spherically symmetric stress field caused by the high pressure gases that entered the tunnel. Figure 3.60 is a sketch of the exploded cavity, tunnel fracture, and incipient stemming.

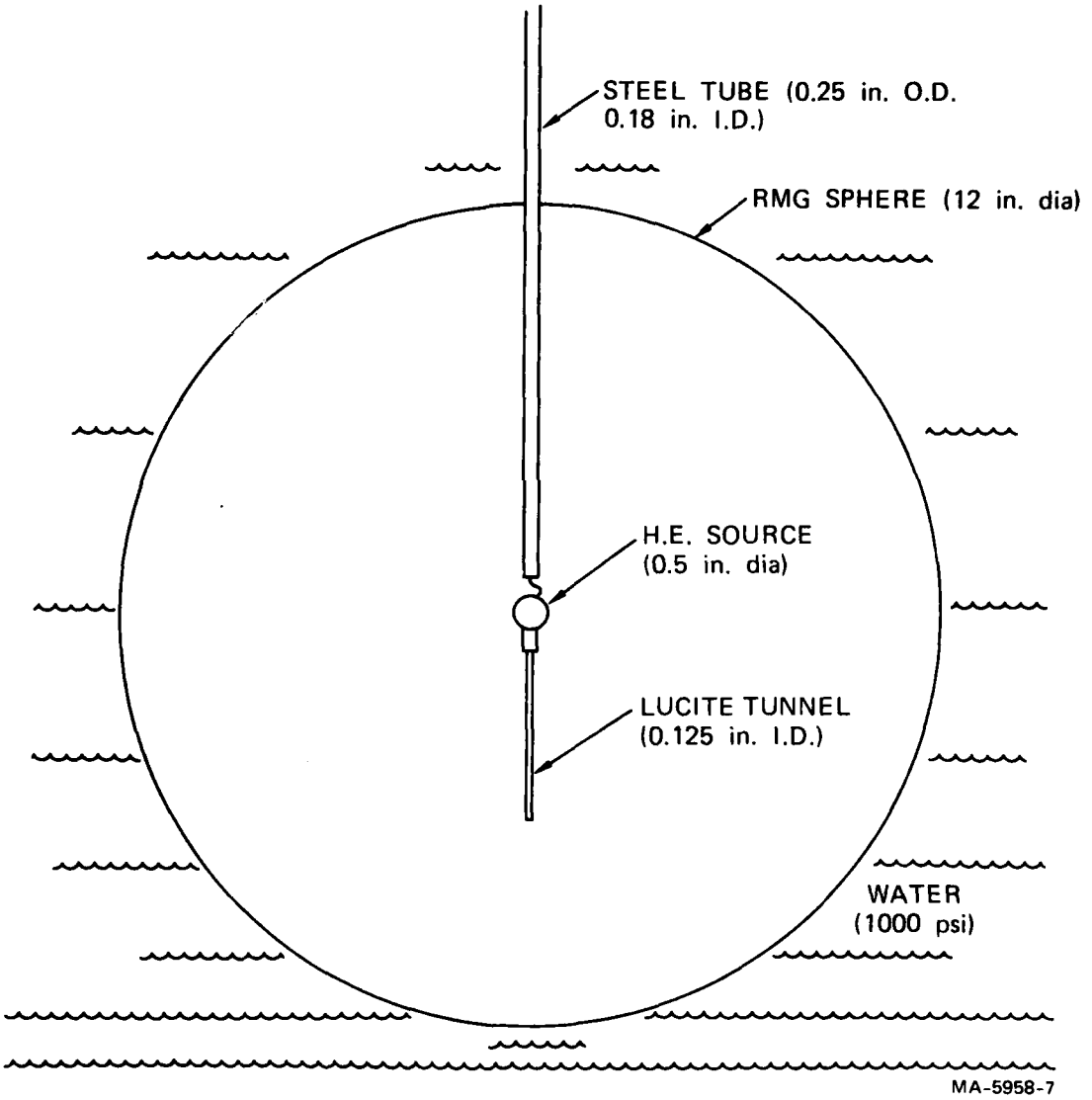

FIGURE 3.48 OVERALL CONFIGURATION FOR HYBLA GOLD EXPERIMENT

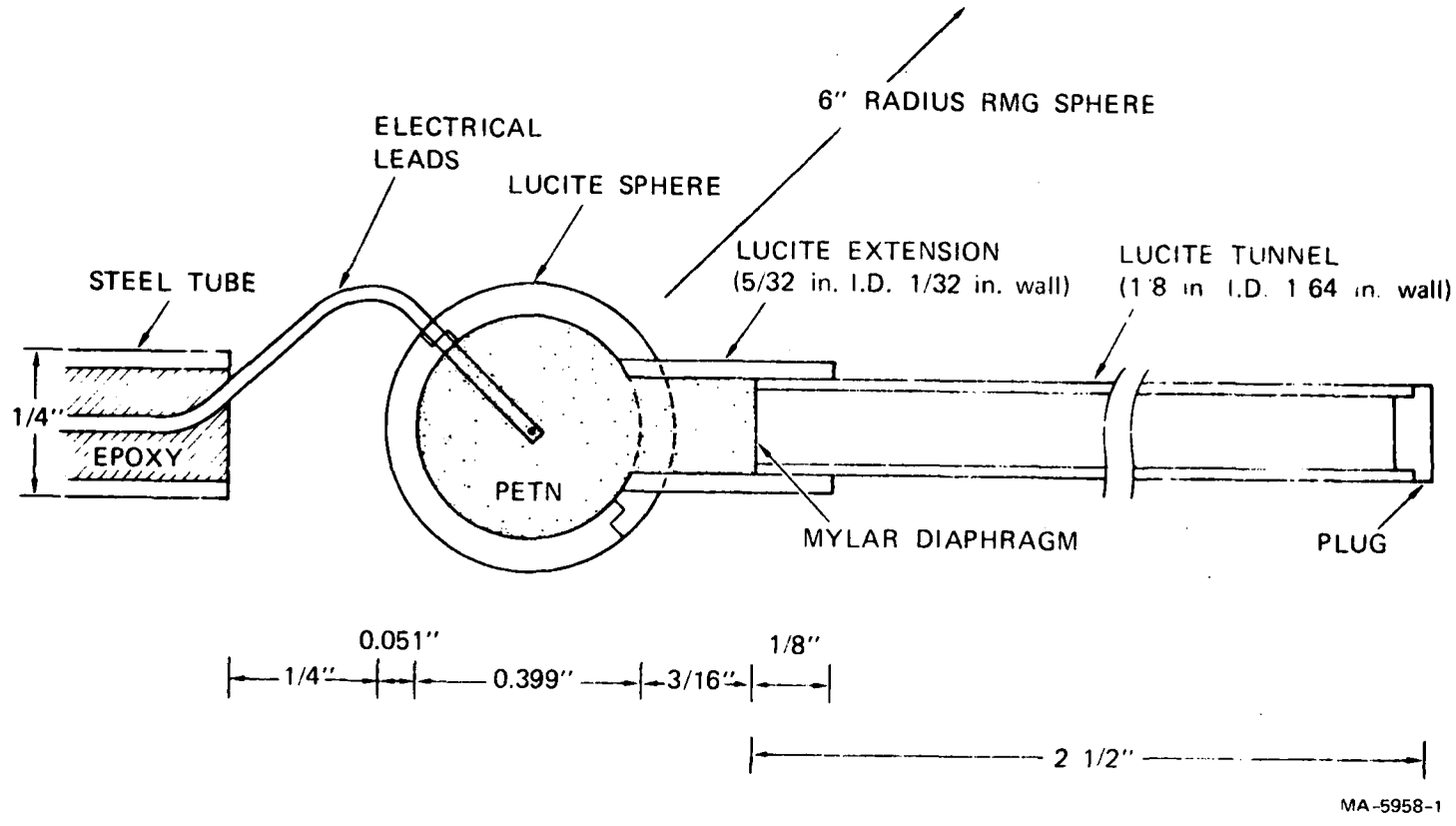

FIGURE 3.49 CONFIGURATION FOR HYBLA GOLD LABORATORY EXPERIMENT

MP 5958 61

FIGURE 3.50 LARGER PIECE OF RMG SPHERE IN HYBLA GOLD TEST 26

MP 5958-62

FIGURE 3.51 SMALLER PIECE OF RMG SPHERE IN HYBLA GOLD TEST 26

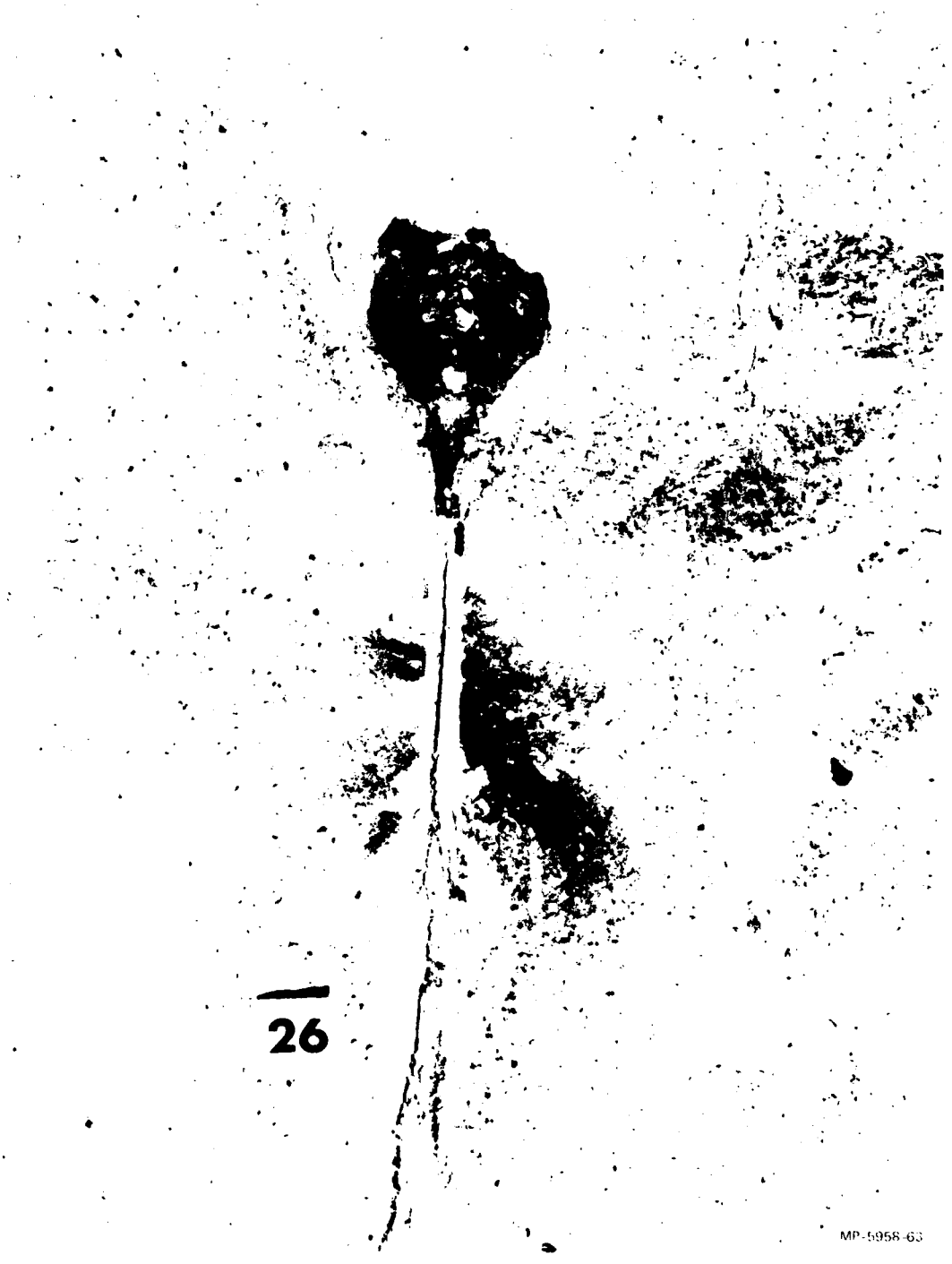

FIGURE 3.52 CLOSE-UP OF FIGURE 3.50 SHOWING CAVITY AND TUNNEL REGION IN HYBLA GOLD TEST 26

FIGURE 3.53 CLOSE-UP OF FIGURE 3.51 SHOWING CAVITY AND TUNNEL REGION IN HYBLA GOLD TEST 26

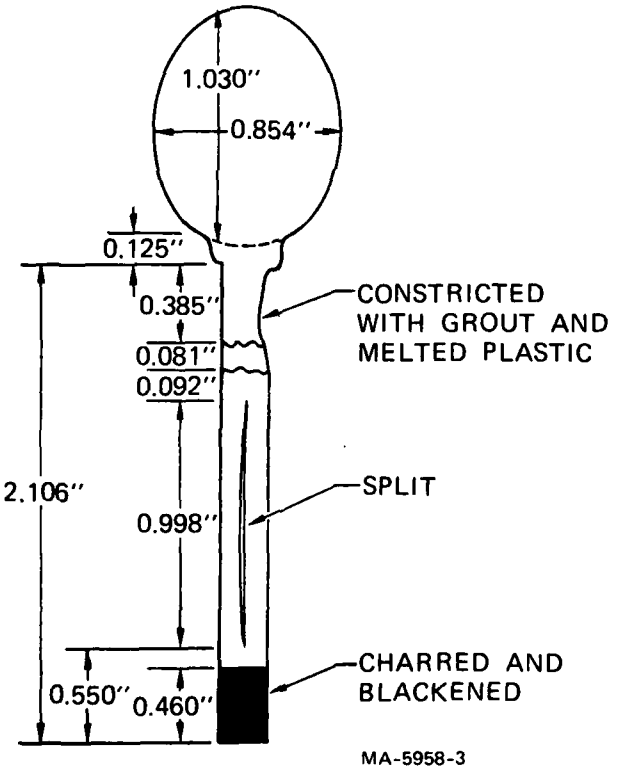

FIGURE 3.54 HYBLA GOLD EXPERIMENT 26

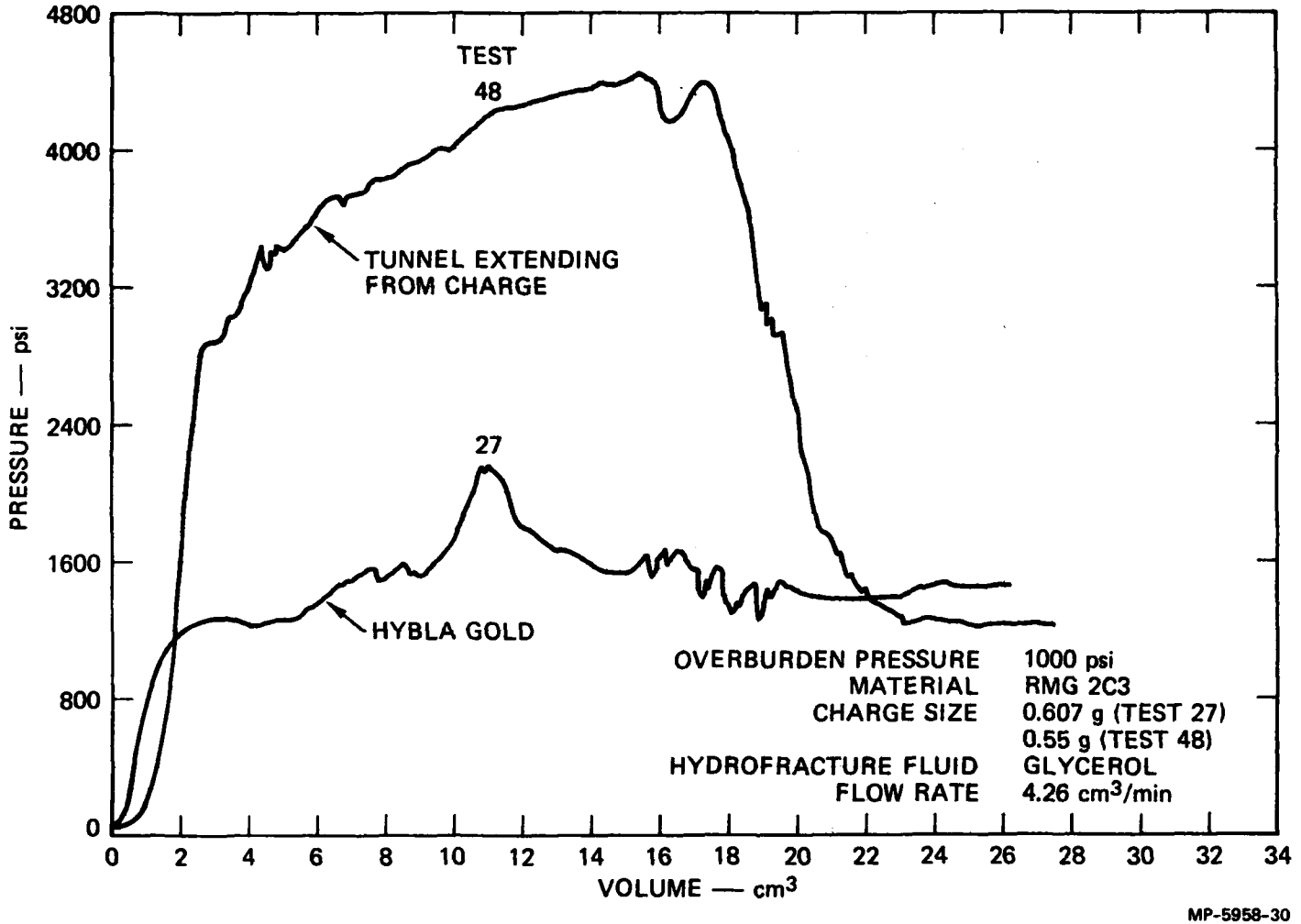

FIGURE 3.55 HYDROFRACTURE PRESSURES FOR TESTS 27 AND 48—TUNNELS

FIGURE 3.56 LARGER PIECE OF RMG SPHERE IN HYBLA GOLD TEST 27

MP-5958-66

FIGURE 3.57 SMALLER PIECE OF RMG SPHERE IN HYBLA GOLD TEST 27

FIGURE 3.58 CLOSE-UP OF FIGURE 3.56 SHOWING CAVITY AND TUNNEL REGION IN HYBLA GOLD TEST 27

FIGURE 3.59 CLOSE-UP OF FIGURE 3.57 SHOWING CAVITY AND TUNNEL REGION IN HYBLA GOLD TEST 27

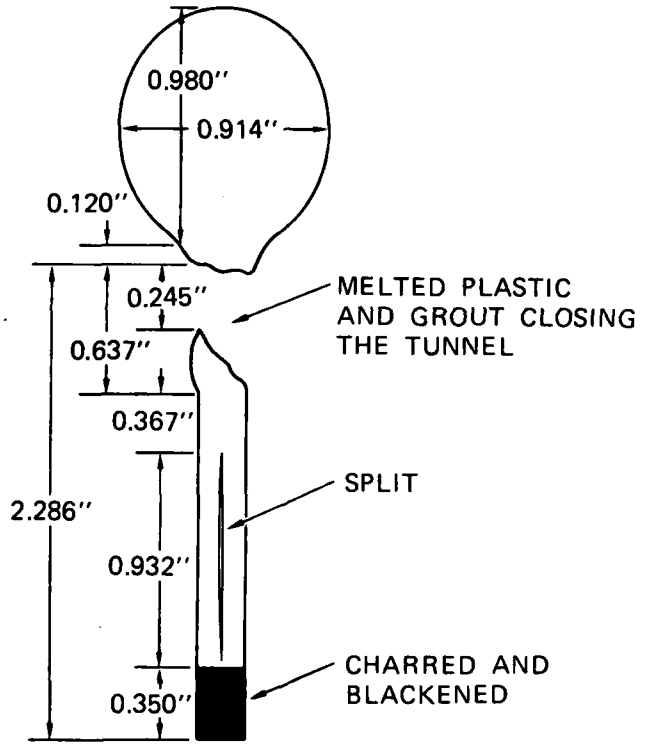

FIGURE 3.60 HYBLA GOLD EXPERIMENT 27

Test 48 was conducted with a configuration similar to the one shown in Figure 3.49 for Hybla Gold. In Test 48 the PETN in the Lucite extension was eliminated and the extension shortened accordingly. The hydrofracture record is shown in Figure 3.55. The 2880-psi fracture initiation pressure is 16% higher than the 2487-psi average for the spherically symmetric 1/2-gram tests of Figure 3.30. Figure 3.61 shows that the fracture surface in Test 48 extended through the tunnel axis similar to the Hybla Gold tests. However, the absence of darkened regions indicates that the detonation gases did not rupture the tunnel, and explains the higher cavity pressures developed in Test 48 as compared with Hybla Gold Test 27.

In Test 29 a 1/2-gram charge was detonated in a RMG 2C3 sphere containing parallel tunnels located as shown in Figure 3.62. The explosive gases expanded the cavity out to the closer tunnel, which was ruptured along a 4-inch length. The sphere was cracked to the surface by the explosion, so hydrofracture was not performed. Wedging the sphere apart resulted in a fracture surface along the axis of the ruptured tunnel as shown in Figure 3.63.

Cavities. Test 28 was performed on a RMG 2C3 sphere with a 1/2-gram charge of PETN and two nearby cavities as shown in Figure 3.64. The hydrofracture record, shown in Figure 3.65, reveals a fracture initiation pressure of 2400 psi, which is 3% less than the 2487-psi average for tests without the cavities. Since the fracture surface intersected the region between the cavities, the perturbation induced by these structures had negligible influence on the test.

The configuration for Test 18 was similar to that shown in Figure 3.64 except that only one cavity was cast, with the center of the cavity 3 inches from the center of the charge. The hydrofracture record is shown in Figure 3.65. The 2700-psi fracture initiation pressure is 9% greater than the 2487-psi average for corresponding tests without the nearby cavity. A sudden drop in cavity pressure, which occurred soon after fracture initiation, is attributed to the fact that the fracture surface passed through the nearby cavity as shown in Figure 3.66. Hence the test provides data on the rate of

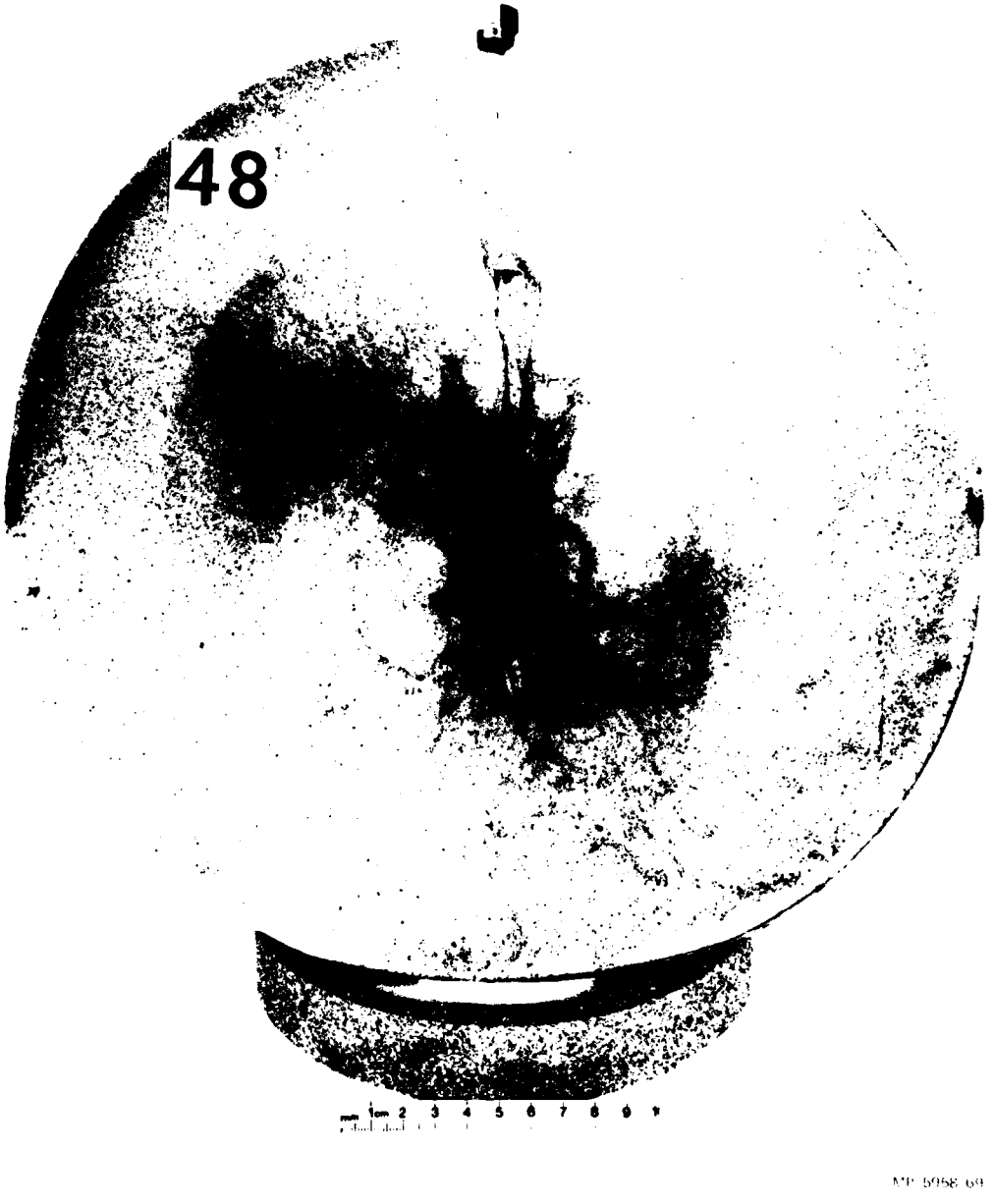

FIGURE 3.61 HYDROFRACTURE FROM EXPLODED CAVITY TEST 48

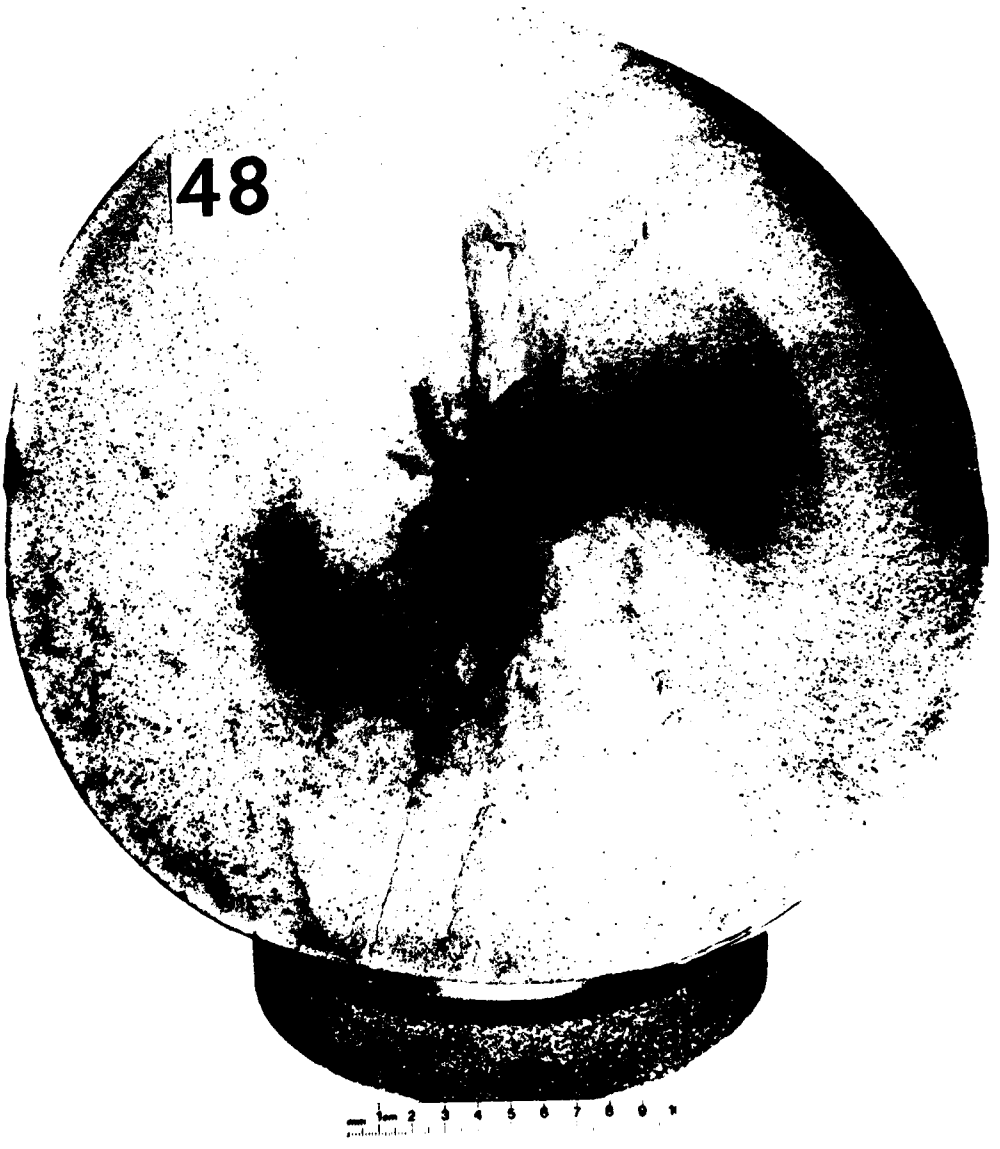

FIGURE 3.61 HYDROFRACTURE FROM EXPLODED CAVITY TEST 48 (CONCLUDED)

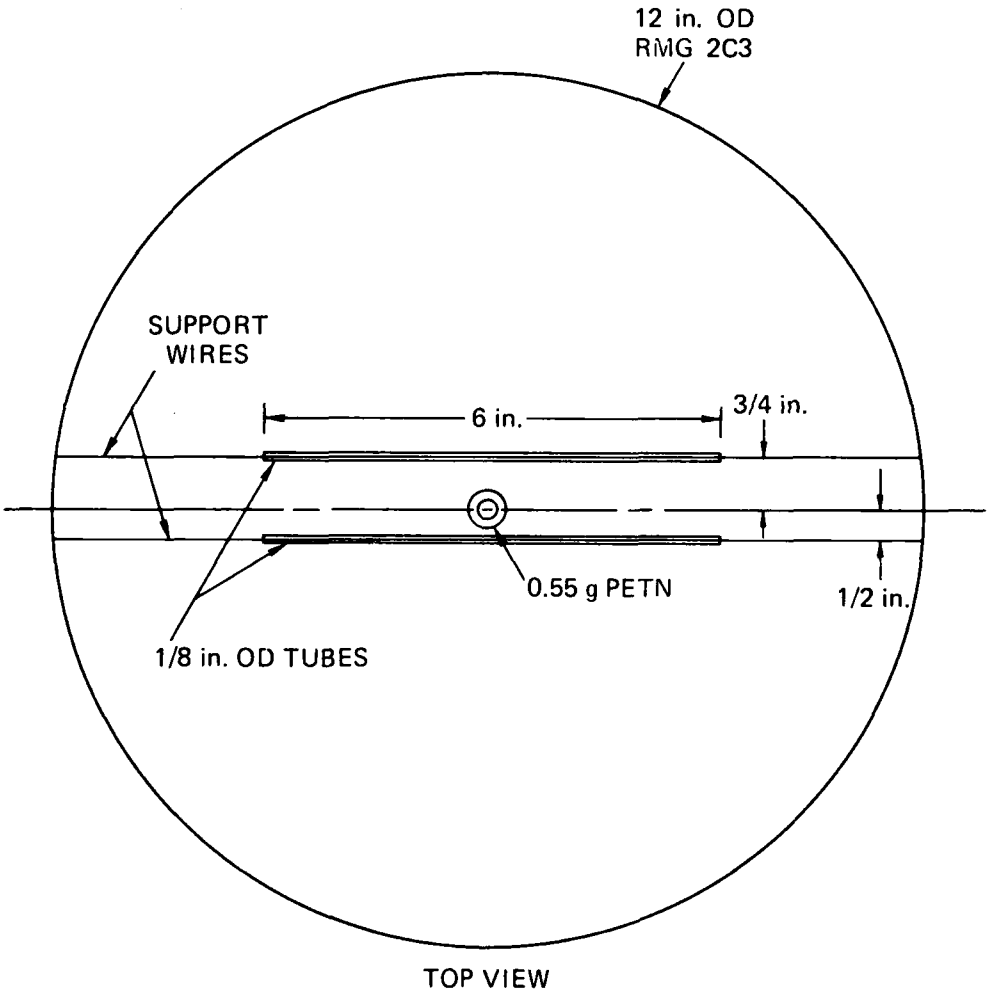

FIGURE 3.62 CONFIGURATION FOR EXPLODED CAVITY TEST 29

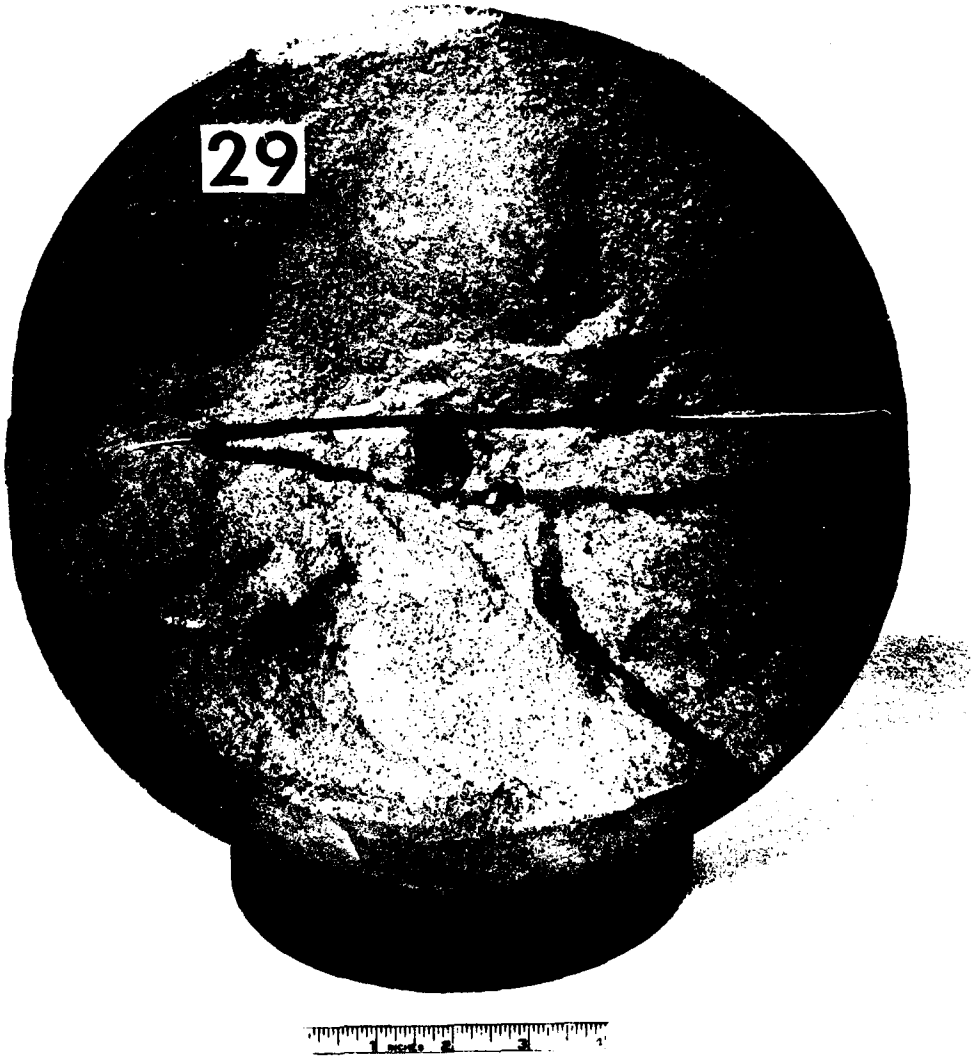

MP-5958-72

FIGURE 3.63 HYDROFRACTURE FROM EXPLODED CAVITY TEST 29

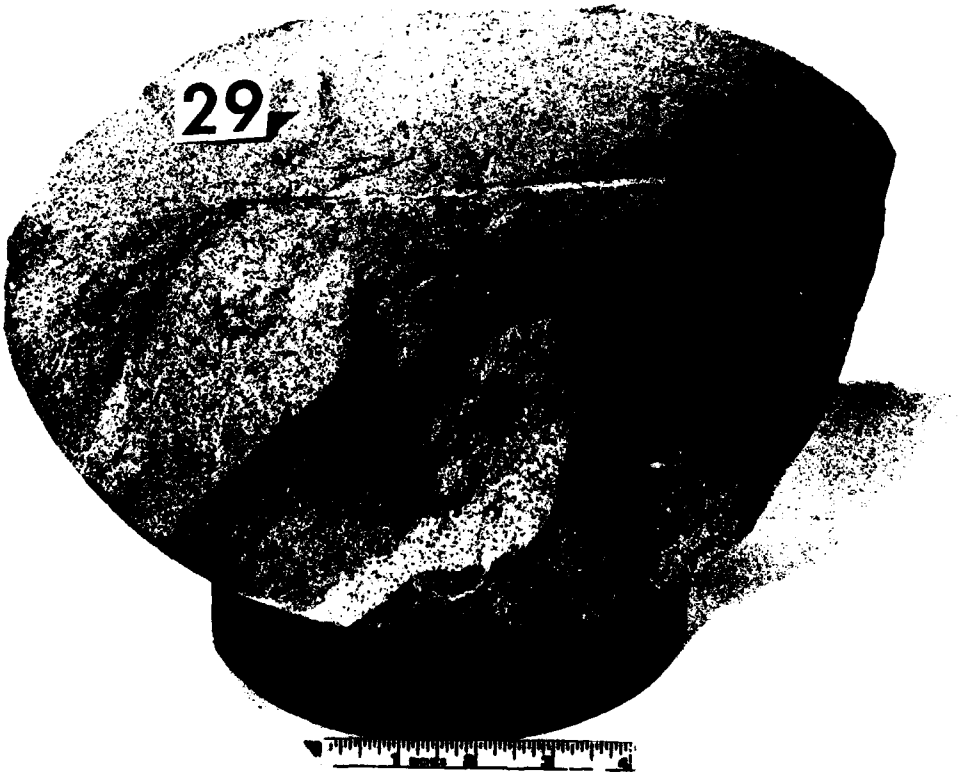

MP 5958-73

FIGURE 3.63 HYDROFRACTURE FROM EXPLODED CAVITY TEST 29 (CONCLUDED)

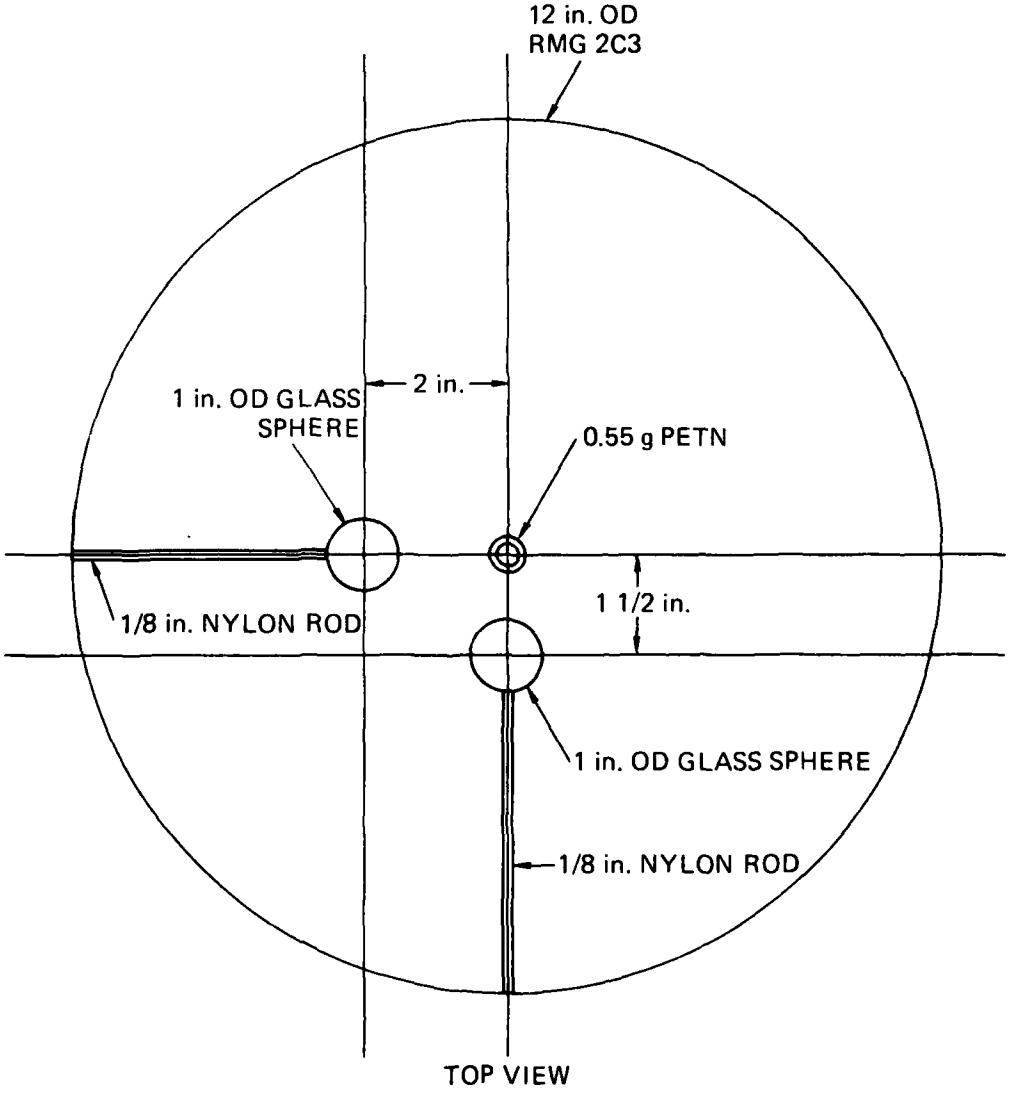

FIGURE 3.64 CONFIGURATION FOR EXPLODED CAVITY TEST 28

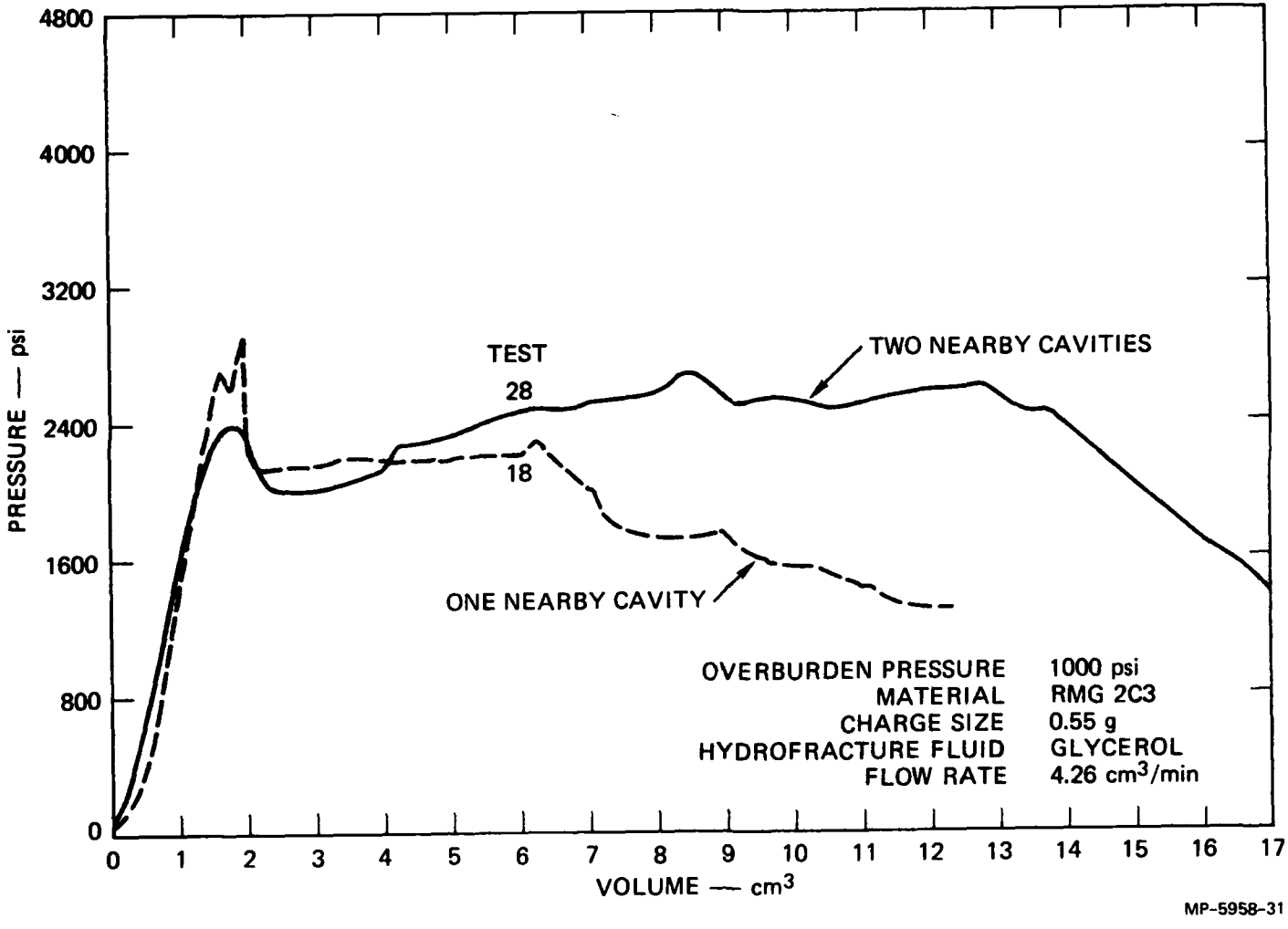

FIGURE 3.65 HYDROFRACTURE PRESSURES FOR EXPLODED CAVITY TESTS 18 AND 28—NEARBY CAVITIES

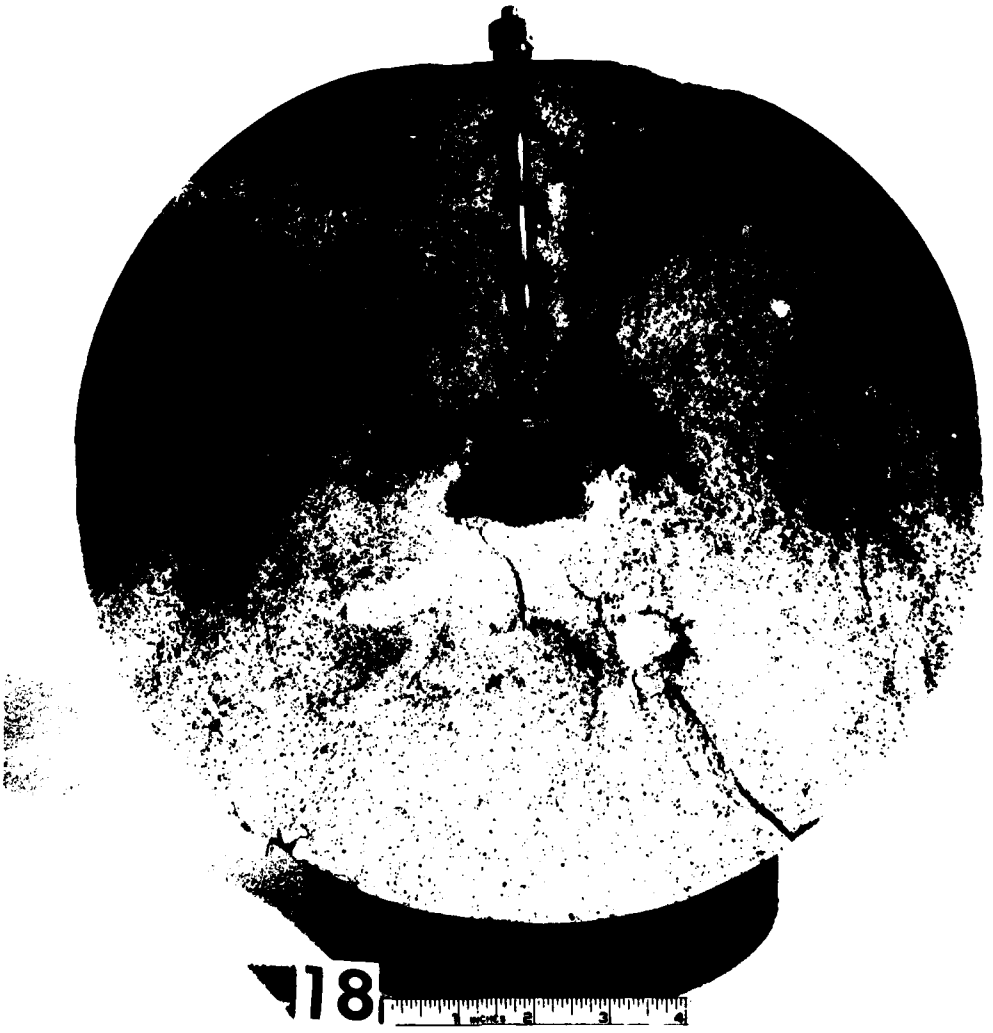

MP-5958-75

FIGURE 3.66 HYDROFRACTURE FROM EXPLODED CAVITY TEST 18

MP-5958-76

FIGURE 3.66 HYDROFRACTURE FROM EXPLODED CAVITY TEST 18 (CONCLUDED)

crack growth in an exploded cavity experiment. In Test 28 the presence of a nearby structure had negligible influence on the orientation of the fracture surface. However, Test 18 showed that when a crack does intersect a nearby structure, loss of containment capability is possible.

Series 18 - Cavity Lining

Tests 5 through 8 were conducted on RMG 2C3 spheres containing a 1/2-gram charge of PETN. The glycerol hydrofracture fluid contained two dyes, one soluble and one insoluble, as in the Series 10 tests for unexploded cavities. Hydrofracture records are shown in Figure 3.67. Fracture initiation pressures were 1940, 2120, 2320, and 2380 psi. The 2190-psi average is 12% lower than the 2487-psi average for the corresponding one dye tests, but maximum pressures following fracture initiation are generally higher in the two dye tests of Figure 3.67. The fracture surface for Test 8 is shown in Figure 3.68. The soluble red dye and the insoluble blue dye appear in nearly equal proportion. This is in contrast to the predominantly blue appearance of the fracture surface found in two dye unexploded cavity tests. Hence, exploded cavities filter out more insoluble material than unexploded cavities. The filtering action provides a cavity lining that restricts flow into a crack and increases hydrofracture pressures.

Series 19 - Fracture Initiation and Growth

Tests 32, 33, 35, and 36 were conducted on RMG 2C3 spheres containing a 1/2-gram charge of PETN. The hydrofracture fluid was dyed glycerol and the flow rate was 4.26 cm^3/min. In Test 32 flow into the cavity was stopped before a spike formed on the pressure record. Cavity pressure reached 1920 psi. Subsequent sawing of the sphere failed to reveal cracks or penetration of dyed glycerol into the grout. In Tests 33, 35, and 36 flow into the cavity was stopped soon after the formation of a spike, as shown in Figure 3.69. Hydrofracture produced cracking to the surface of the sphere in these tests. Figure 3.70 shows the fracture surface and the formation of an intensely dyed region surrounding the exploded cavity in Test 33.

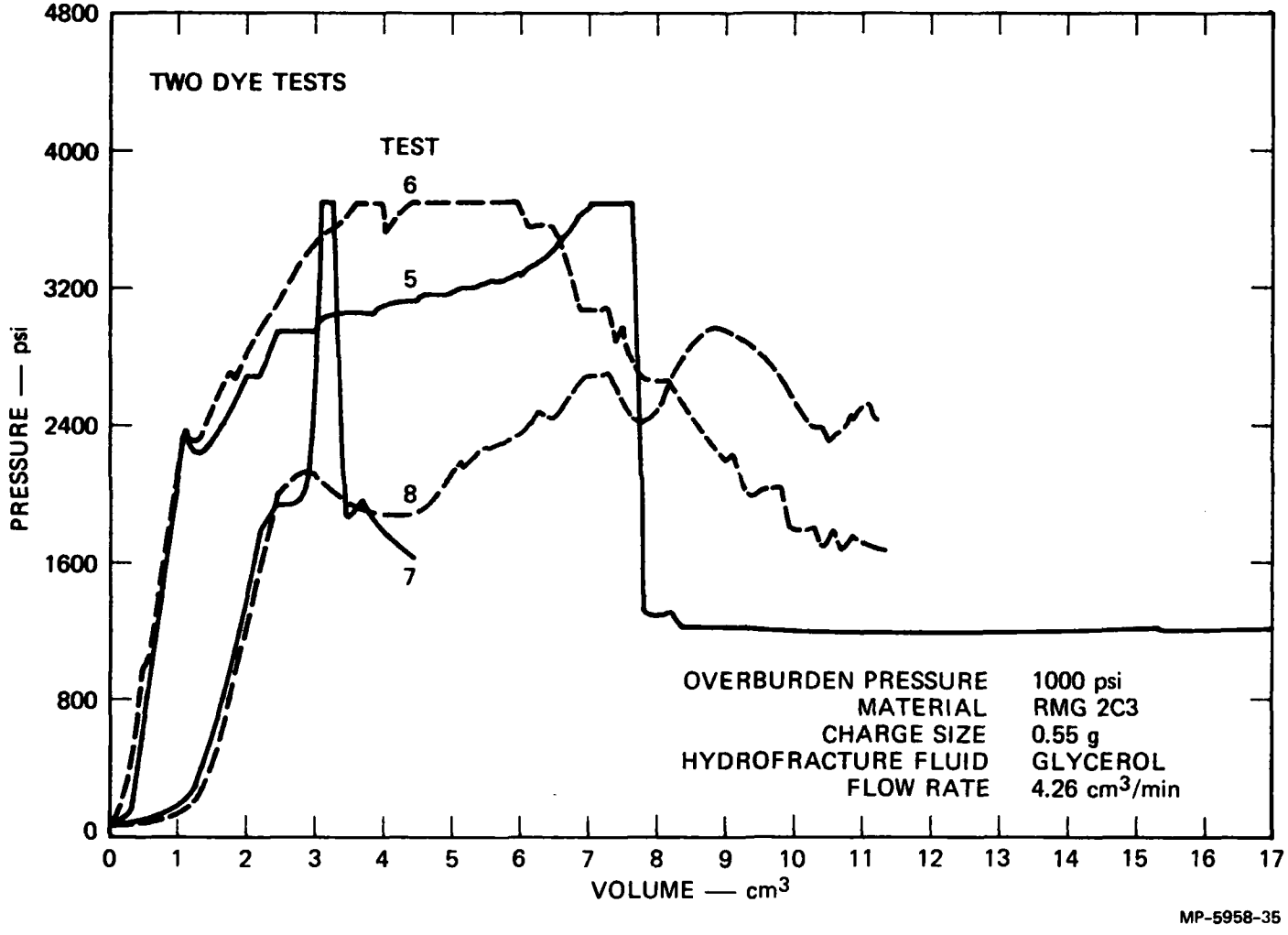

FIGURE 3.67 HYDROFRACTURE PRESSURES FOR EXPLODED CAVITY TESTS 5, 6, 7, AND 8 — CAVITY LINING

MP-5958-77

FIGURE 3.68 HYDROFRACTURE FROM EXPLODED CAVITY TEST 8

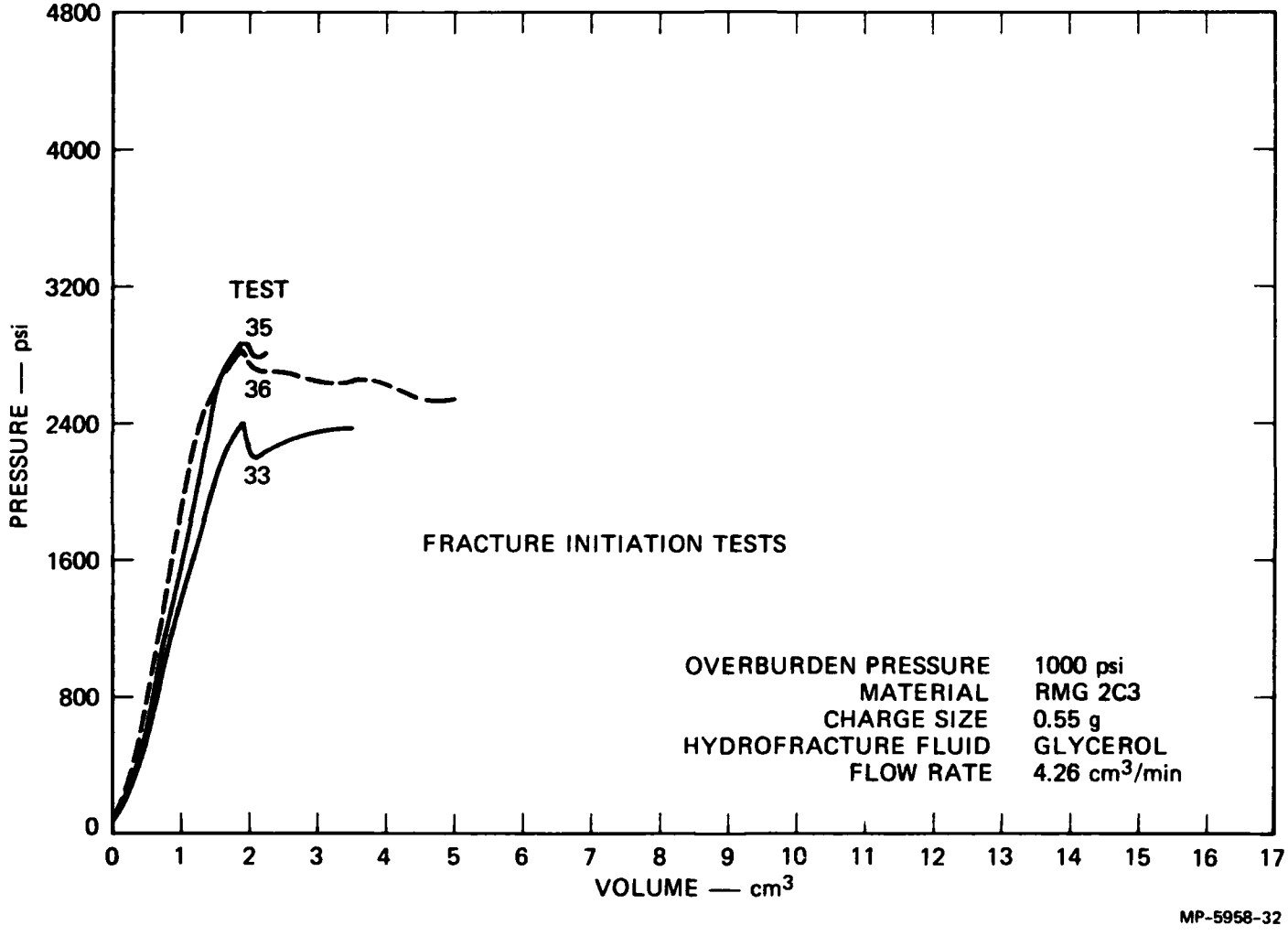

FIGURE 3.69 HYDROFRACTURE PRESSURES FOR EXPLODED CAVITY TESTS 33, 35, AND 36—FRACTURE INITIATION

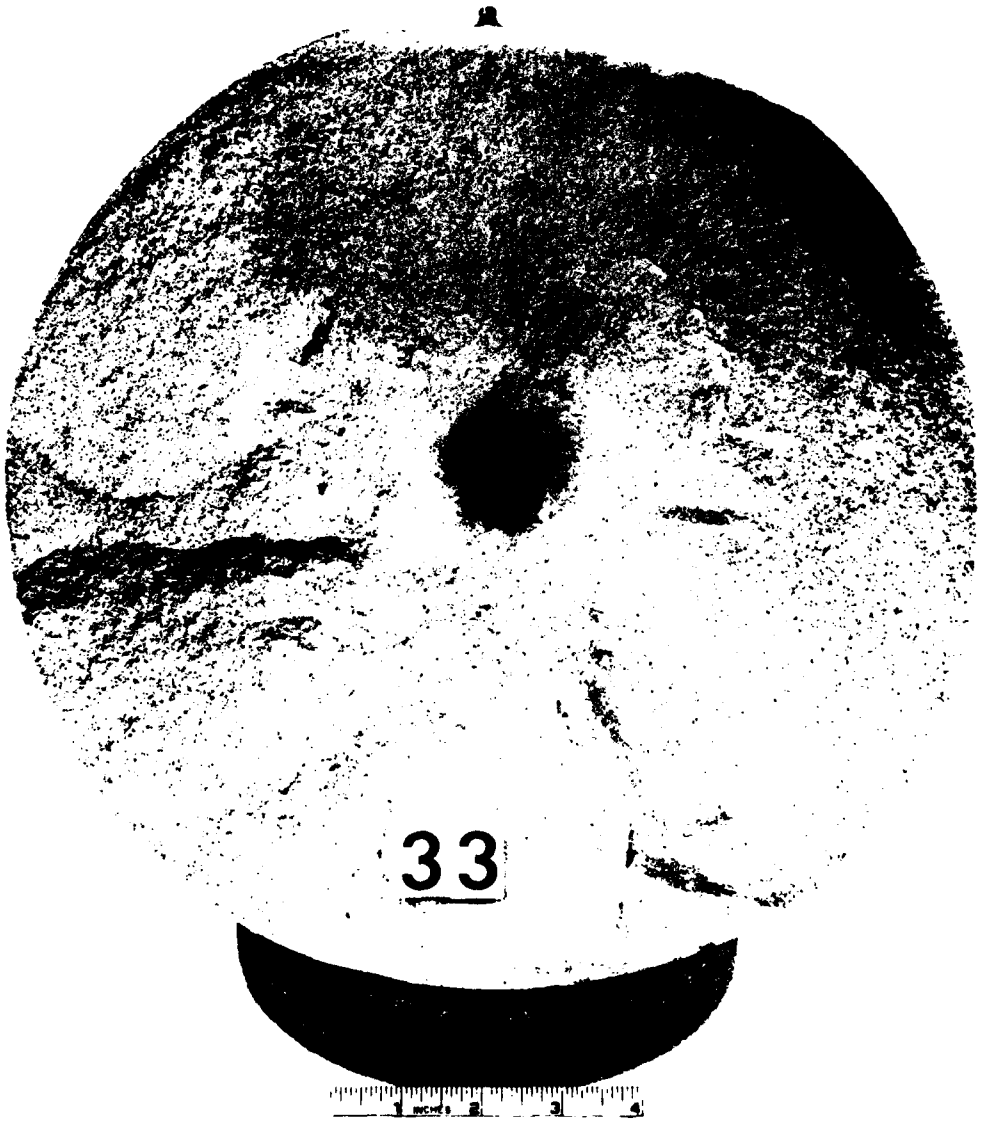

MP-5958-78

FIGURE 3.70 HYDROFRACTURE FROM EXPLODED CAVITY TEST 33

The fracture initiation studies of Series 11 and 19 show that the pressure spike on a hydrofracture record signals fracture initiation in both unexploded and exploded cavity tests. However, the rate of crack growth is much greater in the exploded cavity tests.

4. FUTURE RESEARCH

While risk of explosive cracking increases as the mass of explosive is increased, reproducibility of hydrofracture records dictates the use of 1/2-gram charges rather than the less reliable 1/4-gram charges. However, calibration tests are planned to determine reproducibility of the energy release for all charge sizes, and these tests may explain the spectrum of hydrofracture records associated with the 1/4-gram charges. Also, thinner walled charge holders will reduce inert material and improve reliability.

With an improved charge, exploded cavity investigations will be made to determine:

- Fracture initiation and growth
- Material strength on hydrofracture pressures
- Material relaxation on hydrofracture pressures
- Ways of increasing the range of hydrofracture flow rate and fluid viscosity.

Unexploded cavity investigations are also planned to study:

- Use of imperfection-free cavities
- Explanation of cavity size effect
- Use of flexible cavity lining to prevent porous flow
- Ways of increasing the range of hydrofracture flow rate and fluid viscosity.

Use of embedded stress and strain gages in unexploded and exploded cavity tests are planned to provide further qualitative data for correlation with computer code results.

5. REFERENCES

1. R. W. Gates and C. F. Petersen, "A Laboratory Method for Studying Stemming of Line-of-Sight Tunnels in Underground Nuclear Tests," SRI Final Report DNA 3058Z, Contract DNA001-72-C-0047 (November 1972).

2. R. W. Gates, C. F. Petersen, and A. L. Florence, "Laboratory Method for Studying Stemming of Line-of-Sight Tunnels in Underground Nuclear Tests," SRI Final Report DNA 3592F, Contract DNA001-73-C-0122 (December 1973).

3. A. L. Florence, "Laboratory Investigation of Stemming of Horizontal Line-of-Sight (HLOS) Underground Nuclear Tests," SRI Final Report DNA 3684F, Contract DNA001-74-C-0101 (February 1975).

4. A. L. Florence, "Laboratory Investigation of Stemming and Containment in Underground Nuclear Tests," SRI Final Report DNA 4149F, Contract DNA001-75-C-0083 (October 1976).

5. A. L. Florence and T. C. Kennedy, "A Simple Analysis for Containment Studies," SRI Topical Report 76-3702-2, Contract DNA001-75-C-0083 (August 1976).

6. L. Seaman, "SRI PUFF 3 Computer Code for Stress Wave Propagation," prepared for Air Force Weapons Laboratory, Air Force Systems Command, Kirtland AFB, New Mexico, Technical Report No. AFWL-TR-70-51, SRI International, Menlo Park, California (September 1970).

DISTRIBUTION LIST

DEPARTMENT OF DEFENSE

Assistant to the Secretary of Defense
Atomic Energy
ATTN: Executive Assistant

Defense Nuclear Agency
ATTN: DDST
ATTN: SPTD, T. Kennedy
4 cy ATTN: TITL

Defense Technical Information Center
12 cy ATTN: DD

Field Command
Defense Nuclear Agency
ATTN: FCPR
ATTN: FCTK, C. Keller
ATTN: FCTMD, W. Summa

Field Command
Defense Nuclear Agency
Livermore Division
ATTN: FCPRL

Field Command Test Directorate
Test Construction Division
Defense Nuclear Agency
ATTN: FCTC, J. LaComb

Undersecretary of Def. for Rsch. & Engrg.
ATTN: Strategic & Space Systems (OS)

DEPARTMENT OF THE ARMY

Harry Diamond Laboratories
Department of the Army
ATTN: DELHD-N-P

DEPARTMENT OF THE NAVY

Naval Surface Weapons Center
ATTN: Code F-31

DEPARTMENT OF THE AIR FORCE

Air Force Weapons Laboratory
ATTN: SUL

OTHER GOVERNMENT AGENCY

Department of Interior
U.S. Geological Survey
Special Project Center
ATTN: R. Carroll

DEPARTMENT OF ENERGY

Department of Energy
Nevada Operations Office
ATTN: R. Newman

DEPARTMENT OF ENERGY CONTRACTORS

Lawrence Livermore Laboratory
ATTN: Document Control for D. Oakley
ATTN: Document Control for B. Hudson
ATTN: Document Control for B. Terhune
ATTN: Document Control for J. Shearer

Los Alamos Scientific Laboratory
ATTN: Document Control for R. Brownlee
ATTN: Document Control for E. Jones
ATTN: Document Control for F. App
ATTN: Document Control for A. Davis

Sandia Laboratories
ATTN: C. Mehl
ATTN: C. Smith

DEPARTMENT OF DEFENSE CONTRACTORS

General Electric Company-TEMPO
ATTN: DASIAC

Pacifica Technology
ATTN: G. Kent

Physics International
ATTN: E. Moore

R & D Associates
ATTN: C. MacDonald

SRI International
ATTN: A. Florence

Systems, Science & Software, Inc.
ATTN: R. Duff

Terra Tek, Inc.
ATTN: S. Green


DATE
ILME